Bioorthogonal Noncanonical Amino Acid Tagging for Understanding Bacterial Persistence

Thesis by

Xinyan Liu

In Partial Fulfillment of the Requirements for
the Degree of
Doctor of Philosophy in Chemical
Engineering

CALIFORNIA INSTITUTE OF TECHNOLOGY
Pasadena, California

2023
(Defended on September 2, 2022)

© 2022

Xinyan Liu
ORCID: 0000-0003-3258-5720

All rights reserved except where otherwise noted.

ACKNOWLEDGEMENTS

First of all, I would like to thank my advisor, Prof. David Tirrell, for his support and guidance throughout my entire graduate studies. Dave's knowledge, insights, patience, and enthusiasm were incredibly helpful in moving this project forward. I am continuously impressed by his integrity, leadership, and wisdom. He truly leads by example and emphasizes education and independence. I am so grateful and proud to be one of Dave's students.

I would like to thank the other members of my thesis committee, Prof. Mikhail Shapiro, Prof. Rustem Ismagilov, and Prof. Victoria Orphan, for their time, insights, advice, and support. I really appreciate all the help I got from them.

I would like to thank the entire Tirrell lab. I am deeply impressed by their brilliance. I feel fortunate to have had the opportunity to work with them. They have already made important contributions to the world of science. Many of them, even after they graduated, still keep in touch with me and visit me whenever they are in Pasadena. I have learned so much from them. Special thanks to all the past and current members of the BONCAT subgroup. There is nothing else which could refresh me more than subgroup meetings on Tuesday mornings. Special thanks to Dr. Brett Babin and Dr. Mark van Eldijk for initiating this project.

Many thanks to Ms. Roxana Eggleston-Rangel, Mr. Michael J. Sweredoski, Ms. Annie Moradian, Dr. Jeff Jones, and Mr. Brett Lomenick from Caltech Proteome Exploration Laboratory for the LC-MS/MS experiments and analysis. I would like to thank Dr. Chelsey VanDrisse, Dr. Megan Bergkessel, and Prof. Dianne Newman for everything about *Pseudomonas*.

I would like to thank the Rosen Bioengineering Center for everything during the Biotechnology Leadership Pre-doctoral Training Program. Many thanks to Prof. Frances Arnold, Dr. Kim Mayer, and Ms. Julie Kelly for their contributions, arrangements, and efforts.

I would like to thank everyone I met during my internship at Protomer, Eli Lilly and Company. Special thanks to Dr. Alborz Mahdavi, one of the greatest entrepreneurs I have met, for the internship opportunity and continuous help and support. Many thanks to all the wonderful colleagues, Dr. Diao Chen, Dr. Ryan Spencer, Dr. Sachitanand Mali, Mr. Jack

Steele, Ms. Danielle Sumilang, and Ms. Haley Peters, who made my internship experience so enjoyable.

I would like to thank all my friends at Caltech. Special thanks to all my friends from the Caltech Chinese Association (Caltech C) and US Southwestern Chinese Students and Scholars Association. And also thanks to Mr. Qi Chen for all the teaching and management opportunities at Weichen, which greatly broadens my vision and expands my network.

I would like to thank the Agency for Science, Technology, and Research (A*STAR, Singapore) for awarding me the National Science Scholarship. I would not have been able to be a graduate student without their trust and investment.

I would like to thank everyone who helped me in my past research projects: Prof. Linda Griffith, Prof. Paula Hammond, Dr. Chee Ping Ng, Prof. Daniel Heath, Mr. Sharif Mohamed, and Ms. Jocelyn Sales from Singapore-MIT Alliance for Research and Technology; Prof. Jianwen Jiang, Prof. Lanry Yung, Dr. Narjes Allahrabbi, Dr. Surya Effendy, Mr. Wei Wang, Mr. Junjie Chen, and Ms. Shruti Tandon from National University of Singapore; Dr. Keng-Hwee Chiam, Dr. Yukai Zeng, and Dr. Ai Kia Yip from Bioinformatics Institute, Singapore.

Finally, I would like to thank my family for their support. Especially, I want to thank my parents for their love and support. I grew up in a small city in Shandong, China and it was their vision and unique education that enabled me to study in Singapore, Germany, and the United States. I would like to thank my wife Wenxuan for her unconditional love, and my cat Xiao Mao Mao (little kitten in English) who has decided to devote her lifetime to love me, respect me, and sometimes bite or scratch me (out of goodwill, I believe).

ABSTRACT

Phenotypic heterogeneity in populations of isogenic bacterial cells includes variations in metabolic rates and responses to antibiotic treatment. In particular, sub-populations of "persister" cells exhibit increased antibiotic tolerance. Understanding the mechanisms that underlie bacterial persistence would constitute an important step toward preventing and treating chronic infections. On the other hand, bacteria often have multiple molecular mechanisms to adapt to fluctuating environments. Understanding these mechanisms, and their redundancy, requires examinations in depth at the molecular level. This thesis describes a time- and cell state-selective proteome-labeling approach that enables researchers to investigate heterogeneous systems and molecular redundancy.

In Chapter 1, we review the concept of bacterial persistence. The definition of bacterial persistence is introduced. Both the differences and connections between bacterial persistence and resistance are covered. In particular, we discuss research related to *Pseudomonas aeruginosa* (*P. aeruginosa*), an important opportunistic pathogen found in many cystic fibrosis patients. State-of-the-art technologies to investigate bacterial persistence are discussed, and we conclude that advanced tools are needed to advance research on bacterial persistence further.

In Chapter 2, we highlight the concept of bioorthogonal noncanonical amino acid tagging (BONCAT). BONCAT is a powerful tool developed in the Tirrell and Schuman laboratories allowing the incorporation of noncanonical amino acids (ncAA) into newly-synthesized proteins. We review established strategies for proteomics, especially cell-selective proteomics. We introduce the concept and mechanism of BONCAT and address the advantages of BONCAT in the investigation of phenotypic heterogeneity and bacterial persistence.

In Chapter 3, we describe our work using BONCAT for understanding bacterial persistence. In particular, we investigated the process of persister resuscitation, as it is closely related to the reoccurrence of *P. aeruginosa* infections. The characteristics

of the heterogeneity of persister cells during persister awakening were examined by survival assays and by ScanLag, an automated colony-based system allowing high-throughput acquisition of time-lapse images, quantification, and analysis of growth of bacterial colonies. Two BONCAT methods were developed in the *P. aeruginosa* strain PA14 by treating cells either with L-azidohomoalanine (Aha), which avoids extensive usage of antibiotic markers and allows direct integration with PA14 transposon insertion library, or with L-azidonorleucine (Anl), which has the advantage of specificity, as well as direct application in nutrition-rich medium. Through BONCAT enrichment experiments, we found proteins involved in the biosynthesis of pyochelin, a secondary siderophore involved in bacterial iron acquisition, were up-regulated in the regrowth phase. We further explored whether the up-regulation was a result of the modulation of HigB-HigA toxin-antitoxin system.

In Chapter 4, we describe our work for understanding molecular redundancy. The chapter follows up on our observation of up-regulation of pyochelin-related proteins during persister regrowth. We discuss the hypothesis that pyochelin confers a growth advantage in persister cells subject to carbon-limited conditions. In addition, we discuss the potential role of Fur, a ferric uptake regulator, in bacterial persistence.

TABLE OF CONTENTS

Acknowledgements……...iii
Abstract …….v
Table of Contents…….vii
List of Figures and Tables…….....xi
Nomenclature …….xiv

Chapter I: Bacterial Persistence..... 1
1.1. Introduction 1
1.2. Bacterial persistence and bacterial resistance 2
1.3. General understanding of bacterial persistence 2
1.4. Bacterial persistence in *Pseudomonas aeruginosa* 3
1.5. State-of-the-art technologies related to persistence studies..... 4
1.6. Conclusion..... 6
1.7. List of figures 7
1.8. References 8

Chapter II: Bioorthogonal Noncanonical Amino Acid Tagging 13
2.1. Proteomics as a tool..... 13
2.2. Bioorthogonal noncanonical amino acid tagging (BONCAT)..... 14
2.3. BONCAT for understanding phenotypic heterogeneity..... 15
2.4. Conclusion..... 15
2.5. List of figures 16
2.6. References 17

Chapter III: BONCAT for Understanding Persister Resuscitation..... 20
3.1. Abstract..... 20
3.2. Introduction 21

3.3. Results 24
3.3.1. Recovered *P. aeruginosa* persister cells had similar killing kinetics as untreated cells 24
3.3.2. The regrowth of *P. aeruginosa* persister cells in planktonic culture cannot occur without dilution of cell debris after antibiotic treatment 24
3.3.3. ScanLag analysis showed that the persister population exhibited a heterogeneous distribution in terms of appearance time and colony growth rate 25
3.3.4. Demonstration of labeling with BONCAT in the comparison of recovered persisters and untreated cells in stationary phase 26
3.3.5. The persister resuscitation period is defined as the total regrowth period prior to the beginning of stationary phase 27
3.3.6. Pyochelin-related proteins were found to be up-regulated during persister resuscitation 28
3.3.7. No single gene in the pyochelin biosynthesis pathway altered regrowth behavior 31
3.3.8. A PA14 *higA*::Tn mutant was examined via ScanLag and the regrowth pattern was shown to fit a negative exponential distribution 32
3.3.9. HigA-binding sequence was not found to be directly or indirectly relevant to pyochelin-related genes in PA14 genome 33
3.3.10. BONCAT with Aha as ncAA was established and examined to label PA14 WT and transposon insertion mutant strains 35
3.3.11. Pyochelin-related proteins were also found to be up-regulated during *higA*::Tn persister resuscitation 36
3.4. Discussion 38
3.5. Materials and methods 42
3.5.1. Strains and growth conditions 42
3.5.2. Antibiotic treatment 42
3.5.3. Growth curve characterization and determination of regrowth conditions 43

3.5.4. ScanLag 43
3.5.5. BONCAT labeling visualization and enrichment experiments 44
3.5.6. LC-MS/MS 46
3.5.7. Proteomic data analysis 46
3.5.8. Whole genome searching 47
3.6. Acknowledgements 48
3.7. List of figures and tables 49
3.8. References 57
3.9. Supplementary information 71

Chapter IV: Pyochelin Confers a Fitness Advantage in Bacterial Persister Cells Under Carbon-Limited Conditions 92
4.1. Abstract 92
4.2. Introduction 93
4.3. Results 96
4.3.1. Differences in the abundances of pyoverdine biosynthesis proteins were not observed when we compared the regrowth of persisters and untreated cells 96
4.3.2. Point mutations in PA14 *fur* increase bacterial survival rates under antibiotic treatment 96
4.3.3. Bacteria relying on the pyochelin biosynthesis pathway had a growth advantage under low energy conditions 97
4.4. Discussion 101
4.5. Materials and methods 103
4.5.1. Strains and growth conditions 103
4.5.2. Antibiotic treatment 103
4.5.3. Survival rates characterization 104
4.5.4. Absorbance 104
4.5.5. Statistical analysis 104
4.6. Acknowledgements 105

4.7. List of figures..... 106
4.8. References 109
4.9. Supplementary information..... 117

LIST OF FIGURES AND TABLES

Chapter I: Bacterial Persistence

Figure 1. Drug persistence, recurrent infection, and complexity of persister cells 7

Chapter II: Bioorthogonal Noncanonical Amino Acid Tagging

Figure 2. Mechanism of BONCAT and two labeling methods used in this study 16

Chapter III: BONCAT for Understanding Persister Resuscitation

Figure 3.1. Characteristics of persister cells 49

Figure 3.2. Comparison between persister cells and untreated cells on LB agar plates 50

Figure 3.3. Integrated total proteins identified in the regrowth of persister and untreated cells with Anl approach 51

Figure 3.4. Analysis of appearance times of WT and *higA*::Tn 53

Figure 3.5. Integrated total proteins identified in the regrowth of persister and untreated cells with Aha approach 54

Figure 3.6. Integrated total proteins identified in the regrowth of *higA*::Tn persister and untreated cells with Aha approach..... 55

Table 3.1. Comparison of fold changes involved in various studies in persister formation and persister regrowth 56

Figure 3.S1. Gel visualization of Anl-labeled proteins in each condition. 71

Figure 3.S2. Proteomic comparison between recovered persisters and untreated cells 72

Figure 3.S3. Proteomic comparison at the early exponential phase..... 74

Figure 3.S4. Labeling strategies for cumulatively temporal comparison between untreated cells and persister cells 75

Figure 3.S5. In-gel visualization of Anl-labeled samples..... 76
Figure 3.S6. Effect of pyochelin-related genes on survival rates..... 77
Figure 3.S7. Violin diagrams of the appearance times of the transposon insertion mutants of pyochelin-related genes with ScanLag 78
Figure 3.S8. HigA was located in the identified proteome of BONCAT enrichment results..... 79
Figure 3.S9. In-gel visualization of Aha-labeled samples..... 80
Figure 3.S10. Gel visualization of Aha-labeled proteins in three biological replicates of the samples in sections 3.3.10 and 3.3.11 81
Figure 3.S11. Comparison of proteins identified in the BONCAT enrichment experiments..... 83
Table 3.S1. Table of proteins significantly up- or down-regulated in PA14 NLL-MetRS mutant persisters versus untreated cells..... 84
Table 3.S2. List of all PA14 genes with HigA or HigA-like palindrome (5′-TTAAC GTTAA-3′) in the promoter region identified by whole genome searching..... 91

Chapter IV: Pyochelin Confers a Fitness Advantage in Bacterial Persister Cells Under Carbon-Limited Conditions

Figure 4.1. Pyochelin and pyoverdine..... 106
Figure 4.2. *fur* mutants and Fur binding sites 107
Figure 4.3. Regrowth of persisters of each strain under energy-limited conditions 108
Figure 4.S1. Fold changes involved in the pyoverdine biosynthesis pathway 117
Figure 4.S2. Absorbance at OD 500 of each strain in carbon-limited medium with pyruvate concentrations ranging from 1 mM to 40 mM..... 118
Figure 4.S3. Absorbance at OD 500 of the early-stage of growth for untreated cells in carbon-limited medium with pyruvate concentrations ranging from 1 mM to 40 mM..... 119

Figure 4.S4. Alignment of the protein sequences of PA14 *vfr* and *E. coli* BL21 *crp* 120

NOMENCLATURE

aaRS. Aminoacyl tRNA synthetase

ACN. Acetonitrile

Aha. L-azidohomoalanine

Anl. L-azidonorleucine

BCA. Bicinchoninic acid

BONCAT. Bioorthogonal noncanonical amino acid tagging

CF. Cystic fibrosis

CFU. Colony forming unit

DBCO. Aza-dibenzocyclooctyne

DTT. Dithiothreitol

E. coli. *Escherichia coli*

HiPPR. High Protein and Peptide Recovery

Hpg. Homopropargylglycine

HPLC. High performance liquid chromatography

iBAQ. Intensity based absolute quantification

LB. Luria-Bertani broth

LC-MS. Liquid chromatography-tandem-mass spectrometry

LFQ. Label-free quantitation

Limma. Linear models for microarray data

MEME. Multiple Em for Motif Elicitation

Met. Methionine

MetRS. Methionine tRNA synthetase

MIC. Minimum inhibitory concentration

MS. Mass spectrometry

ncAA. Noncanonical amino acids

P. aeruginosa. *Pseudomonas aeruginosa*

PBS. Phosphate-buffered saline

PCA. Principal component analysis

Pch. Pyochelin

ppGpp. Guanosine tetraphosphate

PseudoCAP. *Pseudomonas* Community Annotation Project

pSILAC. Pulsed stable isotope labeling using amino acids in cell culture

Pvd. Pyoverdine

SDE. Standard deviation

SDS. Sodium dodecyl sulfate

SDS-PAGE. Sodium dodecyl sulfate–polyacrylamide gel electrophoresis

SILAC. Stable isotope labeling using amino acids in cell culture

TA. Toxin-antitoxin

TAMRA. Tetramethylrhodamine

THPTA. Tris(3-hydroxypropyltriazolylmethyl)amine

TMT. Tandem mass tags

WT. Wild-type

Chapter 1

BACTERIAL PERSISTENCE

1.1. Introduction

There is much public attention directed toward misuse of antibiotics due to increasing reports of antibiotic treatment failure (Barbosa & Levy, 2000). Previously, this was thought to be caused by bacterial resistance, which was initially reported shortly after the early clinical usage of antibiotics, but there have also been additional unsuccessful clinical treatments where resistance was not observed (Abraham & Chain, 1940; Maisonneuve & Gerdes, 2014). One possible explanation is bacterial persistence, a physiological state in which a small fraction of bacteria enter a dormant state, allowing for survival after antibiotic treatment. It has also been observed in laboratories that antibiotic treatment of a planktonic bacterial culture leads to a biphasic killing pattern as a result of bacterial persistence (Figure 1A). The bacterial subpopulation exhibiting higher tolerance, but not resistance, to antibiotics is denoted as persister cells (Bigger, 1944).

Bacterial persistence differs fundamentally from bacterial resistance. Unlike resistant populations, persister populations do not proliferate in the presence of antibiotics and will resume growth only after the external bactericidal agent is removed (Cohen et al., 2013). Furthermore, as revealed by killing kinetics, the remaining population after treatment is as sensitive to antibiotics as the initial population (Figure 1A, B) (Keren, Kaldalu, et al., 2004). This evidence indicates that bacterial persistence is a non-heritable phenotype, while resistant mutants exhibit stable, heritable antibiotic insensitivity (Fauvart et al., 2011). In general, persister cells are believed to be genetically identical to susceptible cells, but exhibit a distinct phenotype in terms of their response to antibiotics (Balaban et al., 2004).

1.2. Bacterial persistence and bacterial resistance

Bacterial persistence may be an important factor in the emergence of antibiotic resistance. The mechanism of development of drug resistance remains unclear. Studies have shown that specific mutations toward resistance are typically associated with recurrent persistent isolates; however, evidence of a direct link between bacterial persistence and resistance has yet to be discovered (Hayden et al., 2012). In *vitro* experiments have also revealed a number of altruistic resistant organisms might induce susceptible cells to enter a persister-like state through indole secretion (Lee et al., 2010; Vega et al., 2012). Combined with all these results, a potential link between persistence and resistance might exist despite of the great complexity.

1.3. General understanding of bacterial persistence

Although the formation of persister cells is considered as a result of phenotypic heterogeneity in isogenic populations, one mutation, which produced a higher frequency of persister cells of *Escherichia coli* (*E. coli*), was mapped to *hipA*, a gene that encodes for the toxin of a toxin-antitoxin (TA) module (Balaban et al., 2004; Lewis, 2007; Moyed & Bertrand, 1983). Following the work of Moyed and Bertrand, the contribution of TA loci to cell dormancy, which is considered to play an important role in persistence, has been highlighted (Dörr et al., 2010; Moyed & Bertrand, 1983; Verstraeten et al., 2016). A TA locus consists of two parts: a toxin that inhibits cell metabolism and induces a dormancy-like state, and an antitoxin that reacts with the toxin and nullifies the toxicity (Pu et al., 2016). A hypothesis for this effect on the persistence state is that overproduction of toxin inhibits cell growth and induces a dormant state where lethal effects of the antibiotic molecule have been compromised due to the extremely slow metabolism and proliferation at this state (Maisonneuve & Gerdes, 2014; Pu et al., 2016).

1.4. Bacterial persistence in *Pseudomonas aeruginosa*

Persister cells have been observed in a wide range of organisms, including bacteria, fungi, parasites, and even cancerous human cell populations. In addition, certain bacteria have been reported to be multidrug-tolerant persisters; however, little is known about the persister phenotype (Maisonneuve & Gerdes, 2014; Möker et al., 2010). Bacterial persistence is also increasingly the major cause of recurrent chronic infectious disease; for example, cystic fibrosis (CF), a common fatal hereditary diseases (Hansen et al., 2008). Several studies have also showed that *Pseudomonas aeruginosa* (*P. aeruginosa*), a common pathogen found in CF patients, is extremely tolerant, but rarely resistant, to antibiotics (Burns et al., 1999; Gibson et al., 2003; Gilligan, 2006; Lyczak et al., 2002; Mulcahy et al., 2010). The leading cause of death (85-90%) of CF patients is chronic bacterial infection, which interrupts lung function and causes respiratory failure (Lyczak et al., 2002). Evidence suggests the resuscitation of persister cells may contribute to chronic infection in cystic fibrosis. To test the validity of this assumption, Mulcahy and co-workers studied a group of 14 CF patients and compared their early *P. aeruginosa* isolates to those from late clinical stages (Mulcahy et al., 2010). Ten of the 14 late isolates exhibited a *hip* phenotype, which is absent in the early isolates. This finding suggested, for the first time, a direct link between the presence of persister cells and the clinical manifestation of a chronic infection disease.

Understanding the mechanisms of persister formation and recurrent infection may enhance clinical strategies for preventing and treating chronic diseases. Previous studies have identified various global regulators in persister formation; for example, TA modules might be activated through the alarmone guanosine tetraphosphate (ppGpp) pathway; nevertheless, our understanding of bacterial persistence remains limited (Hansen et al., 2008; Maisonneuve & Gerdes, 2014). Future studies will require technology that can accurately characterize persister metabolism and cellular activities; this is challenging because persister cells are only a small percentage of

the whole population, and are in a dormancy state where they are metabolically inactive.

P. aeruginosa is extremely tolerant, but rarely resistant, and is recalcitrant to both the host immune system and to antibiotic therapies, which suggests *P. aeruginosa* exhibits persistence (Babin et al., 2017; Fauvart et al., 2011; Gilligan, 2006; Möker et al., 2010; Mulcahy et al., 2010). Much effort has been made to understand the mechanisms controlling its intracellular genetic and proteomic activities (Potvin et al., 2008; Wurtzel et al., 2012). Several factors, such as RpoS, a stationary phase sigma factor, have been reported to contribute to persistence; however, there is much work still to be done to understand *P. aeruginosa* persistence (Cohen et al., 2013; Kayama et al., 2009; Murakami et al., 2005). This is, in part, due to the fact that there are limited tools suitable for analysis of cellular heterogeneity (Verstraeten et al., 2016).

1.5. State-of-the-art technologies related to persistence studies

Bacterial persistence is defined as a transient phenotype. Another challenge is the low abundance of the persister subpopulation, which is typically less than 1% (Wood et al., 2013). In addition, persister cells entering dormancy state have low metabolic activities. Therefore, it is hard to use traditional tools of molecular biology to identify differences between persistent and susceptible cells.

Many tools have been developed to study bacterial persistence at the single-cell level. Direct evidence for the preexistence of naturally occurring persistent bacteria was provided by a microfluidic device in 2004 (Balaban et al., 2004). Balaban *et al.* reported that natural persister cells remain dormant during antibiotic treatment and the phenotype switched when the antibiotic pressure was removed. The use of microfluidic devices allowed direct examination of persister cells at the single-cell level and created convenient experimental conditions for observing the phenotypic

switch. In addition, a colony-based assay called ScanLag was developed to quantify phenotypic characteristics of persister cells including appearance times and colony expansion rates (Rotem et al., 2010). Through ScanLag, Rotem *et al.* demonstrated that induction of persistence is toxin-dependent. However, these methods have certain limitations. Due to the low abundance of persister cells, tools targeting single-cell experiments including microfluidic devices or microscopy can only access a limited number of cells. In *vitro* colony-based assays reflect collective growth behaviors, but the readouts, including appearance times or colony growth rates, may not be related to the persistence level.

To overcome these drawbacks, experimental techniques like flow cytometry have been used to isolate persister cells from bacterial populations on a much larger scale (Jõers et al., 2010). For example, Jõers *et al*. used flow cytometry to investigate persister awakening and found many factors affecting the kinetics of awakening. However, these methods may affect context-dependent behavior (Orman & Brynildsen, 2013) and lack temporal resolution.

More recently, transcriptomic and proteomic tools have provided insights into the behavior and metabolism of persister cells (Rowe et al., 2016). Various attempts were made to identify persister-specific information, using RNAseq (Alkasir et al., 2018), DNA microarrays (Keren, Shah, et al., 2004; Shah et al., 2006), and different proteomic approaches and methods (Tsakou et al., 2020). These results presented unbiased information about bacterial persistence and advanced our general understanding of phenotypic heterogeneity. However, these omics approaches are generally applied to the entire population, and average over the differences that arise from cell-to-cell heterogeneity (Babin et al., 2017).

1.6. Conclusion

In conclusion, understanding the mechanisms that underlie bacterial persistence would constitute an important step toward preventing and treating chronic infections. There have been extensive studies of bacterial persistence but our understanding of the phenomenon remains limited. It is challenging to study bacterial persistence not only because of the complexity of phenotypic heterogeneity and the mechanisms that drive the formation and resuscitation of persister subpopulations, but also because of a lack of experimental methods that can target the metabolism of the persister subpopulation. This thesis describes one such method.

1.7. List of figures

Figure 1. Drug persistence, recurrent infection, and complexity of persister cells. (A) Schematic model of killing and persistence kinetics during antibiotic treatment. Introduction of antibiotic kills the majority of the population, but a small fraction of the bacteria survive, though not growing ("dormancy state"). Persister cells in dormancy state recover and resume growth when the external antibiotic pressure is removed. (B) Schematic diagrams of three phases during recurrent infection: (I) bacterial population contains a mixture of phenotypic variants. Some cells may pre-exist in the dormancy state (shown in green), while a majority of the population are metabolically active (shown in brown); (II) during antibiotic treatment, a majority of cells are killed, and some cells are induced into dormancy state as a strategy to survive the treatment; (III) when the antibiotic pressure is removed, these cells switch their phenotypic state and resume growth and division.

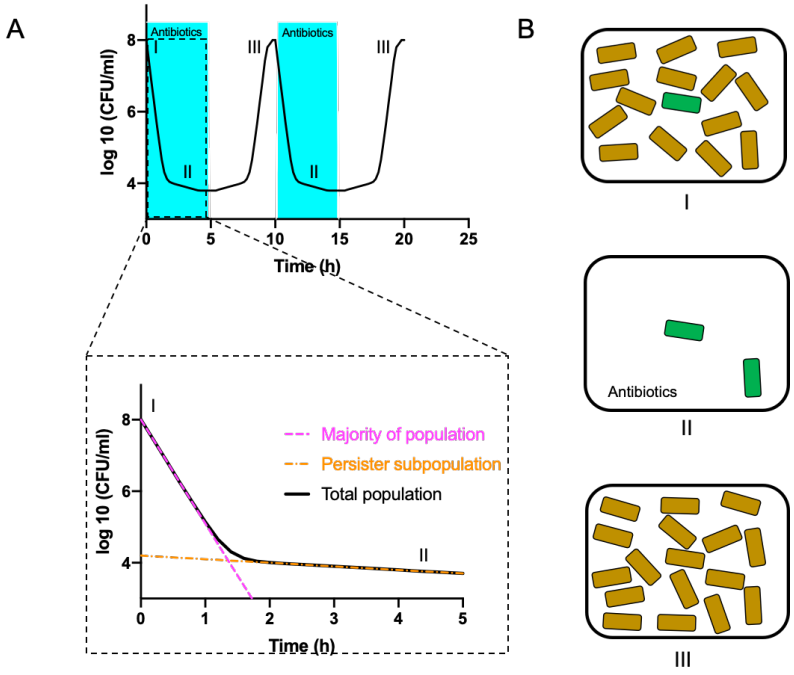

1.8. References

Abraham, E. P., & Chain, E. (1940). An Enzyme from Bacteria Able to Destroy Penicillin. *Nature*, *146*(3713), 837–837. https://doi.org/10.1038/146837a0

Alkasir, R., Ma, Y., Liu, F., Li, J., Lv, N., Xue, Y., Hu, Y., & Zhu, B. (2018). Characterization and Transcriptome Analysis of *Acinetobacter baumannii* Persister Cells. *Microbial Drug Resistance*, *24*(10), 1466–1474. https://doi.org/10.1089/mdr.2017.0341

Babin, B. M., Atangcho, L., van Eldijk, M. B., Sweredoski, M. J., Moradian, A., Hess, S., Tolker-Nielsen, T., Newman, D. K., & Tirrell, D. A. (2017). Selective Proteomic Analysis of Antibiotic-Tolerant Cellular Subpopulations in *Pseudomonas aeruginosa* Biofilms. *MBio*, *8*(5). https://doi.org/10.1128/mBio.01593-17

Balaban, N. Q., Merrin, J., Chait, R., Kowalik, L., & Leibler, S. (2004). Bacterial Persistence as a Phenotypic Switch. *Science*, *305*(5690), 1622–1625. https://doi.org/10.1126/science.1099390

Barbosa, T. M., & Levy, S. B. (2000). The Impact of Antibiotic Use on Resistance Development and Persistence. *Drug Resistance Updates*, *3*(5), 303–311. https://doi.org/10.1054/drup.2000.0167

Bigger, JosephW. (1944). Treatment of Staphylococcal Infections with Penicillin by Intermittent Sterilisation. *The Lancet*, *244*(6320), 497–500. https://doi.org/10.1016/S0140-6736(00)74210-3

Burns, J. L., Van Dalfsen, J. M., Shawar, R. M., Otto, K. L., Garber, R. L., Quan, J. M., Montgomery, A. B., Albers, G. M., Ramsey, B. W., & Smith, A. L. (1999). Effect of Chronic Intermittent Administration of Inhaled Tobramycin on Respiratory Microbial Flora in Patients with Cystic Fibrosis. *The Journal of Infectious Diseases*, *179*(5), 1190–1196. https://doi.org/10.1086/314727

Cohen, N. R., Lobritz, M. A., & Collins, J. J. (2013). Microbial Persistence and the Road to Drug Resistance. *Cell Host & Microbe*, *13*(6), 632–642. https://doi.org/10.1016/j.chom.2013.05.009

Dörr, T., Vulić, M., & Lewis, K. (2010). Ciprofloxacin Causes Persister Formation by Inducing the TisB Toxin in *Escherichia coli*. *PLoS Biology*, *8*(2), e1000317. https://doi.org/10.1371/journal.pbio.1000317

Fauvart, M., de Groote, V. N., & Michiels, J. (2011). Role of Persister Cells in Chronic Infections: Clinical Relevance and Perspectives on Anti-Persister Therapies. *Journal of Medical Microbiology*, *60*(6), 699–709. https://doi.org/10.1099/jmm.0.030932-0

Gibson, R. L., Burns, J. L., & Ramsey, B. W. (2003). Pathophysiology and Management of Pulmonary Infections in Cystic Fibrosis. *American Journal of Respiratory and Critical Care Medicine*, *168*(8), 918–951. https://doi.org/10.1164/rccm.200304-505SO

Gilligan, P. H. (2006). Is There Value in Susceptibility Testing of *Pseudomonas aeruginosa* Causing Chronic Infection in Patients with Cystic Fibrosis? *Expert Review of Anti-Infective Therapy*, *4*(5), 711–715. https://doi.org/10.1586/14787210.4.5.711

Hansen, S., Lewis, K., & Vulić, M. (2008). Role of Global Regulators and Nucleotide Metabolism in Antibiotic Tolerance in *Escherichia coli*. *Antimicrobial Agents and Chemotherapy*, *52*(8), 2718–2726. https://doi.org/10.1128/AAC.00144-08

Hayden, H. S., Lim, R., Brittnacher, M. J., Sims, E. H., Ramage, E. R., Fong, C., Wu, Z., Crist, E., Chang, J., Zhou, Y., Radey, M., Rohmer, L., Haugen, E., Gillett, W., Wuthiekanun, V., Peacock, S. J., Kaul, R., Miller, S. I., Manoil, C., & Jacobs, M. A. (2012). Evolution of *Burkholderia pseudomallei* in Recurrent Melioidosis. *PLoS ONE*, *7*(5), e36507. https://doi.org/10.1371/journal.pone.0036507

Jõers, A., Kaldalu, N., & Tenson, T. (2010). The Frequency of Persisters in *Escherichia coli* Reflects the Kinetics of Awakening from Dormancy. *Journal of Bacteriology*, *192*(13), 3379–3384. https://doi.org/10.1128/JB.00056-10

Kayama, S., Murakami, K., Ono, T., Ushimaru, M., Yamamoto, A., Hirota, K., & Miyake, Y. (2009). The Role of *rpoS* Gene and Quorum-Sensing System in

Ofloxacin Tolerance in *Pseudomonas aeruginosa*. *FEMS Microbiology Letters*, *298*(2), 184–192. https://doi.org/10.1111/j.1574-6968.2009.01717.x

Keren, I., Kaldalu, N., Spoering, A., Wang, Y., & Lewis, K. (2004). Persister Cells and Tolerance to Antimicrobials. *FEMS Microbiology Letters*, *230*(1), 13–18. https://doi.org/10.1016/S0378-1097(03)00856-5

Keren, I., Shah, D., Spoering, A., Kaldalu, N., & Lewis, K. (2004). Specialized Persister Cells and the Mechanism of Multidrug Tolerance in *Escherichia coli*. *Journal of Bacteriology*, *186*(24), 8172–8180. https://doi.org/10.1128/JB.186.24.8172-8180.2004

Lee, H. H., Molla, M. N., Cantor, C. R., & Collins, J. J. (2010). Bacterial Charity Work Leads to Population-Wide Resistance. *Nature*, *467*(7311), 82–85. https://doi.org/10.1038/nature09354

Lewis, K. (2007). Persister Cells, Dormancy and Infectious Disease. *Nature Reviews Microbiology*, *5*(1), 48–56. https://doi.org/10.1038/nrmicro1557

Lyczak, J. B., Cannon, C. L., & Pier, G. B. (2002). Lung Infections Associated with Cystic Fibrosis. *Clinical Microbiology Reviews*, *15*(2), 194–222. https://doi.org/10.1128/CMR.15.2.194-222.2002

Maisonneuve, E., & Gerdes, K. (2014). Molecular Mechanisms Underlying Bacterial Persisters. *Cell*, *157*(3), 539–548. https://doi.org/10.1016/j.cell.2014.02.050

Möker, N., Dean, C. R., & Tao, J. (2010). *Pseudomonas aeruginosa* Increases Formation of Multidrug-Tolerant Persister Cells in Response to Quorum-Sensing Signaling Molecules. *Journal of Bacteriology*, *192*(7), 1946–1955. https://doi.org/10.1128/JB.01231-09

Moyed, H. S., & Bertrand, K. P. (1983). *hipA*, a Newly Recognized Gene of *Escherichia coli* K-12 that Affects Frequency of Persistence after Inhibition of Murein Synthesis. *Journal of Bacteriology*, *155*(2), 768–775. https://doi.org/10.1128/jb.155.2.768-775.1983

Mulcahy, L. R., Burns, J. L., Lory, S., & Lewis, K. (2010). Emergence of *Pseudomonas aeruginosa* Strains Producing High Levels of Persister Cells in

Patients with Cystic Fibrosis. *Journal of Bacteriology*, *192*(23), 6191–6199. https://doi.org/10.1128/JB.01651-09

Murakami, K., Ono, T., Viducic, D., Kayama, S., Mori, M., Hirota, K., Nemoto, K., & Miyake, Y. (2005). Role for *rpoS* Gene of *Pseudomonas aeruginosa* in Antibiotic Tolerance. *FEMS Microbiology Letters*, *242*(1), 161–167. https://doi.org/10.1016/j.femsle.2004.11.005

Orman, M. A., & Brynildsen, M. P. (2013). Establishment of a Method To Rapidly Assay Bacterial Persister Metabolism. *Antimicrobial Agents and Chemotherapy*, *57*(9), 4398–4409. https://doi.org/10.1128/AAC.00372-13

Potvin, E., Sanschagrin, F., & Levesque, R. C. (2008). Sigma Factors in *Pseudomonas aeruginosa*. *FEMS Microbiology Reviews*, *32*(1), 38–55. https://doi.org/10.1111/j.1574-6976.2007.00092.x

Pu, Y., Zhao, Z., Li, Y., Zou, J., Ma, Q., Zhao, Y., Ke, Y., Zhu, Y., Chen, H., Baker, M. A. B., Ge, H., Sun, Y., Xie, X. S., & Bai, F. (2016). Enhanced Efflux Activity Facilitates Drug Tolerance in Dormant Bacterial Cells. *Molecular Cell*, *62*(2), 284–294. https://doi.org/10.1016/j.molcel.2016.03.035

Rotem, E., Loinger, A., Ronin, I., Levin-Reisman, I., Gabay, C., Shoresh, N., Biham, O., & Balaban, N. Q. (2010). Regulation of Phenotypic Variability by a Threshold-Based Mechanism Underlies Bacterial Persistence. *Proceedings of the National Academy of Sciences*, *107*(28), 12541–12546. https://doi.org/10.1073/pnas.1004333107

Rowe, S. E., Conlon, B. P., Keren, I., & Lewis, K. (2016). *Persisters: Methods for Isolation and Identifying Contributing Factors—A Review* (pp. 17–28). https://doi.org/10.1007/978-1-4939-2854-5_2

Shah, D., Zhang, Z., Khodursky, A. B., Kaldalu, N., Kurg, K., & Lewis, K. (2006). Persisters: A Distinct Physiological State of *E. coli*. *BMC Microbiology*, *6*(1), 53. https://doi.org/10.1186/1471-2180-6-53

Tsakou, F., Jersie-Christensen, R., Jenssen, H., & Mojsoska, B. (2020). The Role of Proteomics in Bacterial Response to Antibiotics. *Pharmaceuticals*, *13*(9), 1–27. https://doi.org/10.3390/ph13090214

Vega, N. M., Allison, K. R., Khalil, A. S., & Collins, J. J. (2012). Signaling-Mediated Bacterial Persister Formation. *Nature Chemical Biology*, *8*(5), 431–433. https://doi.org/10.1038/nchembio.915

Verstraeten, N., Knapen, W., Fauvart, M., & Michiels, J. (2016). *A Historical Perspective on Bacterial Persistence* (pp. 3–13). https://doi.org/10.1007/978-1-4939-2854-5_1

Wood, T. K., Knabel, S. J., & Kwan, B. W. (2013). Bacterial Persister Cell Formation and Dormancy. *Applied and Environmental Microbiology*, *79*(23), 7116–7121. https://doi.org/10.1128/AEM.02636-13

Wurtzel, O., Yoder-Himes, D. R., Han, K., Dandekar, A. A., Edelheit, S., Greenberg, E. P., Sorek, R., & Lory, S. (2012). The Single-Nucleotide Resolution Transcriptome of *Pseudomonas aeruginosa* Grown in Body Temperature. *PLoS Pathogens*, *8*(9), e1002945. https://doi.org/10.1371/journal.ppat.1002945

Chapter 2

BIOORTHOGONAL NONCANONICAL AMINO ACID TAGGING

2.1. Proteomics as a tool

With the advancement of experimental instruments and computational software, researchers now have various options to acquire transcriptomic data, which have provided deep insight into cellular processes and enabled discovery of antibacterial strategies (Domínguez et al., 2017). Transcriptomic tools like DNA microarrays and RNAseq yield measurements of mRNA abundances, and are used frequently in these scenarios. However, measurements and quantification based on the transcriptome are usually not direct measures of cellular activity. For example, in the case of a toxin-antitoxin (TA) systems, the TA modules often modulate protein expression post-transcriptionally (Yamaguchi et al., 2011), so it is likely that information is missing from the transcriptomic data.

Proteomic approaches by mass spectrometry (MS) have drawn attention with the establishment of bioinformatic approaches and the development of full genome sequencing techniques (Tsakou et al., 2020). But the results of conventional proteomic approaches, in which information is acquired through mass spectrometry on whole cell lysates (Macek et al., 2019) can be compromised if the proteins of interest are low in abundance. In particular, it is challenging to quantify transcriptional activity when the cells are not actively dividing (Bergkessel, 2021).

To investigate proteins in low abundance, an enrichment step is often required (Tsakou et al., 2020). Established methods for enrichment and identification of these proteins often involve labeling by modifications on the proteins of interest (Macek et

al., 2019), including metabolic labeling, for example, using stable isotope labeling using amino acids in cell culture (SILAC) (Ong et al., 2002) and chemical labeling, for example, using tandem mass tags (TMT) (Thompson et al., 2003). Recent techniques include pulsed SILAC (pSILAC), which labels only newly-synthesized proteins after injection of amino acid isotopologs (Schwanhäusser et al., 2009).

2.2. Bioorthogonal noncanonical amino acid tagging (BONCAT)

To address the challenges and identify newly-synthesized proteins in low abundance, we introduced a time- and cell state-selective proteome-labeling approach designated bioorthogonal noncanonical amino acid tagging (BONCAT, Figure 2A). The BONCAT method, which was developed in the Tirrell and Schuman laboratories (Dieterich et al., 2006), allows the incorporation of noncanonical amino acids (ncAA) into newly-synthesized proteins through two routes. The first uses ncAAs that are structurally similar to the corresponding canonical amino acid (cAA): for example, azidohomoalanine (Aha, Figure 2B. II) and homopropargylglycine (Hpg) have been used as methionine (Met) analogues (Figure 2B. I), which take the advantage of the promiscuity of the cell's endogenous aminoacyl tRNA synthetase (aaRS) (Figure 2A) (Ngo & Tirrell, 2011). The second route is through engineered mutant aaRSs, which allow the introduction of ncAAs in a cell-specific manner. The mutant synthetase used in the experiments described here has been designated NLL-MetRS (mutations of L13N, Y260L, and H301L in the *E. coli* methionyl-tRNA synthetase), which allows the incorporation of azidonorleucine (Anl) (Figure 2B. III) into cellular proteins (Tanrikulu et al., 2009). The azide side chains of Aha and Anl then enable conjugation reactions to alkyne affinity probes or beads via azide-alkyne cycloaddition, allowing the newly synthesized proteins to be separated from pre-existing proteins (Figure 2C). Newly-synthesized proteins bearing ncAAs can also be conjugated to fluorescent probes *in situ* and visualized by in-gel fluorescence on SDS-PAGE protein gels (Beatty et

al., 2005), or identified and quantified by mass spectrometry (Szychowski et al., 2010).

2.3. BONCAT for understanding phenotypic heterogeneity

Proteomic approaches have been widely applied to study bacterial responses to antibiotics (Pérez-Llarena & Bou, 2016; Sulaiman & Lam, 2019). Many of these studies revealed that the biological processes involved in response to antibiotics are regulated by post-translational modifications, which are further complicated by phenotypic heterogeneity (Germain et al., 2013; Kaspy et al., 2013; Macek et al., 2019; Schumacher et al., 2015; Semanjski et al., 2018; Vang Nielsen et al., 2019).

Previously, BONCAT has been shown to be able to target the subpopulation of *P. aeruginosa* biofilm cells that showed increased antibiotic tolerance (Babin et al., 2017), and proteins synthesized at extremely low growth rates (Babin et al., 2016). These examples illustrated the power of BONCAT as a powerful tool to identify and quantify cellular activity, which can bridge the gap between proteomic analysis and phenotypic heterogeneity and enhance our understanding of the metabolism of bacterial systems.

2.4. Conclusion

Proteomic methods provide powerful tools to investigate the metabolism of microbial systems. In particular, BONCAT, a cell-selective, time-resolved proteomic approach which is able to target distinct phenotypic variants and examine metabolism at low growth rates, offers a promising tool to investigate bacterial persistence, a challenging problem defined by its transient nature, heterogeneous phenotypes, and low metabolic activity.

2.5. List of figures

Figure 2. Mechanism of BONCAT and two labeling methods used in this study. (A) Wild-type aminoacyl-tRNA synthetases (aaRS, shown in blue) charges tRNAs (shown in black) with 20 natural amino acids (shown in yellow). Occasionally, it loads non-canonical amino acids (ncAA, shown in green). Engineered mutant aaRS (shown in purple) can charge tRNAs with selected ncAAs (shown in red). (B) Structures of methionine (I) and ncAAs that have been used for BONCAT. Methionyl-tRNA synthetase (MetRS) can recognize analogues like Aha (II) and load them on tRNA, while Anl (III) requires a mutant MetRS. (C) Gel visualization of ncAA-labeled (top: Aha, bottom: Anl) and unlabeled proteins. In each panel, left: InstantBlue; right: TAMRA labeling. In each gel, Lane 1 contains labeled proteins extracted from cell lysates in stationary phase; lane 2 contains unlabeled proteins extracted from cell lysates.

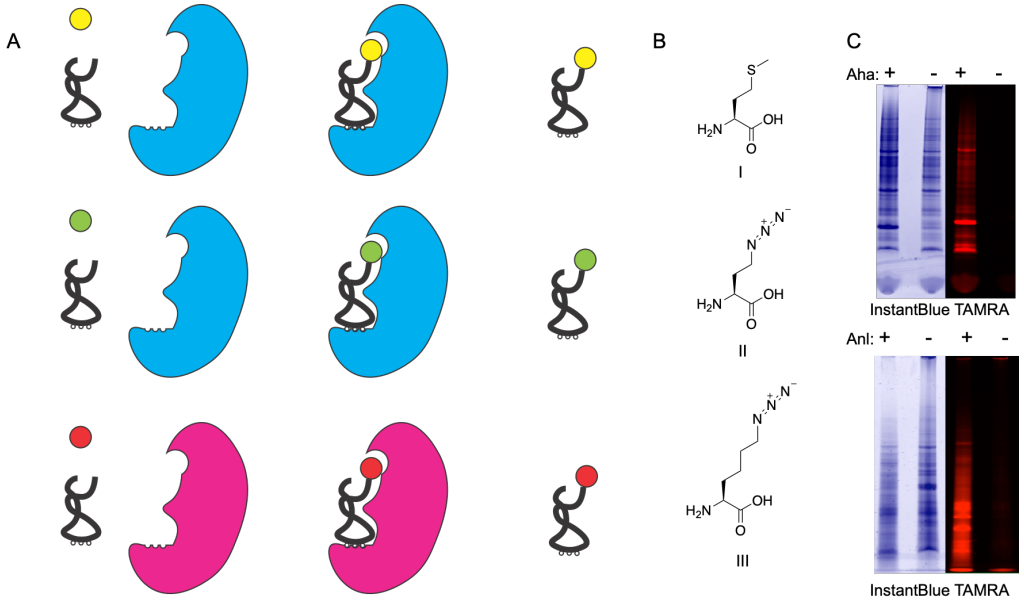

2.6. References

Babin, B. M., Atangcho, L., van Eldijk, M. B., Sweredoski, M. J., Moradian, A., Hess, S., Tolker-Nielsen, T., Newman, D. K., & Tirrell, D. A. (2017). Selective Proteomic Analysis of Antibiotic-Tolerant Cellular Subpopulations in *Pseudomonas aeruginosa* Biofilms. *MBio*, *8*(5). https://doi.org/10.1128/mBio.01593-17

Babin, B. M., Bergkessel, M., Sweredoski, M. J., Moradian, A., Hess, S., Newman, D. K., & Tirrell, D. A. (2016). SutA Is a Bacterial Transcription Factor Expressed during Slow Growth in *Pseudomonas aeruginosa*. *Proceedings of the National Academy of Sciences*, *113*(5). https://doi.org/10.1073/pnas.1514412113

Beatty, K. E., Xie, F., Wang, Q., & Tirrell, D. A. (2005). Selective Dye-Labeling of Newly Synthesized Proteins in Bacterial Cells. *Journal of the American Chemical Society*, *127*(41), 14150–14151. https://doi.org/10.1021/ja054643w

Bergkessel, M. (2021). Bacterial Transcription during Growth Arrest. *Transcription*, *12*(4), 232–249. https://doi.org/10.1080/21541264.2021.1968761

Dieterich, D. C., Link, A. J., Graumann, J., Tirrell, D. A., & Schuman, E. M. (2006). Selective Identification of Newly Synthesized Proteins in Mammalian Cells using Bioorthogonal Noncanonical Amino Acid Tagging (BONCAT). *Proceedings of the National Academy of Sciences*, *103*(25), 9482–9487. https://doi.org/10.1073/pnas.0601637103

Domínguez, Á., Muñoz, E., López, M. C., Cordero, M., Martínez, J. P., & Viñas, M. (2017). Transcriptomics as a Tool to Discover New Antibacterial Targets. In *Biotechnology Letters* (Vol. 39, Issue 6, pp. 819–828). Springer Netherlands. https://doi.org/10.1007/s10529-017-2319-0

Germain, E., Castro-Roa, D., Zenkin, N., & Gerdes, K. (2013). Molecular Mechanism of Bacterial Persistence by HipA. *Molecular Cell*, *52*(2), 248–254. https://doi.org/10.1016/j.molcel.2013.08.045

Kaspy, I., Rotem, E., Weiss, N., Ronin, I., Balaban, N. Q., & Glaser, G. (2013). HipA-Mediated Antibiotic Persistence via Phosphorylation of the Glutamyl-tRNA-Synthetase. *Nature Communications*, *4*(1), 3001. https://doi.org/10.1038/ncomms4001

Macek, B., Forchhammer, K., Hardouin, J., Weber-Ban, E., Grangeasse, C., & Mijakovic, I. (2019). Protein Post-Translational Modifications in Bacteria. In *Nature Reviews Microbiology* (Vol. 17, Issue 11, pp. 651–664). Nature Publishing Group. https://doi.org/10.1038/s41579-019-0243-0

Ngo, J. T., & Tirrell, D. A. (2011). Noncanonical Amino Acids in the Interrogation of Cellular Protein Synthesis. *Accounts of Chemical Research*, *44*(9), 677–685. https://doi.org/10.1021/ar200144y

Ong, S. E., Blagoev, B., Kratchmarova, I., Kristensen, D. B., Steen, H., Pandey, A., & Mann, M. (2002). Stable Isotope Labeling by Amino Acids in Cell Culture, SILAC, as a Simple and Accurate Approach to Expression Proteomics. *Molecular & Cellular Proteomics : MCP*, *1*(5), 376–386. https://doi.org/10.1074/mcp.M200025-MCP200

Pérez-Llarena, F. J., & Bou, G. (2016). Proteomics as a Tool for Studying Bacterial Virulence and Antimicrobial Resistance. In *Frontiers in Microbiology* (Vol. 7, Issue MAR). Frontiers Media S.A. https://doi.org/10.3389/fmicb.2016.00410

Schumacher, M. A., Balani, P., Min, J., Chinnam, N. B., Hansen, S., Vulić, M., Lewis, K., & Brennan, R. G. (2015). HipBA–Promoter Structures Reveal the Basis of Heritable Multidrug Tolerance. *Nature*, *524*(7563), 59–64. https://doi.org/10.1038/nature14662

Schwanhäusser, B., Gossen, M., Dittmar, G., & Selbach, M. (2009). Global Analysis of Cellular Protein Translation by Pulsed SILAC. *Proteomics*, *9*(1), 205–209. https://doi.org/10.1002/pmic.200800275

Semanjski, M., Germain, E., Bratl, K., Kiessling, A., Gerdes, K., & Macek, B. (2018). The Kinases HipA and HipA7 Phosphorylate Different Substrate Pools in *Escherichia coli* to Promote Multidrug Tolerance. *Science Signaling*, *11*(547). https://doi.org/10.1126/scisignal.aat5750

Sulaiman, J. E., & Lam, H. (2019). Application of Proteomics in Studying Bacterial Persistence. *Expert Review of Proteomics*, *16*(3), 227–239. https://doi.org/10.1080/14789450.2019.1575207

Szychowski, J., Mahdavi, A., Hodas, J. J. L., Bagert, J. D., Ngo, J. T., Landgraf, P., Dieterich, D. C., Schuman, E. M., & Tirrell, D. A. (2010). Cleavable Biotin Probes for Labeling of Biomolecules via Azide−Alkyne Cycloaddition. *Journal of the American Chemical Society*, *132*(51), 18351–18360. https://doi.org/10.1021/ja1083909

Tanrikulu, I. C., Schmitt, E., Mechulam, Y., Goddard, W. A., & Tirrell, D. A. (2009). Discovery of *Escherichia coli* Methionyl-tRNA Synthetase Mutants for Efficient Labeling of Proteins with Azidonorleucine in *vivo*. *Proceedings of the National Academy of Sciences*, *106*(36), 15285–15290. https://doi.org/10.1073/pnas.0905735106

Thompson, A., Schäfer, J., Kuhn, K., Kienle, S., Schwarz, J., Schmidt, G., Neumann, T., & Hamon, C. (2003). Tandem Mass Tags: A Novel Quantification Strategy for Comparative Analysis of Complex Protein Mixtures by MS/MS. *Analytical Chemistry*, *75*(8), 1895–1904. https://doi.org/10.1021/ac0262560

Tsakou, F., Jersie-Christensen, R., Jenssen, H., & Mojsoska, B. (2020). The Role of Proteomics in Bacterial Response to Antibiotics. *Pharmaceuticals*, *13*(9), 1–27. https://doi.org/10.3390/ph13090214

Vang Nielsen, S., Turnbull, K. J., Roghanian, M., Bærentsen, R., Semanjski, M., Brodersen, D. E., Macek, B., & Gerdes, K. (2019). Serine-Threonine Kinases Encoded by Split *hipA* Homologs Inhibit Tryptophanyl-tRNA Synthetase. *MBio*, *10*(3). https://doi.org/10.1128/mBio.01138-19

Yamaguchi, Y., Park, J. H., & Inouye, M. (2011). Toxin-Antitoxin Systems in Bacteria and Archaea. *Annual Review of Genetics*, *45*, 61–79. https://doi.org/10.1146/annurev-genet-110410-132412

Chapter 3

BONCAT FOR UNDERSTANDING PERSISTER RESUSCITATION

3.1. Abstract

Phenotypic heterogeneity in populations of isogenic bacterial cells includes variations in metabolic rates and responses to antibiotic treatment. In particular, sub-populations of "persister" cells exhibit increased antibiotic tolerance. Understanding the mechanisms that underlie bacterial persistence would constitute an important step toward preventing and treating chronic infections. There are extensive studies investigating how persisters arise; however, how persister cells resuscitate from the persistence state has received less attention and remains unclear. In this work, we demonstrate the use of Bioorthogonal Noncanonical Amino Acid Tagging (BONCAT) for time- and cell state-selective proteomic analysis of cultures of *P. aeruginosa* that exhibit persistence upon antibiotic treatment. Two methods were developed in the *P. aeruginosa* strain PA14 by treating cells either with L-azidohomoalanine (Aha) or with L-azidonorleucine (Anl). Comparing the proteomic profiles of untreated cells and persister cells showed that proteins involved in the biosynthesis of pyochelin, a secondary siderophore involved in bacterial iron acquisition, were down-regulated in the dormancy phase and up-regulated in the regrowth phase. Previous studies have suggested expression and repression of pyochelin-related genes might be modulated by the HigB-HigA toxin-antitoxin (TA) system. However, through our proteomic analysis, the up-regulation of pyochelin-related proteins was still observed during the resuscitation of persisters of *higA* transposon insertion mutant, which indicated the up-regulation might not be dependent on the HigA antitoxin.

3.2. Introduction

The persistence state of bacteria is generally defined as a transient physiological state in which bacterial cells enter dormancy and remain viable but non-dividing and non-growing. Bacteria persistence was first discovered in 1942 (Hobby et al., 1942). The bacterial subpopulation denoted as persister cells exhibits increased tolerance to antibiotics. It has been shown that increased antibiotic tolerance is not a result of genetic mutations (Chowdhury et al., 2016; Kwan et al., 2015). Persistent bacteria are considered to be phenotypic variants (Balaban et al., 2004), unlike resistant bacteria; persistence is a non-heritable phenotype while resistant mutants exhibit stable and heritable antibiotic insensitivity.

Understanding the mechanisms of persister formation and recurrent infection may enhance clinical strategies for preventing and treating chronic diseases (Goneau et al., 2014; Mulcahy et al., 2010). Currently, there is no agreement on how bacterial persistence arises or how bacteria cells enter the persistence state. Persister cells are generally thought to arise under various environmental stresses, for example, antibiotic or nutritional stress (Maisonneuve & Gerdes, 2014), although direct evidence for the preexistence of naturally occurring persistent bacteria has been obtained in microfluidic studies (Balaban et al., 2004). The predominant theory to explain the mechanism of formation of persistent population is the modulation of toxin-antitoxin (TA) systems (Lewis, 2007). A TA locus consists of two parts: a toxin that inhibits cell metabolism and induces a dormancy-like state, and an antitoxin that reacts with the toxin and nullifies the toxicity (Pu et al., 2016). A hypothesis for this effect on the persistence state is that the overproduction of toxin inhibits cell growth and causes the cell to enter dormancy, where the lethal effects of the antibiotic have been compromised by the extremely slow metabolism and proliferation (Maisonneuve & Gerdes, 2014; Pu et al., 2016). However, the contribution of TA modules to bacterial persistence has been recently challenged by studies that did not find direct evidence for linkage between bacterial persistence and TA systems

(Goormaghtigh et al., 2018; Svenningsen et al., 2019). Therefore, the molecular mechanisms underlying persister formation remain unclear.

Compared to the formation of persister cells, how persister cells resuscitate (switch back to the normal growing state or 'wake up') is even more poorly understood. There is general agreement, however, that persister resuscitation is initiated stochastically (Buerger et al., 2012). In addition, it is commonly observed that antibiotic-induced persisters exhibit longer lag phases once transferred into fresh medium compared to untreated normal cells (Jõers et al., 2010). In line with this observation, various methods were established to investigate whether the duration of the prolonged lag phase would be affected by deletions of certain genes (Fridman et al., 2014; Wilmaerts et al., 2019). In addition, external factors such as nutrients in environmental conditions have been shown to affect persister awakening (Yamasaki et al., 2020).

It is hard to use traditional tools in molecular biology to study the difference between persistent and non-persistent cells. Many platforms have been invented or adapted to study bacterial persistence, for example, microfluidic devices (Balaban et al., 2004), and colony-based methods (Rotem et al., 2010). More recently, transcriptomic and proteomic tools have provided insights into the behavior and metabolism of persister cells (Rowe et al., 2016). These studies have accelerated progress in elucidating the mechanism of persistence. However, very few studies have investigated the mechanisms of persister resuscitation. In order to gain insights into the metabolism of the switching between phenotypic states of persister cells and achieve specific labeling of newly-synthesized proteins during persister resuscitation, we employed a time-selective proteome-labeling method called bioorthogonal noncanonical amino acid tagging (BONCAT, Figure 2A), a method developed in the Tirrell and Schuman laboratories that relies on the incorporation of non-canonical amino acids (ncAAs) into newly-synthesized proteins (Dieterich et al., 2006). The incorporated ncAAs then enable conjugation to different probes,

allowing the newly-synthesized proteins to be distinguished and separated from pre-existing proteins. Identification of newly synthesized proteins allows us to compare the proteomic profiles of persister cells to those of normal cells, and offers insight into the mechanisms that underlie bacterial persistence.

In this study, we examined the switching of phenotypic states of *P. aeruginosa*, a common pathogen found in cystic fibrosis (CF) patients. They are extremely tolerant, but rarely resistant, to antibiotics (Burns et al., 1999; Gibson et al., 2003; Gilligan, 2006; Lyczak et al., 2002; Mulcahy et al., 2010). Research found that the leading cause of death (85-90%) of CF patients is chronic bacterial infection, which continuously interrupts lung function and causes respiratory failures (Lyczak et al., 2002). This evidence suggests the resuscitation of persister cells may contribute to the chronic infection in cystic fibrosis.

Here we demonstrated the heterogenous nature of *P. aeruginosa* that resume growth upon the removal of antibiotics. We further employed BONCAT for proteomic analysis and compared the proteome of persister cells during resuscitation with the proteome of untreated cells to sort out proteins important for persister awakening. Our results, which showed up-regulation of proteins involved in the biosynthesis of pyochelin, are complementary to evidence from other literature. We further explored whether the HigB-HigA TA system could affect the up-regulation of pyochelin-related proteins. We found the up-regulation of pyochelin-related proteins was independent from the modulation of antitoxin HigA.

3.3. Results

3.3.1. Recovered P. aeruginosa persister cells had similar killing kinetics as untreated cells

Wild-type (WT) *P. aeruginosa* PA14 culture in stationary phase were treated with ciprofloxacin (20 μg/mL, 100x the reported minimum inhibitory concentration (MIC) (Möker et al., 2010)) for 4 h. The viable cell population, as measured by colony forming units (CFU), dropped from 10^8~10^9 per mL (CFU/mL, stationary phase concentration) to 10^5~10^6 CFU/mL (stable persister region) (Figure 3.1A). This indicated a survival rate of ~0.1% and was consistent with literature values (Maisonneuve & Gerdes, 2014; Möker et al., 2010; Spoering & Lewis, 2001). Persisters were isolated from the antibiotic environment and resuspended into fresh Luria-Bertani broth (LB) (resuspension conditions discussed later). At the same time, a separate untreated *P. aeruginosa* culture in stationary phase was diluted into fresh LB medium. After the lag phase period, persister cells started to regrow into exponential phase at a constant growth rate. The doubling time of persisters for 100x dilution was 39.5 min (Figure 3.1C), slightly larger than 32.6 min, the doubling time of untreated cells (Høyland-Kroghsbo et al., 2018).

We found no significant changes in killing kinetics in stationary phase between recovered persister cells and untreated cells (Figure 3.1A). The final concentration of viable cells (persisters) after 4-h treatment was still approximately 10^5~10^6 CFU/mL, consistent with the idea that persistence is a non-heritable phenotype.

3.3.2. The regrowth of P. aeruginosa persister cells in planktonic culture cannot occur without dilution of cell debris after antibiotic treatment

P. aeruginosa is known to secrete a variety of pigments, including pyocyanin (blue-green), pyoverdine (yellow-green and fluorescent), and pyorubin (red-brown); these pigments can be used to identify the organism (King et al., 1954). It is known that laboratory cultures of *P. aeruginosa* in LB medium will turn green from the original yellow when the population reaches stationary phase (LaBauve & Wargo, 2012). To

optimize experimental conditions for the resuscitation of persisters, cell pellets (after centrifugation at 5,000 g for 5 min) containing cell debris and persisters were resuspended in fresh LB medium with dilution factors of 1x (no dilution), 10x, and 100x (Figure 3.1B). Regrowth required dilution of the mixture of cell debris and persisters. Regrowth was completed within 20 h after 100x dilution, within 40 h for 10x dilution, and was not observed for the 1x culture (Figure 3.1C-F). This phenomenon may indicate that persister cells sense the presence of cell debris before exiting the persistence state. This mechanism seems unlikely to be related to quorum-sensing because secreted signaling molecules (as well as the antibiotic) were eliminated by thorough washing prior to resuspending persister cells in fresh medium.

In addition, a heterogeneous distribution of colony sizes, shown as a pattern of a normal distribution with large variance (Figure 3.2D), was observed on the survival assays of persister cells, which was dramatically different from the pattern of untreated cells, where the appearance of them exhibited a normal distribution of small variance, or nearly a uniform colony size (Figure 3.2A). From this point, observations on the single-cell platform could be useful to further characterize to the regrowth of persister cells.

3.3.3. ScanLag analysis showed that the persister population exhibited a heterogeneous distribution in terms of appearance time and colony growth rate

We used ScanLag to track the regrowth behavior of persister cells on LB agar plates. ScanLag is an automated colony-based system allowing high-throughput acquisition of time-lapse images, quantification, and analysis of the growth bacterial colonies (Levin-Reisman et al., 2010, 2014; Levin-Reisman & Balaban, 2016). After antibiotic treatment and washes, cell pellets containing cell debris and persisters were resuspended into fresh medium and diluted onto LB agar plates at a density of approximately 100 cells per plate (calculated from the killing curves). The majority of colonies derived from the persister population exhibited appearance times between

21 and 34 h (Figure 3.2F), while colonies from the untreated population appeared between 13 and 14 h (Figure 3.2C), which is consistent with the prolonged lag phase observed in planktonic culture. In addition, persister cells exhibited a broader distribution of growth rates, defined as the colony expansion rate (Figure 3.2B and 3.2E).

Although recovered persisters that had reached stationary phase demonstrated similar killing kinetics as untreated cells, there were obvious differences in terms of the duration of lag phase and growth rates before cells reach stationary phase. The reason may be related to the occurrence of phenotypic switching between the persistence and non-persistence states, which is generally thought to be stochastic (Buerger et al., 2012). Unlike untreated cells, the regrowth of persister cells may be led by a few individuals that resuscitated from the persistence state early. The understanding of the characteristics of growth phases is critical for follow-up experiments, as bacterial persistence level varies at different growth phases (Harms et al., 2016). For example, expression of RpoS, a stationary phase sigma factor that modulates various stress pathways, has been reported to increase the percentage of the persistent population in stationary phase as compared to exponential phase (Kayama et al., 2009; Murakami et al., 2005). The determination of persister resuscitation period will help differentiate factors in phenotypic switching.

3.3.4. Demonstration of labeling with BONCAT in the comparison of recovered persisters and untreated cells in stationary phase

We used BONCAT to identify the newly synthesized proteins that persisters rely on during regrowth. To visualize whether Anl could be incorporated into cellular proteins, we performed BONCAT experiments on the mutant strain PA14::Tn7:P_{trc}-NLL-MetRS (Babin et al., 2017), which contains a chromosomally-integrated mutant methionyl-tRNA synthetase (L13N, Y260L, and H301L). Separate cultures of untreated cells and persisters were grown to stationary phase and then labeled with

Anl at 37˚C for 20 h. As shown by TAMRA-alkyne staining (Figure 3.S1), both recovered persisters and untreated cells showed strong incorporation of Anl. We then investigated whether there are differences between the recovered persisters and untreated cells in stationary phase.

Proteins synthesized during regrowth, as they contained azido groups, were enriched by reacting with alkyne-containing DBCO-agarose beads. After washing, desalting, trypsin digestion, and purification, multiple peptide fragments from the newly-synthesized proteins could be collected for liquid chromatography-tandem-mass spectrometry (LC-MS/MS) analysis. Tryptic digestion often resulted in multiple peptide fragments detectable by LC-MS/MS (Babin et al., 2017). MaxQuant was used to process the data (Tsakou et al., 2020). Information on protein abundances was obtained, including label-free quantification (LFQ) for comparison of protein abundances across samples (Cox et al., 2014), and intensity-based absolute quantification (iBAQ) for comparison of protein abundances within the same sample (Schwanhäusser et al., 2011).

We were able to identify 1629 proteins common to both samples (Figure 3.S2A). Not many significantly up- or down-regulated proteins were identified (using a correlation R^2=0.92, Figure 3.S2 B-C for LFQ and iBAQ comparisons, respectively), supporting our hypothesis that after recovery to stationary phase, cultures derived from persisters are similar to those derived from untreated cells.

3.3.5. The persister resuscitation period is defined as the total regrowth period prior to the beginning of stationary phase

We first labeled the cultures in their early exponential phase. We introduced a 30-min Anl pulse into the growth media (i.e. 7-7.5 h for 100x, 17-17.5 h for 10x). Proteins were obtained from the lysates and conjugated to TAMRA-alkyne; however, there was no TAMRA signal detected from the SDS-PAGE gel after the click reaction (Figure 3.S3A). Following enrichment, the newly-synthesized proteins were

quantified by traces obtained by High Performance Liquid Chromatography (HPLC) (Figure 3.S3B). The ratios of the mass of newly-synthesized proteins (measured by HPLC after enrichment) over the total loaded proteins (measured by BCA assays before enrichment), were less than 1%; this small ratio may not be easily identified by in-gel fluorescence, which could explain the absence of the TAMRA signal in the SDS-PAGE gel.

In order to increase the amount of labeled protein and collect sufficient signal during regrowth, we adjusted our labeling strategy and defined the labeling period to be from the time when cells were suspended into antibiotic-free medium to the end of exponential phase, which is the first 10 h for untreated cells, and the first 20 h for persister cells with a dilution factor of 100 (based on the growth curves, Figure 3.S4). We avoided collecting signals from stationary phase as the ratio of cells entering the persistence state to cells leaving the persistence state will significantly increase in stationary phase (Kayama et al., 2009; Murakami et al., 2005). As shown in Figure 3.S5, SDS-PAGE gels showed strong TAMRA-alkyne staining, indicating sufficient amount of proteins being tagged with Anl.

3.3.6. Pyochelin-related proteins were found to be up-regulated during persister resuscitation

Following the protocols described in section 3.3.4, we performed BONCAT enrichment experiments on the samples (3 replicates for each condition) discussed in section 3.3.5. In total 1,956 proteins were identified and quantified. Of these, 1880 were shared between untreated cells and persister cells; 64 proteins were found only during persister regrowth; and 12 proteins were found only during regrowth of untreated cells. For the 1,880 proteins shared by both groups, LFQ was used to compare protein abundances across samples. Of these proteins, 22 were up-regulated by persisters ($p<0.05$) and 38 were down-regulated by persisters ($p<0.05$), compared to untreated cells (See Table 3.S1). To investigate whether these proteins were functionally related, we used the *Pseudomonas* Community Annotation Project

(PseudoCAP) genome database to classify each of the proteins on the list (Winsor et al., 2011). In addition, we investigated proteins that appeared only in the persister group.

We found the functional group *pyochelin biosynthesis and metabolism* to be strikingly up-regulated during the regrowth of persisters. Specifically, we found PchE, PchA, PchR, PchB, PchD, PchF and FptA to be at least 4-fold more abundant in persister samples ($p<0.05$), and TonB to be 1.6-fold more abundant ($p<0.05$) (Figure 3.3A). In addition, PchH, PchG, and PchC were found only in the persister population. The *pchDCBA* and *pchEFGH* operons (Reimmann et al., 2001) are essential for the biosynthesis of pyochelin (Figure 3.3B), one of the two major siderophores used for iron acquisition in *P. aeruginosa* (Cox et al., 1981). Pyochelin is also known as a virulence factor, which increases the lethality of the pathogen (Cox, 1982). PchR is a regulatory protein, acting as a regulator for the *pchDCBA* and *pchEFGH* operons, as well as an activator for the production of FptA, which is the outer membrane ferric pyochelin receptor (Ankenbauer & Quan, 1994; Heinrichs & Poole, 1996). TonB is essential for siderophore-mediated iron acquisition in *P. aeruginosa* and receptors for iron uptake like FptA and FpvA are both TonB-dependent receptors (Takase et al., 2000).

We compared our studies with other bacterial persistence studies using proteomic approaches, especially two papers that also studied persister resuscitation (Semanjski et al., 2021; Spanka et al., 2019). Spanka et al used pSILAC for investigation of the post-ampicillin recovery of persisters of Δ1-41 Δ*istR*, a double deletion mutant of *E. coli* K-12 MG1655 in which the regulatory RNA elements and the antitoxin IstR-1 are deleted, allowing overexpression of the toxin TisB in the TisB/IstR-1 TA system (Spanka et al., 2019). They identified a number of proteins involved in iron sequestration and iron storage with significantly decreased protein synthesis in the killing phase of TisB-dependent persister cells, including Dps (a protein that oxidizes ferrous ions and accumulates them within its protein cavity (Antipov et al., 2017)),

FtnA (the iron storage protein ferritin), and Bfr (the iron storage protein bacterioferritin) (Honarmand Ebrahimi et al., 2015; Spanka et al., 2019). They also identified IscA (an iron-binding protein) and HscB (a co-chaperone protein in iron-sulfur assembly) with significantly increased abundance during recovery of persisters (Spanka et al., 2019; Takahashi & Nakamura, 1999). In addition, Semanjski et al used pSILAC for investigation of the post-ampicillin recovery of persisters of *E. coli* K-12 MG1655 by ectopically inducing *hipA*, which encodes for toxin HipA in the HipA-HipB TA system, allowing overexpression of toxin HipA (Semanjski et al., 2021). They reported that the abundances of proteins involved in metal cluster binding were significantly increased during the onset of resuscitation, especially from 10 to 30 min after induction of resuscitation. Several proteins present in increased abundance are closely related to iron uptake in *E. coli*, for example, IscA, IscU, IscR, ErpA, and NfuA (which are involved in iron-sulfur cluster assembly (Py et al., 2018; Takahashi & Nakamura, 1999)), EfeO (part of the iron uptake system EfeUOB (Nakatsuji et al., 2022)), and Fur (a ferric uptake regulation protein (Stojiljkovic et al., 1994)). We did not find proteins directly involved in the biosynthesis of siderophores being highlighted in their results, although EfeO and Fur are closely related to siderophores (Nakatsuji et al., 2022; Stojiljkovic et al., 1994). One possible reason is that *E. coli* might use different iron uptake strategies other than siderophore-mediated pathways. Nevertheless, these results, together with our results showing the up-regulation of pyochelin-related proteins, suggest the importance of iron uptake in the resuscitation of persister cells.

In *P. aeruginosa*, pyochelin has been reported previously to be associated with bacterial persistence (Li et al., 2016; Wood & Wood, 2016). In a PA14 *hig*A deletion mutant, which favors the activity of the HigB toxin and increases survival under ciprofloxacin treatment, DNA microarray data indicated down-regulation of pyochelin-related genes (*pchA-G*, *pchR*, and *fptA*) (Wood & Wood, 2016), compared with the PA14 WT strain. RNAseq analysis of a PA14 *higA*::Tn mutant showed similar down-regulation of pyochelin-related genes (*pchB-D, pchF* and *fptA*) (Li et

al., 2016). Furthermore, Mark van Eldijk in our laboratory used BONCAT to examine the killing of PA14 NLL-MetRS by ciprofloxacin. His proteomic results also showed down-regulation of pyochelin-related proteins (PchA-G, PchR, and FptA) (unpublished). Collectively, these results (Table 3.1), obtained through different methods, suggest a link between pyochelin down-regulation and bacterial persistence. Furthermore, compared to the methods Li et al and Wood and Wood have used in their experiments (DNA microarrays and RNAseq), a proteomic approach is a direct measurement of cellular metabolism. This approach is particularly important in the study of bacterial persistence because persister cells remain metabolically dormant.

Our observation of up-regulation of pyochelin-related proteins during persister resuscitation confirms the involvement of pyochelin-related proteins in the regulation of *P. aeruginosa* persistence. The magnitude of fold changes of exiting the persistence state matches that of entering the persistence state (Table 3.1), reflecting the need for recovering persisters to return pyochelin synthesis to a normal level. Compared to *E. coli* TisB-dependent persister cells (Spanka et al., 2019), where proteins involved in multiple iron uptake pathways were down-regulated in entering the persistence state and up-regulated in exiting the persistence state, our study demonstrated that bacteria were able to activate the expression of same genetic operons in one phenotypic state and repress them in the reverse phenotypic state, which indicates the importance of iron uptake pathways in the regulation of bacterial persistence state-switching.

3.3.7. No single gene in the pyochelin biosynthesis pathway altered regrowth behavior

We then investigated whether a single gene in the pyochelin pathway could affect bacterial response to antibiotics and persistence-related phenotypes. The corresponding transposon insertion mutants were obtained from a PA14 transposon insertion library (Liberati et al., 2006), including *pchA*::Tn*, pchB*::Tn*, pchC*::Tn and

pchD::Tn, which disrupt the *pchDCBA* operon and interrupt the synthesis of pyochelin, *pchE*::Tn and *pchF*::Tn, which disrupt the *pchEFGH* operon and interrupt the synthesis of pyochelin, *pchR*::Tn, which disrupts the regulator *pchR*, and *fptA*::Tn, which disrupts the outer membrane transporter for pyochelin (Kaplan et al., 2021; Schalk et al., 2020). The survival rates after antibiotic treatment (Figure 3.S6) and the appearance times of the mutant persisters were investigated (Figure 3.S7). We found no significant differences among *pchA*::Tn, *pchB*::Tn, *pchC*::Tn, *pchD*::Tn, *pchE*::Tn, and *pchF*::Tn. These results are not surprising, as *P. aeruginosa* has many genes that enable adaptation to environmental stresses (Silby et al., 2011). In fact, only 35 and 79 PA14 transposon insertion mutants, out of a total of 20,530 unique mutants in the library, were found to have increased or decreased susceptibilities, respectively, to ciprofloxacin (Breidenstein et al., 2008). We noticed that *pchR*::Tn had increased survival rate and different appearance time distribution but PchR does not participate the biosynthesis directly (Kaplan et al., 2021) and the transcription of *pchDCBA* and *pchEFGH* can still occur (Roche et al., 2022).

3.3.8. A PA14 higA::Tn mutant was examined via ScanLag and the regrowth pattern was shown to fit a negative exponential distribution

Although it was reported the expression of pyochelin-related genes were down-regulated during the process of persister formation (Li et al., 2016; Wood & Wood, 2016), the molecular mechanisms involved are not understood. Reduction of pyochelin is thought to be correlated with decreased bacterial virulence (Cox, 1982; Sokol, 1987; Wang et al., 1996). Therefore, the authors argued the down-regulation of pyochelin biosynthesis was a sign of decreased bacterial virulence in the persistence state due to the overall decrease of bacterial metabolism.

The studies of Li et al and of Wood and Wood used PA14 *higA* transposon insertion mutants to create ciprofloxacin-triggered persister cells, and both groups suggested that down-regulation of transcription of pyochelin-related genes was modulated by the HigB-HigA TA system (Li et al., 2016; Wood & Wood, 2016). HigB-HigA is

one of the four TA systems, ParD/ParE (Muthuramalingam et al., 2019), HicA/HicB (Li et al., 2016), RelE/RelB (Coskun, 2018), and HigB/HigA (Wood & Wood, 2016), found in *P. aeruginosa* so far (Zhou et al., 2021). HigB is an RNase, which cleaves mRNAs and functions as the toxin; HigA is the antitoxin and neutralizes the toxicity of HigB. HigB-HigA systems are found in many other organisms, although the genetic arrangement is different from that in *P. aeruginosa*, where *higB* is upstream of *higA* (Wood & Wood, 2016).

While it has been observed that *higA*::Tn mutants exhibit higher survival rates than the WT strain (Li et al., 2016), it is unclear what role the HigB-HigA system plays during persister resuscitation.

To explore whether the fold changes of pyochelin-related proteins during the regrowth of persister cells is caused by the HigB-HigA TA system, we used ScanLag to characterize the regrowth behavior of a PA14 *higA*::Tn mutant (there is no *higB*::Tn mutant available in the library) (Liberati et al., 2006). To generate *higA*::Tn persisters, *higA*::Tn culture in stationary phase were treated with ciprofloxacin (20 μg/mL) for 4 h. Cell pellets containing cell debris and *higA*::Tn persisters were resuspended into fresh medium and diluted onto LB agar plates at a density of approximately 100 cells per plate. Surprisingly, persisters of the *higA*::Tn mutant exhibited an uncommon appearance pattern on LB agar plates. Instead of a normal distribution, the distribution of *higA*::Tn persisters followed a negative exponential distribution, suggesting that the HigB-HigA system modulates persister awakening and regrowth (Figure 3.4).

3.3.9. HigA-binding sequence was not found to be directly or indirectly relevant to pyochelin-related genes in PA14 genome

To further investigate the role of the HigB-HigA system in persister regrowth, we examined the role of antitoxin HigA. According to toxin-antitoxin theory, in order for persisters to initiate awakening, HigA should be up-regulated to neutralize the

toxicity of HigB. HigA is thought to bind to the promoters of certain genes, including *higB*, to activate or repress their transcription (Guo et al., 2019). DNase I footprinting has shown that HigA binds to a specific palindrome sequence, 5'-TTAAC GTTAA-3'. In *P. aeruginosa* PAO1, HigA represses expression of *higB* by binding to the sequence 5'-TTAAC GTTAA-3' in the promoter region of *higB*. The same palindromic sequence is found in the promoter region of PAO1 *mvfR*, an important regulator of *P. aeruginosa* virulence which is also repressed by HigA (Xiao et al., 2006). Because pyochelin is also thought to be a virulence factor in *P. aeruginosa*, we wondered whether HigA might affect the expression of pyochelin-related genes through a similar mechanism. Upon checking the whole genome of *P. aeruginosa* PA14, we found that the promoter region of PA14 *mvfR* does not contain the 5'-TTAAC GTTAA-3' sequence. We also note that *mvfR* is not known to directly regulate the expression of pyochelin-related genes.

To further investigate whether HigA directly affects pyochelin-related genes through other regulatory sequences that contain 5'-TTAAC GTTAA-3', we performed whole genome searching for potential binding motifs of HigA via Multiple Em for Motif Elicitation (MEME) Suite (Bailey et al., 2015). The results are summarized in Table 3.S2. PseudoCAP was used to check the correlation between each gene on the list and pyochelin-related genes. However, no other locations, other than the promoter of *higB*, were found to contain the perfect palindrome sequences in PA14 genome. In addition, no direct link was found between genes carrying similar palindrome structures and pyochelin-related genes.

We reviewed the results of our BONCAT enrichments to determine whether HigB or HigA is altered in abundance during regrowth (Figure 3.S8). Only HigA was found, and its abundance was not significantly different between persisters and untreated cells ($p>0.05$).

3.3.10. BONCAT with Aha as ncAA was established and examined to label PA14 WT and transposon insertion mutant strains

To elucidate what causes the *higA* mutant to exhibit the uncommon appearance pattern, to understand what metabolic pathways in the *higA* mutant differ from those in other strains, and to check whether the HigB-HigA system modulates the expression of pyochelin-related genes, we performed BONCAT enrichment experiments to identify proteins made during regrowth of *higA* persisters.

In order to label proteins from the *higA*::Tn strain, we used Aha as the ncAA to avoid extensive use of antibiotic markers, since all of the strains in the library use the MAR2xT7 transposon, which contains a gentamicin marker (Liberati et al., 2006). We adapted and revised the conditions used in some of the pioneer BONCAT experiments in other organisms (Dieterich et al., 2006, 2007) and optimized the protocols for *P. aeruginosa*. In particular, we replaced LB medium with M9 medium supplemented with Aha, and reduced the methionine concentration (to achieve an Aha:Met ratio of 30:1). The concentrations of the 19 other natural amino acids were kept at 40 mg/L. These conditions allowed efficient incorporation of Aha into newly-synthesized proteins (Figure 3.S9).

The change of ncAA and growth medium might affect cellular metabolism and regrowth behavior (Ngo et al., 2009; Tanrikulu et al., 2009). To determine whether the proteome profile would be affected by the switch from Anl to Aha, we performed BONCAT enrichment experiments on samples collected during the regrowth of WT untreated cells and WT persister cells (Figure 3.S10). Starting from the time when the cells were suspended into fresh medium, untreated cells were labeled with Aha for 10 h and persister cells were labeled for 20 h. A total of 1,949 proteins were found in common between Anl-labeled proteins and Aha-labeled proteins, while 388 were found only in Anl-labeled proteins and 241 were found only in Aha-labeled proteins (Figure 3.S11). Most importantly, Aha-labeling again showed that pyochelin-related proteins are up-regulated in PA14 WT persisters (Figure 3.5) as compared to

untreated cells, supporting our previous observations derived from Anl-labeling of the PA14 NLL-MetRS mutant.

3.3.11. Pyochelin-related proteins were also found to be up-regulated during higA::Tn persister resuscitation

Following the protocols described in section 3.3.4, we performed BONCAT enrichment experiments on samples collected during regrowth of *higA*::Tn untreated cells and *higA*::Tn persister cells labeled with Aha (Figure 3.S10). For the enrichment results, the pyochelin-related proteins were still found up-regulated in the newly-synthesized Aha-labeled proteins of PA14 *higA*::Tn persisters (Figure 3.6), indicating the up-regulation of pyochelin biosynthetic pathways was independent from the modulation HigB-HigA TA system.

In fact, the theory that toxin-antitoxin systems modulate bacterial persistence has been challenged. Evidence supporting that the activation of toxins promote persister formation is that deletions of several toxins leads to reduction in persistence and deletions of several antitoxins leads to increase in persistence (Dörr et al., 2010; Harrison et al., 2009; Kim & Wood, 2010). But recent studies that have found no direct linkage between bacterial persistence and TA systems (Conlon et al., 2016; Goormaghtigh et al., 2018; Pontes & Groisman, 2019; Shan et al., 2017; Svenningsen et al., 2019). Goormaghtigh et al demonstrated deletion of 10 TA systems in *E. coli* did not affect persistence to ofloxacin or ampicillin. In addition, the correlation between the fluorescence of YefM-YeoB TA system and persister resuscitation could not be established (Goormaghtigh et al., 2018). Svenningsen et al confirmed high (p)ppGpp levels were critical for *E. coli* persister formation but they could not confirm the post-transcriptional effects of (p)ppGpp were through the activation of TA modules (Svenningsen et al., 2019). Shan et al also found induction of TA systems did not necessarily increase *E. coli* persistence and concluded ATP levels led to persister formation, which was independent from TA systems (Shan et al., 2017). Similar observations and conclusions showing that bacterial persistence is

independent from TA systems were reported in other bacteria including *Salmonella enterica* (Pontes & Groisman, 2019) and *Staphylococcus aureus* (Conlon et al., 2016).

Furthermore, the role of antitoxin remains questionable during persister resuscitation. Although some studies suggested that cells might be resuscitated by reversing the effects of toxins (Cheverton et al., 2016; Semanjski et al., 2021), there is no evidence confirming that antitoxin can initiate persister resuscitation without changes in the external environment. In our study, we observed an uncommon appearance pattern through ScanLag, which indicates the HigB-HigA TA system affects bacterial resuscitation on LB agar plates. However, our BONCAT data in *higA*::Tn persisters could not confirm that the changes in abundance of pyochelin-related proteins, which were observed in planktonic cultures, resulted from the modulation of the HigB-HigA system.

3.4. Discussion

Recent advances in the study of bacterial persistence revealed that several mechanisms can induce cells to enter the persistence state, a transient and phenotypic state in which bacteria exhibit increased antibiotic tolerance. However, due to lack of direct reporters of persister cells, many traditional molecular methods cannot be applied to investigate bacterial persistence, and there is controversy over the definition of bacterial persistence. It is now generally agreed among many research groups that persistence refers to the ability of a subset of the bacterial population that survives under antibiotic treatment (Balaban et al., 2019). Previous studies have shown that bacterial persistence is a non-heritable phenotype, as the population after the regrowth of the persister population is as sensitive to antibiotics as the initial population (Fauvart et al., 2011; Keren et al., 2004). In the meantime, heterogeneity is the key that makes antibiotic persistence different from antibiotic tolerance. The most obvious observation is that heterogenous bacteria exhibit a biphasic killing curve (Maisonneuve & Gerdes, 2014), as we observed upon antibiotic treatment of either previously untreated cells or recovered persisters cells after regrowth to stationary phase. Another observation related to the post-antibiotic recovery is that persistent bacteria exhibit longer lag phases in planktonic culture (Fridman et al., 2014; Jõers et al., 2010; Wilmaerts et al., 2019). In our study focusing on persister resuscitation, we adapted an automated colony-based method called ScanLag and observed heterogenous characteristics that persister cells exhibited when they exit the persistence state. Therefore, heterogeneity is a feature present in entering and exiting the persistence state. The reasons causing the phenomenon are unclear. As we have shown, the phenomenon could be related to the presence of cell debris or it could be related to the stochastic nature of exiting the persistence state. Nevertheless, our experimental set-up with ScanLag provided a useful platform to observe heterogenous population and determine the persistence level.

The phenotypic switching between the persistence state and non-persistence state is thought to be the cause leading to the general heterogeneity of microbial population (Buerger et al., 2012). We have applied BONCAT to selectivity label newly-synthesized proteins of persister cells in the heterogenous population, allowing direct measurements of the translational activities during persister regrowth. In this work, newly-synthesized proteins were tagged with either Anl or Aha. The Anl approach has the advantage of specificity, as well as direct application in nutrition-rich medium. The Aha approach avoids extensive use of antibiotic markers and allows direct interrogation of strains drawn from the PA14 transposon insertion mutant library. In our experimental results, the up-regulation of pyochelin-related proteins was demonstrated as a reproducible observation, which are closely related to reports from other research groups (Li et al., 2016; Wood & Wood, 2016). Understanding the ribosomal activities or ribosome-dependent metabolism has been one of the major interests of many research groups in the field of bacterial persistence (Bokinsky et al., 2013; Cho et al., 2015; Lemke et al., 2011; Potrykus et al., 2011). The usage of BONCAT demonstrates itself as a feasible, robust, and reliable proteomic platform to investigate bacterial persistence.

Furthermore, we compared our approaches with these two papers which also studied persister resuscitation using proteomic approaches (Semanjski et al., 2021; Spanka et al., 2019). Both studies labeled persisters with stable isotope-containing amino acids (SILAC) to obtain information about active translational activities of persister cells. Although the application of SILAC allowed the quantification and identification by mass spectrometry, both studies had to use mutant strains, in which the antitoxin module was knocked out, to increase the persistence level and abundances of proteins of interest so that enough proteomic signals of persisters could be collected. However, in our BONCAT experiments, we avoided beginning with antitoxin knockouts, and used PA14 WT strains in Aha-labeling experiments and the NLL-MetRS mutant in Anl-labeling experiments. This allowed us to examine whether the proteomic profiles of persisters during regrowth were affected by the HigB-HigA TA system. TA

modules were not shown to be either up- or down-regulated in our proteomic analysis. For the HigB-HigA TA system, we detected HigA (PA14_61840; $p>0.05$) but did not detect HigB under any conditions. It is possible that cells did not make new HigA or HigB under our conditions, or that these proteins, especially the antitoxin proteins (Wilmaerts et al., 2019), were unstable and yielded no signals detectable by LC-MS/MS. As a follow-up, we did BONCAT enrichments on *higA*::Tn persisters, which also revealed an up-regulation of pyochelin-related proteins and indicated that the changes in expression of pyochelin-related genes reported earlier were independent of modulation by antitoxin HigA (Li et al., 2016; Wood & Wood, 2016). In addition, Mark van Eldijk in our laboratory has demonstrated down-regulation of pyochelin-related proteins during ciprofloxacin-mediated killing of the PA14 NLL-MetRS mutant, and he also did not observe significant changes of HigA or detect any HigB (unpublished results). Recent studies have reported that persisters require repair systems to sustain antibiotic-induced damage and initiate post-antibiotic regrowth (Mok & Brynildsen, 2018; Völzing & Brynildsen, 2015). Noting that the previous studies and our studies all used ciprofloxacin as the generator of antibiotic-induced stress, the down-regulation of pyochelin-related genes/proteins during persister formation and up-regulation of pyochelin-related proteins during persister resuscitation might be related to ciprofloxacin, instead of the downstream effects of the modulation of antitoxin HigB. Further studies are needed to elucidate the connection between ciprofloxacin and pyochelin.

Finally, while our proteomic investigation highlights the up-regulation of genetic operons involved in the biosynthesis of pyochelin, the mechanism governing up-regulation during persister resuscitation is not known. Although DNA repair has also been found to be up-regulated during persister resuscitation (Mok & Brynildsen, 2018; Völzing & Brynildsen, 2015), it was only required during the recovery phase, not during persister formation. To the best of our knowledge, the pyochelin biosynthetic pathway is the first pathway discovered in *P. aeruginosa* which has been shown to be reversely-regulated in response to persistence-related phenotypic state

switching. In addition, pyochelin, because it has lower affinity for iron than pyoverdine, is known as the secondary siderophore for iron uptake in *P. aeruginosa* (Brandel et al., 2012). Previous studies (Li et al., 2016; Wood & Wood, 2016), and our BONCAT results (including van Eldijk's independent BONCAT studies of persister formation) did not detect significant changes in pyoverdine-related genes/proteins, which constitute the predominant iron acquisition pathway in *P. aeruginosa* (Cornelis & Dingemans, 2013). This observation raises the question of why persisters rely on pyochelin instead of pyoverdine if iron uptake is essential for persistence-related phenotypic state switching. In addition, it is also interesting to investigate whether pyochelin has other functions, including some related to bacterial persistence. These extensions of our work will enhance our understanding of bacterial siderophores and bacterial persistence.

3.5. Materials and methods

3.5.1. Strains and growth conditions

The *P. aeruginosa* PA14 strain was used in this study. The PA14 NLL-MetRS mutant was obtained from Dr. Mark B. van Eldijk in the Tirrell laboratory at the California Institute of Technology (Babin et al., 2017). All the transposon insertion mutants, including *pchA*::Tn*, pchB*::Tn*, pchC*::Tn*, pchD*::Tn*, pchR*::Tn*, pchE*::Tn*, pchF*::Tn*, fptA*::Tn*,* and *higA*::Tn mutants, were obtained from the PA14 transposon insertion library held in the Newman laboratory at the California Institute of Technology. The library was first constructed by the Ausubel laboratory at Massachusetts General Hospital (Liberati et al., 2006).

Planktonic cultures were grown at 37˚C with shaking. The growth medium used in Anl labeling experiments was LB medium (1 L recipe: 950 mL H_2O, 10 g tryptone, 10 g NaCl, and 5 g Yeast extract). The growth medium used in Aha labeling experiments was modified minimal medium (1L recipe: 780 mL H_2O, 200 mL M9 salts (5X; Sigma-Aldrich), 20 mL glucose (20%; Sigma-Aldrich), 2 mL $MgSO_4$ (1 M; Fisher Scientific), 100 µL $CaCl_2$ (1 M; Fisher Scientific)). For control experiments, 20 natural amino acids (Life Technologies) were added to M9 medium at a concentration of 40 mg/L. For labeling experiments, the concentration of methionine was 5 mg/L, the 19 other natural amino acids were at 40 mg/L. Trace metals were also added to the minimal medium to ensure sufficient metals especially iron. 1000x trace metals (per L) contains $Fe(III)Cl_3 \cdot 6H_2O$ (2.03g), $Co(II)Cl_2 \cdot 6H_2O$ (190mg); $Mn(II)Cl_2 \cdot 4H_2O$ (99mg); $ZnCl_2$ (68mg); $NaMoO_4 \cdot 2H_2O$ (48 mg); $Ni(II)SO_4 \cdot 6H_2O$ (26 mg); $Cu(II)SO_4 \cdot 5H_2O$ (2.5 mg); H_3BO_3 (6 mg) (Sigma-Aldrich).

3.5.2. Antibiotic treatment

Bacterial cells were cultured overnight with shaking at 37˚C to reach stationary phase. Ciprofloxacin (Life Technologies) was dissolved in 0.1 M NaOH solution and the pH was adjusted to 7. The ciprofloxacin was then filtered and added to cultures

at stationary phase at a final concentration of 20 μg/mL, 100x the reported minimum inhibitory concentration (MIC). The duration of antibiotic treatment was 4 h. Culture tubes containing the persister cells and cell debris were centrifuged at 5,000 g for 5 mins and the cell pellets were washed with sterile 0.9% NaCl solution twice.

3.5.3. Growth curve characterization and determination of regrowth conditions

Growth curves were characterized by counting colony forming unit (CFU) as a function of time. At the desired timepoint, 100 mL of cell suspension was collected from the culture tubes, followed by washing with 0.9% NaCl solution (an extra wash was performed if the cell suspension contained antibiotics). The cells were then diluted in series, up to 10^9 for untreated cells and up to 10^7 for persisters. Three drops from each diluted sample were collected and plated on LB agar plates. The plates were then cultured overnight at 37˚C.

The regrowth period was defined as the total length of the lag phase plus the exponential phase (i.e., the time required to reach stationary phase). Starting from the time where the cells were suspended into fresh medium, the regrowth period was determined to be 10 h for untreated cells and 20 h for persister cells diluted 100-fold.

3.5.4. ScanLag

Detailed protocols for ScanLag can be found at (Levin-Reisman et al., 2014). Prior to plating, cells were centrifuged at 5,000 g and washed with 0.9% NaCl solution. Sterile glass plating beads (diameter: 3 mm; Fisher Scientific) were placed onto pre-warmed LB agar plates. Aliquots (10-100 μL) of cell suspension containing roughly 100 to 200 cells were placed on the glass beads and mixed well before the beads were removed. Plates were transferred onto the scanner (EPSON Perfection V37). The lids of the plates were removed and black paper (Neenah Creative Collection™ FSC Certified Paper, Eclipse Black) was used to cover the plates. Scanning Manager (provided by the Balaban Lab at The Hebrew University of Jerusalem) was used to acquire images of the plates.

For analysis, the software version used in this study was V15 with Matlab 2017a (Mathworks). Parameters were slightly revised from the default settings of ScanLag software based on our experimental settings. For example, a value of 0.03, corresponding to 10 pixels, was used as the intensity threshold indicating minimum colony size. Merging colonies and corner colonies were manually excluded from the analysis.

3.5.5. BONCAT labeling visualization and enrichment experiments

In our ncAA labeling experiments, the concentration of pH-7 Anl (Iris-Biotech) or Aha (Iris-Biotech) was 1 mM. ncAA solutions were added to the culture tubes or flasks in the 37˚C incubator with shaking for a specified time. Labeled lysates (according to section 3.5.3) were then centrifuged at 5,000 g for 5 min. Cell pellets were resuspended in 4% SDS (Sigma-Aldrich) in PBS (Life Technologies) containing 20 mM chloroacetamide (Life Technologies) and kept in the dark. Cell suspensions were then heated at 95˚C for 5 min and sonicated for 1 min with 30% amplitude on a 5-second-on-5-second-off mode (Qsonica). Heating and sonication were repeated if necessary. The lysed cell suspensions were centrifuged at 10,000 g for 15 min at room temperature. Supernatants were collected for analysis by BCA protein assay (Thermo Scientific) and other downstream processing, or stored at -80˚C.

To visualize labeled proteins, 54 µL lysates containing 200 µg of protein supplemented with 4% SDS in PBS for each reaction were reacted with 4 µL alkyne-remix (recipe: 10 µL $CuSO_4$ (3.2 mg/mL), 20 µL THPTA (50 mM), and 4 µL alkyne-TAMRA (20 mM); incubated for 3 min), 12.5 µL aminoguanidine (11 mg/mL), 12.5 µL sodium ascorbate (20 mg/mL). The reaction mixes were incubated in the dark at room temperature for 30 min. Chloroform-methanol precipitation and four methanol washes were performed to remove excess TAMRA. Samples were then resuspended in 40 µL 4% SDS in PBS and 10 µL 5X SDS loading dye (Fisher Scientific). Aliquots

(5-10 µL) of suspensions for each reaction were loaded on protein gels (NuPAGE Novex 4-12% Bis-Tris Protein Gels; Fisher Scientific) and separated via SDS-PAGE. The separated SDS-PAGE gels were resuspended in water for destaining and then imaged on a Typhoon Trio Scanner (GE Healthcare). After TAMRA images were obtained, gels were stained with InstantBlue (Fisher Scientific) stain and placed at room temperature with gentle shaking on a rotator for 20 min. The gels were then washed with DI water twice, placed at room temperature on a rotator for 20 min, and imaged on the Typhoon Scanner.

For enrichment experiments, lysates containing 3 mg protein was diluted up to 1 mL with 1% SDS in PBS. 0.2 mL 600 mM chloroacetamide in 0.8% SDS in PBS was added. To alkylate free thiol groups, the samples were then incubated at 65˚C with shaking for 30 min. Aliquot (0.2 mL) of the fresh solution of 8 M urea (Life Technologies)/0.85 M NaCl/protease inhibitor (cOmplete, Mini, EDTA-free Protease Inhibitor Cocktail; Roche) in PBS was then added into each sample. Aliquot (35 µL) of washed DBCO-agarose beads (Click Chemistry Tools) was then added to each sample. The whole samples were then transferred to 2 mL polypropylene tubes (Fisher Scientific) and placed on a rotor in a dark room for overnight incubation. The reacted resins were then washed with water and treated with 0.5 mL 1 mM dithiothreitol (DTT; Life Technologies) at 70˚C for 15 min. After the supernatant was removed, 0.5 mL of iodoacetamide (Life Technologies) solution (7.4 mg/mL) was added and the samples were incubated in the dark on the rotor for 30 min. The resins were then transferred to spin columns (Bio-Rad) and washed with 0.8% SDS in PBS, 8M urea in tris pH 8.0 (Life Technologies), and 20% acetonitrile (ACN; Sigma-Aldrich) for four rounds. During the second wash, the columns were capped, allowing the resins to be incubated for 10 minutes before draining. The beads were then transferred to Eppendorf tubes with 10% ACN in 50 mM ammonium bicarbonate (AmmBic; Life Technologies). The tubes were then centrifuged at 2,000 g for 5 min and supernatant was removed down to leave a final volume of 100 µL. Ten µL 10% ACN in 50 mM AmmBic with 0.1 µg trypsin (Life Technologies) were

added to each tube. The samples were then incubated overnight on a shaker at 37˚C and 1,200 rpm. The supernatants were collected. The beads were washed twice with 150 µL 20% ACN and combined with the previous supernatants. The beads were then filtered through spin filters and dried by Speedvac (Thermo Fisher). To further remove the detergents in the samples, HiPPR kit (Thermo Fisher) was used. Finally, the samples were desalted with ZipTip (EMD Millipore).

3.5.6. LC-MS/MS

The identification and quantification of newly-synthesized proteins were performed using established protocols (Babin et al., 2016, 2017; Kalli & Hess, 2012). The untreated versus persisters experiments and Aha versus Anl experiments were performed on a nanoflow LC system, the EASY-nLC 1000, coupled to an hybrid ion trap-Orbitrap Elite mass spectrometer (Thermo Fisher Scientific). For the EASY-nLC 1000 system, solvent A consisted of 97.8% H_2O, 2% ACN, and 0.2% formic acid, and solvent B consisted of 19.8% H_2O, 80% ACN, and 0.2% formic acid. For the LC-MS/MS experiments, digested peptides were directly loaded at a flow rate of 500 nL/min onto a PicoFrit column (New Objective) packed in-house with ReproSil-Pur C_{18}AQ 3-µm resin (120 Å pore size; Maisch). The column was enclosed in a column heater operating at 60 °C. After 30 min of loading time, the peptides were separated with a 120-min gradient at a flow rate of 220 nL/min. The gradient was as follows: 0 to 30% B (120 min). Eluted peptides were ionized using a nanoelectrospary ion source (Thermo Fisher Scientific) and introduced into the mass spectrometer. The Orbitrap was operated in data-dependent acquisition mode to automatically alternate between a full scan (m/z 400-1600) in the Orbitrap and top 20 MS/MS scans in the linear ion trap.

3.5.7. Proteomic data analysis

The data files obtained from LC-MS/MS were processed with MaxQuant (v 1.6.1.0) (Babin et al., 2016; Cox & Mann, 2008) Database used was *P. aeruginosa* PA14 UniProt (5,886 sequences), in addition to a contaminant database (246 sequences).

Trypsin was specified as the digestion enzyme, with up to two missed cleavages. Carbamidomethylation of cysteine was set as a fixed modification, and protein N-terminal acetylation and methionine oxidation were variable modifications. Protein abundances were estimated with MaxLFQ (Cox et al., 2014), and for each experiment peptides were matched between runs. LFQ values were normalized and used to calculate abundance ratios between samples and to estimate variance using the limma package in R version (v 3.5.1) (Ritchie et al., 2015). P values were adjusted for false discovery by using the Benjamini-Hochberg procedure (Benjamini & Hochberg, 1995).

3.5.8. Whole genome searching

The full genome of *P. aeruginosa* PA14 was downloaded from the *Pseudomonas* Genome Database (Winsor et al., 2016). MEME Suite was used to detect motifs containing HigA-like palindromes in the PA14 genome (Bailey et al., 2015).

3.6. Acknowledgements

We thank Dr. Brett M. Babin for his help in BONCAT experiments and Dr. Mark van Eldijk for his assistance in ScanLag experiments and proteomic analysis. We thank Roxana Eggleston-Rangel, Michael J. Sweredoski, Annie Moradian, Dr. Jeff Jones, and Brett Lomenick from Caltech Proteome Exploration Laboratory for LC-MS/MS experiments and analysis. We also thank Dr. Megan Bergkessel and Prof. Dianne K. Newman for their help in PA14 strains and their insights in this project.

3.7. List of figures and tables

Figure 3.1. Characteristics of persister cells. (A) PA14 WT culture in stationary phase of recovered persister cells (red) and untreated cells (blue) were treated with ciprofloxacin for 4 h. Killing kinetics revealed a biphasic killing and survival rates were around 0.1%. The error bars refers to SDE. (B) Schematic diagram of the regrowth experiment with different dilution factors. Antibiotic-treated cell pellets (after washing and centrifugation at 5,000 g for 5 min) containing cell debris and persisters were resuspended in fresh LB medium with dilution factors of 1x (no dilution), 10x, and 100x. (C) Growth kinetics of the three conditions (1x in red, 10x in green, and 100x in blue) for 40 hours showed that regrowth does not occur without dilution of cell debris. Error bars refer to SDE. The growth conditions of the three planktonic cultures were recorded in (D)(E)(F). The culture exhibit green color when the cells complete exponential growth phase.

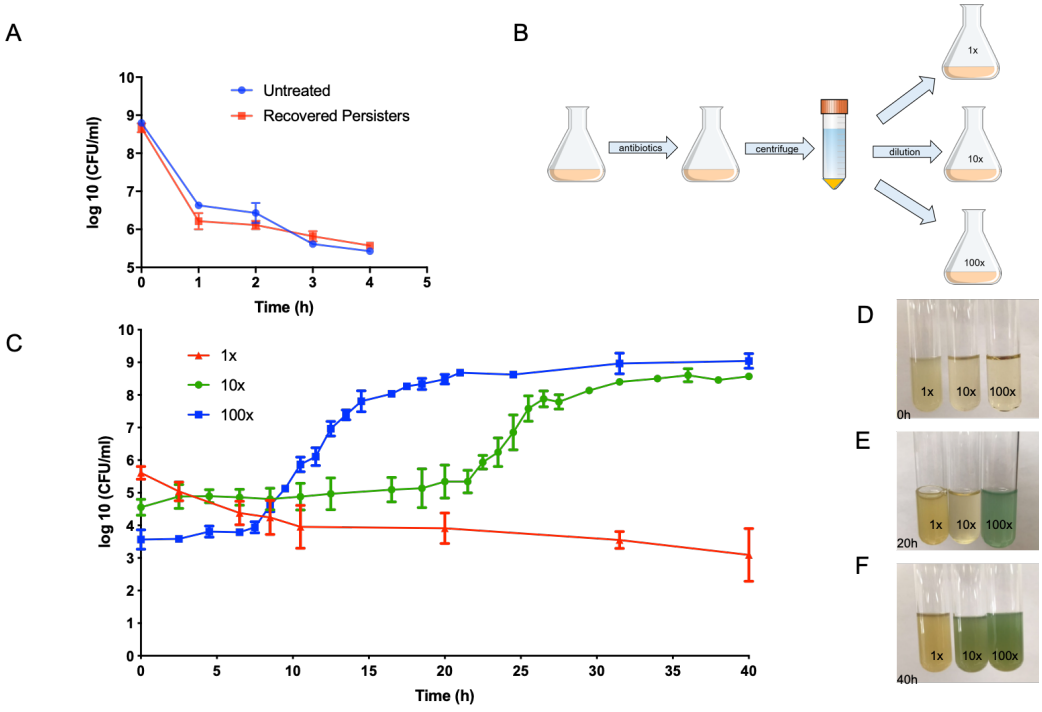

Figure 3.2. Comparison between persister cells and untreated cells on LB agar plates. Scanned pictures of colonies of untreated (A) and persister cells (D). Ciprofloxacin treatment causes the cell population in the stationary phase to drop from 10^8~10^9 to 10^5~10^6 CFU/mL. Time-lapse monitoring of the growth of untreated (B) and persister (E) cells reveals they exhibit distinct characteristics in terms of appearance time and colony expansion rates. The frequency distribution of the appearance time of untreated (C) and persister (F) cells showed a delay and a broader distribution in persister population.

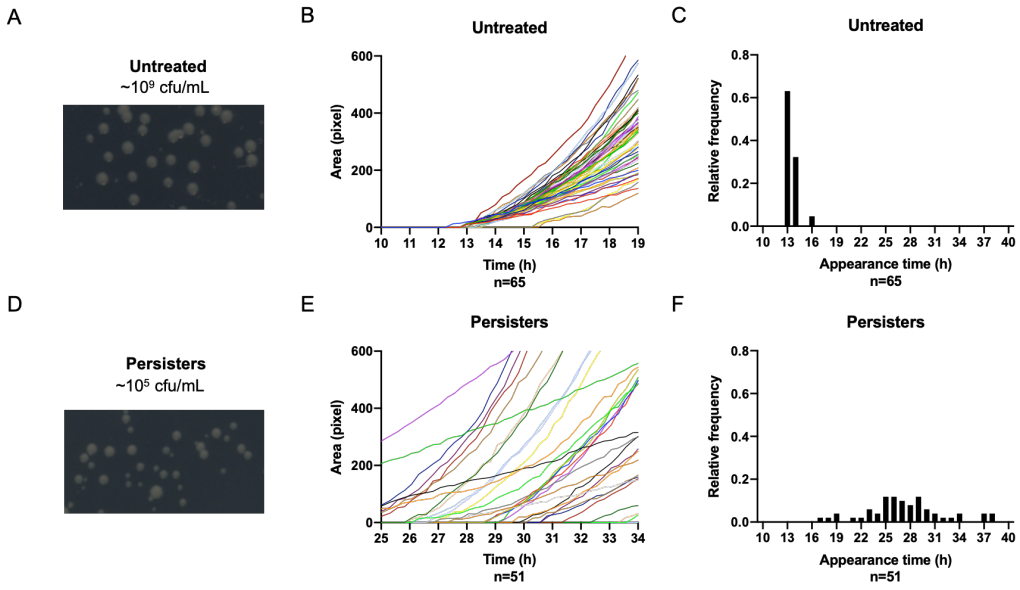

Figure 3.3. Integrated total proteins identified in the regrowth of persister and untreated cells with Anl approach. (A) A volcano plot showing the ratios of the shared proteins during the regrowth of NLL-MetRS persister cells versus untreated cells, calculated via label free quantification (LFQ). Persisters were obtained by treating stationary-phase cells with ciprofloxacin for 4 h. The persister regrowth experiments were labeled with Anl. Newly synthesized proteins were enriched for LC-MS/MS analysis. Red points indicate proteins involved in pyochelin pathway. Samples were collected from three replicates. (B) A brief biosynthetic pathway to pyochelin in *P. aeruginosa*, adapted from (Kaplan et al., 2021). Chorismate is converted to salicylate by PchA and PchB. Salicylate is then activated by PchD, loaded to PchE, and condensed. Another cysteine molecule is incorporated by PchF, after which the tailoring protein, PchG, reduces this second thiazoline to a thiazolidine, which is then N-methylated. Pyochelin is then released.

A

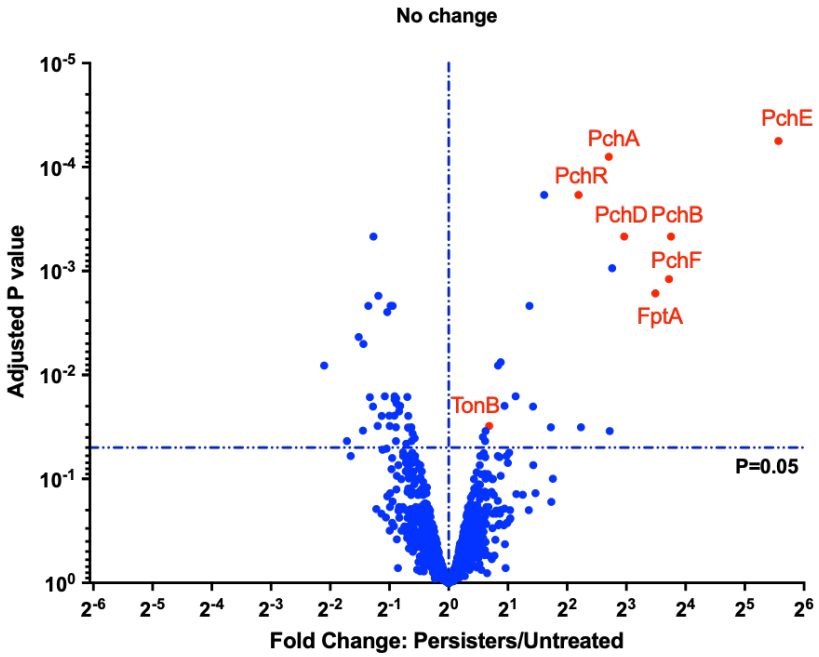
No change
Adjusted P value
Fold Change: Persisters/Untreated
P=0.05
PchE
PchA
PchR
PchD
PchB
PchF
FptA
TonB

B

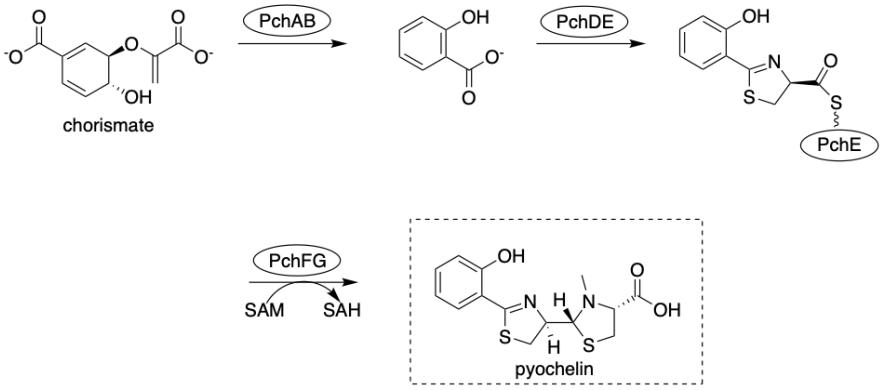
chorismate
PchAB
PchDE
PchE
PchFG
SAM
SAH
pyochelin

Figure 3.4. Analysis of appearance times of WT and *higA*::Tn. The frequency distributions of the appearance times of persisters of (A) PA14 WT strain and (B) *higA*::Tn strain. Persisters were obtained by treating stationary-phase cells with ciprofloxacin for 4 h. The appearance times were recorded with ScanLag.

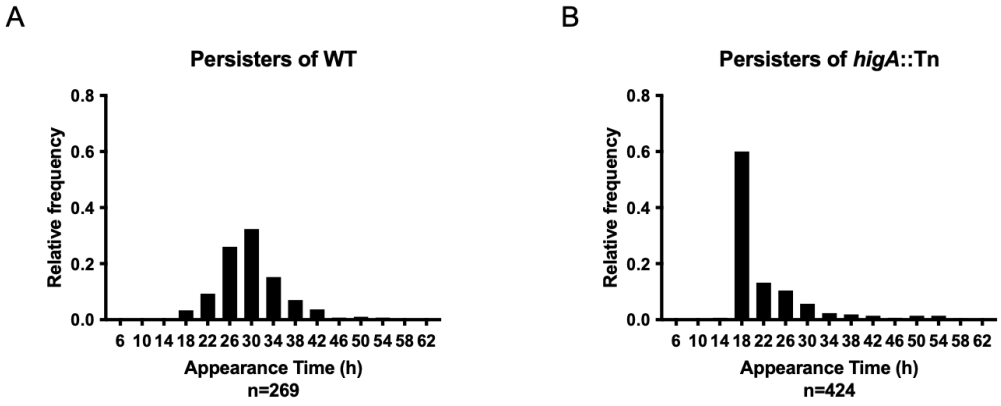

Figure 3.5. Integrated total proteins identified in the regrowth of persister and untreated cells with Aha approach. A volcano plot showing the ratios of the shared proteins during the regrowth of WT persister cells versus untreated cells, calculated via label free quantification (LFQ). Persisters were obtained by treating stationary-phase cells with ciprofloxacin for 4 h. The persister regrowth experiments were labeled with Aha. Newly synthesized proteins were enriched for LC-MS/MS analysis. Red points indicate proteins involved in pyochelin pathway. Samples were collected from three replicates.

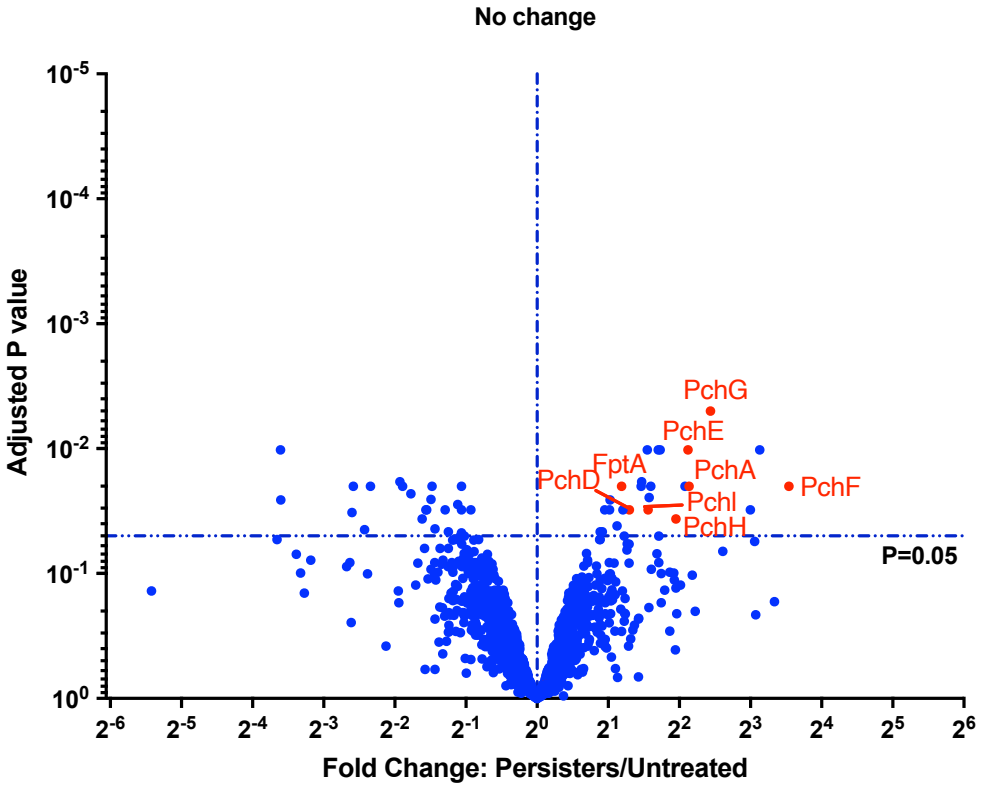

Figure 3.6. Integrated total proteins identified in the regrowth of *higA*::Tn persister and untreated cells with Aha approach. A volcano plot showing the ratios of the shared proteins during the regrowth of *higA*::Tn persister cells versus untreated cells, calculated via label free quantification (LFQ). Persisters were obtained by treating stationary-phase cells with ciprofloxacin for 4 h. The persister regrowth experiments were labeled with Aha. Newly synthesized proteins were enriched for LC-MS/MS analysis. Red points indicate proteins involved in pyochelin pathway. Samples were collected from three replicates.

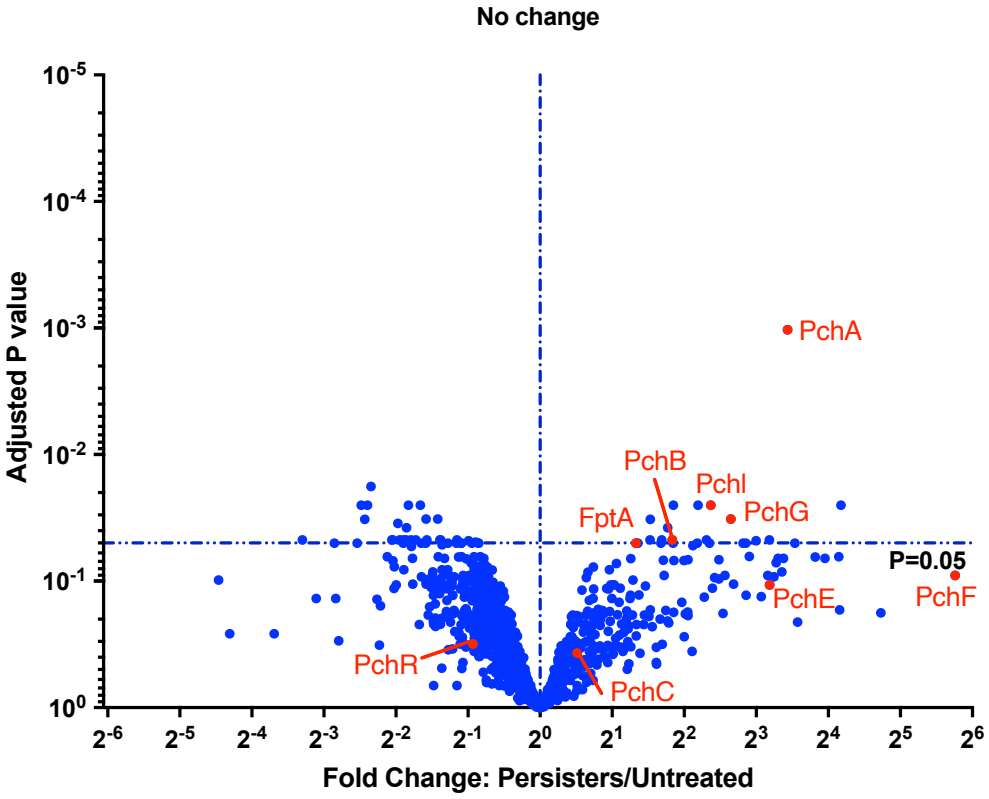

Table 3.1. Comparison of fold changes involved in various studies in persister formation and persister regrowth. Data of DNA microarray and RNAseq were retrieved from (Li et al., 2016; Wood & Wood, 2016). Both studies used HigB overproduction to induce a higher percentage of persister cells. BONCAT for entering persister was conducted by Mark van Eldijk from Tirrell laboratory at the California Institute of Technology (results are not published). Pyochelin-related genes/proteins showed a down-regulation in entering the persistence state and an up-regulation in exiting the persistence state.

	Overproduction of HigB		Entering persister	Exiting persister	Exiting persister
Gene/Protein	Fold change	Fold change	Fold change	Fold change	Fold change
Method	DNA microarray	RNAseq	BONCAT (Anl)	BONCAT (Anl)	BONCAT (Aha)
Comparison	P/U (*higA*::Tn)	P/U (*higA*::Tn)	P/U (NLL-MetRS)	P/U (NLL-MetRS)	P/U (WT)
fptA/FptA	-6.1	-2.7	-1.8	3.5	2.3
pchA/PchA	-7.5	N.A.	-3.7	2.7	4.4
pchB/PchB	-9.2	-3.0	-2.5	3.8	2.4
pchC/PchC	-6.1	-2.2	-4.2	Appear only in persister	1.5
pchD/PchD	-4.6	-2.8	-1.5	3.0	2.5
pchE/PchE	-4.9	N.A.	-2.8	5.6	4.4
pchF/PchF	-4.0	-2.9	-4.3	3.7	11.6
pchG/PchG	-4.9	N.A.	-1.6	Appear only in persister	5.4
pchH/PchH	N.A.	N.A.	-0.4	Appear only in persister	3.9
pchR/PchR	-2.6	N.A.	-2.8	2.2	1.1

3.8. References

Ankenbauer, R. G., & Quan, H. N. (1994). FptA, the Fe(III)-Pyochelin Receptor of *Pseudomonas aeruginosa*: a Phenolate Siderophore Receptor Homologous to Hydroxamate Siderophore Receptors. *Journal of Bacteriology*, *176*(2), 307–319. https://doi.org/10.1128/jb.176.2.307-319.1994

Antipov, S. S., Tutukina, M. N., Preobrazhenskaya, E. v., Kondrashov, F. A., Patrushev, M. v., Toshchakov, S. v., Dominova, I., Shvyreva, U. S., Vrublevskaya, V. v., Morenkov, O. S., Sukharicheva, N. A., Panyukov, V. v., & Ozoline, O. N. (2017). The Nucleoid Protein Dps Binds Genomic DNA of *Escherichia coli* in a Non-Random Manner. *PLOS ONE*, *12*(8), e0182800. https://doi.org/10.1371/journal.pone.0182800

Babin, B. M., Atangcho, L., van Eldijk, M. B., Sweredoski, M. J., Moradian, A., Hess, S., Tolker-Nielsen, T., Newman, D. K., & Tirrell, D. A. (2017). Selective Proteomic Analysis of Antibiotic-Tolerant Cellular Subpopulations in *Pseudomonas aeruginosa* Biofilms. *MBio*, *8*(5). https://doi.org/10.1128/mBio.01593-17

Babin, B. M., Bergkessel, M., Sweredoski, M. J., Moradian, A., Hess, S., Newman, D. K., & Tirrell, D. A. (2016). SutA is a Bacterial Transcription Factor Expressed during Slow Growth in *Pseudomonas aeruginosa*. *Proceedings of the National Academy of Sciences*, *113*(5). https://doi.org/10.1073/pnas.1514412113

Bailey, T. L., Johnson, J., Grant, C. E., & Noble, W. S. (2015). The MEME Suite. *Nucleic Acids Research*, *43*(W1), W39–W49. https://doi.org/10.1093/nar/gkv416

Balaban, N. Q., Helaine, S., Lewis, K., Ackermann, M., Aldridge, B., Andersson, D. I., Brynildsen, M. P., Bumann, D., Camilli, A., Collins, J. J., Dehio, C., Fortune, S., Ghigo, J.-M., Hardt, W.-D., Harms, A., Heinemann, M., Hung, D. T., Jenal, U., Levin, B. R., … Zinkernagel, A. (2019). Definitions and Guidelines for

Research on Antibiotic Persistence. *Nature Reviews Microbiology*, *17*(7), 441–448. https://doi.org/10.1038/s41579-019-0196-3

Balaban, N. Q., Merrin, J., Chait, R., Kowalik, L., & Leibler, S. (2004). Bacterial Persistence as a Phenotypic Switch. *Science*, *305*(5690), 1622–1625. https://doi.org/10.1126/science.1099390

Benjamini, Y., & Hochberg, Y. (1995). Controlling the False Discovery Rate: A Practical and Powerful Approach to Multiple Testing. *Journal of the Royal Statistical Society: Series B (Methodological)*, *57*(1), 289–300. https://doi.org/10.1111/j.2517-6161.1995.tb02031.x

Bokinsky, G., Baidoo, E. E. K., Akella, S., Burd, H., Weaver, D., Alonso-Gutierrez, J., Garcia-Martin, H., Lee, T. S., & Keasling, J. D. (2013). HipA-Triggered Growth Arrest and -Lactam Tolerance in *Escherichia coli* Are Mediated by RelA-Dependent ppGpp Synthesis. *Journal of Bacteriology*, *195*(14), 3173–3182. https://doi.org/10.1128/JB.02210-12

Brandel, J., Humbert, N., Elhabiri, M., Schalk, I. J., Mislin, G. L. A., & Albrecht-Gary, A.-M. (2012). Pyochelin, a Siderophore of *Pseudomonas aeruginosa*: Physicochemical Characterization of the Iron(iii), Copper(ii) and Zinc(ii) Complexes. *Dalton Transactions*, *41*(9), 2820. https://doi.org/10.1039/c1dt11804h

Breidenstein, E. B. M., Khaira, B. K., Wiegand, I., Overhage, J., & Hancock, R. E. W. (2008). Complex Ciprofloxacin Resistome Revealed by Screening a *Pseudomonas aeruginosa* Mutant Library for Altered Susceptibility. *Antimicrobial Agents and Chemotherapy*, *52*(12), 4486–4491. https://doi.org/10.1128/AAC.00222-08

Buerger, S., Spoering, A., Gavrish, E., Leslin, C., Ling, L., & Epstein, S. S. (2012). Microbial Scout Hypothesis, Stochastic Exit from Dormancy, and the Nature of Slow Growers. *Applied and Environmental Microbiology*, *78*(9), 3221–3228. https://doi.org/10.1128/AEM.07307-11

Burns, J. L., Van Dalfsen, J. M., Shawar, R. M., Otto, K. L., Garber, R. L., Quan, J. M., Montgomery, A. B., Albers, G. M., Ramsey, B. W., & Smith, A. L. (1999).

Effect of Chronic Intermittent Administration of Inhaled Tobramycin on Respiratory Microbial Flora in Patients with Cystic Fibrosis. *The Journal of Infectious Diseases*, *179*(5), 1190–1196. https://doi.org/10.1086/314727

Cheverton, A. M., Gollan, B., Przydacz, M., Wong, C. T., Mylona, A., Hare, S. A., & Helaine, S. (2016). A Salmonella Toxin Promotes Persister Formation through Acetylation of tRNA. *Molecular Cell*, *63*(1), 86–96. https://doi.org/10.1016/j.molcel.2016.05.002

Cho, J., Rogers, J., Kearns, M., Leslie, M., Hartson, S. D., & Wilson, K. S. (2015). *Escherichia coli* Persister Cells Suppress Translation by Selectively Disassembling and Degrading Their Ribosomes. *Molecular Microbiology*, *95*(2), 352–364. https://doi.org/10.1111/mmi.12884

Chowdhury, N., Wood, T. L., Martínez-Vázquez, M., García-Contreras, R., & Wood, T. K. (2016). DNA-Crosslinker Cisplatin Eradicates Bacterial Persister Cells. *Biotechnology and Bioengineering*, *113*(9), 1984–1992. https://doi.org/10.1002/bit.25963

Conlon, B. P., Rowe, S. E., Gandt, A. B., Nuxoll, A. S., Donegan, N. P., Zalis, E. A., Clair, G., Adkins, J. N., Cheung, A. L., & Lewis, K. (2016). Persister Formation in *Staphylococcus aureus* Is Associated with ATP Depletion. *Nature Microbiology*, *1*(5), 16051. https://doi.org/10.1038/nmicrobiol.2016.51

Cornelis, P., & Dingemans, J. (2013). *Pseudomonas aeruginosa* Adapts Its Iron Uptake Strategies in Function of the Type of Infections. *Frontiers in Cellular and Infection Microbiology*, *3*. https://doi.org/10.3389/fcimb.2013.00075

Coskun, U. S. S. (2018). Effect of MazEF, HigBA and RelBE Toxin-Antitoxin Systems on Antibiotic Resistance in *Pseudomonas aeruginosa* and *Staphylococcus* Isolates. *Malawi Medical Journal*, *30*(2), 67. https://doi.org/10.4314/mmj.v30i2.3

Cox, C. D. (1982). Effect of Pyochelin on the Virulence of *Pseudomonas aeruginosa*. *Infection and Immunity*, *36*(1), 17–23. https://doi.org/10.1128/iai.36.1.17-23.1982

Cox, C. D., Rinehart, K. L., Moore, M. L., & Cook, J. C. (1981). Pyochelin: Novel Structure of an Iron-Chelating Growth Promoter for *Pseudomonas aeruginosa*. *Proceedings of the National Academy of Sciences*, *78*(7), 4256–4260. https://doi.org/10.1073/pnas.78.7.4256

Cox, J., Hein, M. Y., Luber, C. A., Paron, I., Nagaraj, N., & Mann, M. (2014). Accurate Proteome-Wide Label-Free Quantification by Delayed Normalization and Maximal Peptide Ratio Extraction, Termed MaxLFQ. *Molecular & Cellular Proteomics*, *13*(9), 2513–2526. https://doi.org/10.1074/mcp.M113.031591

Cox, J., & Mann, M. (2008). MaxQuant Enables High Peptide Identification Rates, Individualized p.p.b.-Range Mass Accuracies and Proteome-Wide Protein Quantification. *Nature Biotechnology*, *26*(12), 1367–1372. https://doi.org/10.1038/nbt.1511

Dieterich, D. C., Lee, J. J., Link, A. J., Graumann, J., Tirrell, D. A., & Schuman, E. M. (2007). Labeling, Detection and Identification of Newly Synthesized Proteomes with Bioorthogonal Non-Canonical Amino-Acid Tagging. *Nature Protocols*, *2*(3), 532–540. https://doi.org/10.1038/nprot.2007.52

Dieterich, D. C., Link, A. J., Graumann, J., Tirrell, D. A., & Schuman, E. M. (2006). Selective Identification of Newly Synthesized Proteins in Mammalian Cells using Bioorthogonal Noncanonical Amino Acid Tagging (BONCAT). *Proceedings of the National Academy of Sciences*, *103*(25), 9482–9487. https://doi.org/10.1073/pnas.0601637103

Dörr, T., Vulić, M., & Lewis, K. (2010). Ciprofloxacin Causes Persister Formation by Inducing the TisB Toxin in *Escherichia coli*. *PLoS Biology*, *8*(2), e1000317. https://doi.org/10.1371/journal.pbio.1000317

Fauvart, M., de Groote, V. N., & Michiels, J. (2011). Role of Persister Cells in Chronic Infections: Clinical Relevance and Perspectives on Anti-Persister Therapies. *Journal of Medical Microbiology*, *60*(6), 699–709. https://doi.org/10.1099/jmm.0.030932-0

Fridman, O., Goldberg, A., Ronin, I., Shoresh, N., & Balaban, N. Q. (2014). Optimization of Lag Time Underlies Antibiotic Tolerance in Evolved Bacterial Populations. *Nature*, *513*(7518), 418–421. https://doi.org/10.1038/nature13469

Gibson, R. L., Burns, J. L., & Ramsey, B. W. (2003). Pathophysiology and Management of Pulmonary Infections in Cystic Fibrosis. *American Journal of Respiratory and Critical Care Medicine*, *168*(8), 918–951. https://doi.org/10.1164/rccm.200304-505SO

Gilligan, P. H. (2006). Is There Value in Susceptibility Testing of *Pseudomonas aeruginosa* Causing Chronic Infection in Patients with Cystic Fibrosis? *Expert Review of Anti-Infective Therapy*, *4*(5), 711–715. https://doi.org/10.1586/14787210.4.5.711

Goneau, L. W., Yeoh, N. S., MacDonald, K. W., Cadieux, P. A., Burton, J. P., Razvi, H., & Reid, G. (2014). Selective Target Inactivation Rather than Global Metabolic Dormancy Causes Antibiotic Tolerance in Uropathogens. *Antimicrobial Agents and Chemotherapy*, *58*(4), 2089–2097. https://doi.org/10.1128/AAC.02552-13

Goormaghtigh, F., Fraikin, N., Putrinš, M., Hallaert, T., Hauryliuk, V., Garcia-Pino, A., Sjödin, A., Kasvandik, S., Udekwu, K., Tenson, T., Kaldalu, N., & van Melderen, L. (2018). Reassessing the Role of Type II Toxin-Antitoxin Systems in Formation of Escherichia coli Type II Persister Cells. *MBio*, *9*(3). https://doi.org/10.1128/mBio.00640-18

Guo, Y., Sun, C., Li, Y., Tang, K., Ni, S., & Wang, X. (2019). Antitoxin HigA Inhibits Virulence Gene *mvfR* Expression in *Pseudomonas aeruginosa*. *Environmental Microbiology*, *21*(8), 2707–2723. https://doi.org/10.1111/1462-2920.14595

Harms, A., Maisonneuve, E., & Gerdes, K. (2016). Mechanisms of Bacterial Persistence during Stress and Antibiotic Exposure. *Science*, *354*(6318). https://doi.org/10.1126/science.aaf4268

Harrison, J. J., Wade, W. D., Akierman, S., Vacchi-Suzzi, C., Stremick, C. A., Turner, R. J., & Ceri, H. (2009). The Chromosomal Toxin Gene *yafQ* Is a

Determinant of Multidrug Tolerance for *Escherichia coli* Growing in a Biofilm. *Antimicrobial Agents and Chemotherapy*, *53*(6), 2253–2258. https://doi.org/10.1128/AAC.00043-09

Heinrichs, D. E., & Poole, K. (1996). PchR, a Regulator of Ferripyochelin Receptor Gene (*fptA*) Expression in *Pseudomonas aeruginosa*, Functions Both as an Activator and as a Repressor. *Journal of Bacteriology*, *178*(9), 2586–2592. https://doi.org/10.1128/jb.178.9.2586-2592.1996

Hobby, G. L., Meyer, K., & Chaffee, E. (1942). Observations on the Mechanism of Action of Penicillin. *Experimental Biology and Medicine*, *50*(2), 281–285. https://doi.org/10.3181/00379727-50-13773

Honarmand Ebrahimi, K., Hagedoorn, P.-L., & Hagen, W. R. (2015). Unity in the Biochemistry of the Iron-Storage Proteins Ferritin and Bacterioferritin. *Chemical Reviews*, *115*(1), 295–326. https://doi.org/10.1021/cr5004908

Høyland-Kroghsbo, N. M., Muñoz, K. A., & Bassler, B. L. (2018). Temperature, by Controlling Growth Rate, Regulates CRISPR-Cas Activity in *Pseudomonas aeruginosa*. *MBio*, *9*(6). https://doi.org/10.1128/mBio.02184-18

Jõers, A., Kaldalu, N., & Tenson, T. (2010). The Frequency of Persisters in *Escherichia coli* Reflects the Kinetics of Awakening from Dormancy. *Journal of Bacteriology*, *192*(13), 3379–3384. https://doi.org/10.1128/JB.00056-10

Kalli, A., & Hess, S. (2012). Effect of Mass Spectrometric Parameters on Peptide and Protein Identification Rates for Shotgun Proteomic Experiments on an LTQ-Orbitrap Mass Analyzer. *PROTEOMICS*, *12*(1), 21–31. https://doi.org/10.1002/pmic.201100464

Kaplan, A. R., Musaev, D. G., & Wuest, W. M. (2021). Pyochelin Biosynthetic Metabolites Bind Iron and Promote Growth in *Pseudomonads* Demonstrating Siderophore-like Activity. *ACS Infectious Diseases*, *7*(3), 544–551. https://doi.org/10.1021/acsinfecdis.0c00897

Kayama, S., Murakami, K., Ono, T., Ushimaru, M., Yamamoto, A., Hirota, K., & Miyake, Y. (2009). The Role of *rpoS* Gene and Quorum-Sensing System in

Ofloxacin Tolerance in *Pseudomonas aeruginosa*. *FEMS Microbiology Letters*, *298*(2), 184–192. https://doi.org/10.1111/j.1574-6968.2009.01717.x

Keren, I., Kaldalu, N., Spoering, A., Wang, Y., & Lewis, K. (2004). Persister Cells and Tolerance to Antimicrobials. *FEMS Microbiology Letters*, *230*(1), 13–18. https://doi.org/10.1016/S0378-1097(03)00856-5

Kim, Y., & Wood, T. K. (2010). Toxins Hha and CspD and Small RNA Regulator Hfq Are Involved in Persister Cell Formation through MqsR in *Escherichia coli*. *Biochemical and Biophysical Research Communications*, *391*(1), 209–213. https://doi.org/10.1016/j.bbrc.2009.11.033

King, E. O., Ward, M. K., & Raney, D. E. (1954). Two Simple Media for the Demonstration of Pyocyanin and Fluorescin. *The Journal of Laboratory and Clinical Medicine*, *44*(2), 301–307.

Kwan, B. W., Chowdhury, N., & Wood, T. K. (2015). Combatting Bacterial Infections by Killing Persister Cells with Mitomycin C. *Environmental Microbiology*, *17*(11), 4406–4414. https://doi.org/10.1111/1462-2920.12873

LaBauve, A. E., & Wargo, M. J. (2012). Growth and Laboratory Maintenance of *Pseudomonas aeruginosa*. *Current Protocols in Microbiology*, *25*(1). https://doi.org/10.1002/9780471729259.mc06e01s25

Lemke, J. J., Sanchez-Vazquez, P., Burgos, H. L., Hedberg, G., Ross, W., & Gourse, R. L. (2011). Direct Regulation of *Escherichia coli* Ribosomal Protein Promoters by the Transcription Factors ppGpp and DksA. *Proceedings of the National Academy of Sciences*, *108*(14), 5712–5717. https://doi.org/10.1073/pnas.1019383108

Levin-Reisman, I., & Balaban, N. Q. (2016). *Quantitative Measurements of Type I and Type II Persisters Using ScanLag* (pp. 75–81). https://doi.org/10.1007/978-1-4939-2854-5_7

Levin-Reisman, I., Fridman, O., & Balaban, N. Q. (2014). ScanLag: High-Throughput Quantification of Colony Growth and Lag Time. *Journal of Visualized Experiments*, *89*. https://doi.org/10.3791/51456

Levin-Reisman, I., Gefen, O., Fridman, O., Ronin, I., Shwa, D., Sheftel, H., & Balaban, N. Q. (2010). Automated Imaging with ScanLag Reveals Previously Undetectable Bacterial Growth Phenotypes. *Nature Methods*, *7*(9), 737–739. https://doi.org/10.1038/nmeth.1485

Lewis, K. (2007). Persister Cells, Dormancy and Infectious Disease. *Nature Reviews Microbiology*, *5*(1), 48–56. https://doi.org/10.1038/nrmicro1557

Li, G., Shen, M., Lu, S., Le, S., Tan, Y., Wang, J., Zhao, X., Shen, W., Guo, K., Yang, Y., Zhu, H., Rao, X., Hu, F., & Li, M. (2016). Identification and Characterization of the HicAB Toxin-Antitoxin System in the Opportunistic Pathogen *Pseudomonas aeruginosa*. *Toxins*, *8*(4), 113. https://doi.org/10.3390/toxins8040113

Li, M., Long, Y., Liu, Y., Liu, Y., Chen, R., Shi, J., Zhang, L., Jin, Y., Yang, L., Bai, F., Jin, S., Cheng, Z., & Wu, W. (2016). HigB of *Pseudomonas aeruginosa* Enhances Killing of Phagocytes by Up-Regulating the Type III Secretion System in Ciprofloxacin Induced Persister Cells. *Frontiers in Cellular and Infection Microbiology*, *6*. https://doi.org/10.3389/fcimb.2016.00125

Liberati, N. T., Urbach, J. M., Miyata, S., Lee, D. G., Drenkard, E., Wu, G., Villanueva, J., Wei, T., & Ausubel, F. M. (2006). An Ordered, Nonredundant Library of *Pseudomonas aeruginosa* Strain PA14 Transposon Insertion Mutants. *Proceedings of the National Academy of Sciences*, *103*(8), 2833–2838. https://doi.org/10.1073/pnas.0511100103

Lyczak, J. B., Cannon, C. L., & Pier, G. B. (2002). Lung Infections Associated with Cystic Fibrosis. *Clinical Microbiology Reviews*, *15*(2), 194–222. https://doi.org/10.1128/CMR.15.2.194-222.2002

Maisonneuve, E., & Gerdes, K. (2014). Molecular Mechanisms Underlying Bacterial Persisters. *Cell*, *157*(3), 539–548. https://doi.org/10.1016/j.cell.2014.02.050

Mok, W. W. K., & Brynildsen, M. P. (2018). Timing of DNA Damage Responses Impacts Persistence to Fluoroquinolones. *Proceedings of the National Academy of Sciences*, *115*(27). https://doi.org/10.1073/pnas.1804218115

Möker, N., Dean, C. R., & Tao, J. (2010). *Pseudomonas aeruginosa* Increases Formation of Multidrug-Tolerant Persister Cells in Response to Quorum-Sensing Signaling Molecules. *Journal of Bacteriology*, *192*(7), 1946–1955. https://doi.org/10.1128/JB.01231-09

Mulcahy, L. R., Burns, J. L., Lory, S., & Lewis, K. (2010). Emergence of *Pseudomonas aeruginosa* Strains Producing High Levels of Persister Cells in Patients with Cystic Fibrosis. *Journal of Bacteriology*, *192*(23), 6191–6199. https://doi.org/10.1128/JB.01651-09

Murakami, K., Ono, T., Viducic, D., Kayama, S., Mori, M., Hirota, K., Nemoto, K., & Miyake, Y. (2005). Role for *rpoS* Gene of *Pseudomonas aeruginosa* in Antibiotic Tolerance. *FEMS Microbiology Letters*, *242*(1), 161–167. https://doi.org/10.1016/j.femsle.2004.11.005

Muthuramalingam, M., White, J. C., Murphy, T., Ames, J. R., & Bourne, C. R. (2019). The Toxin from a ParDE Toxin-Antitoxin System Found in *Pseudomonas aeruginosa* Offers Protection to Cells Challenged with Anti-Gyrase Antibiotics. *Molecular Microbiology*, *111*(2), 441–454. https://doi.org/10.1111/mmi.14165

Nakatsuji, S., Okumura, K., Takase, R., Watanabe, D., Mikami, B., & Hashimoto, W. (2022). Crystal Structures of EfeB and EfeO in a Bacterial Siderophore-Independent Iron Transport System. *Biochemical and Biophysical Research Communications*, *594*, 124–130. https://doi.org/10.1016/j.bbrc.2022.01.055

Ngo, J. T., Champion, J. A., Mahdavi, A., Tanrikulu, I. C., Beatty, K. E., Connor, R. E., Yoo, T. H., Dieterich, D. C., Schuman, E. M., & Tirrell, D. A. (2009). Cell-Selective Metabolic Labeling of Proteins. *Nature Chemical Biology*, *5*(10), 715–717. https://doi.org/10.1038/nchembio.200

Pontes, M. H., & Groisman, E. A. (2019). Slow Growth Determines Nonheritable Antibiotic Resistance in *Salmonella enterica*. *Science Signaling*, *12*(592). https://doi.org/10.1126/scisignal.aax3938

Potrykus, K., Murphy, H., Philippe, N., & Cashel, M. (2011). ppGpp is the Major Source of Growth Rate Control in *E. coli*. *Environmental Microbiology*, *13*(3), 563–575. https://doi.org/10.1111/j.1462-2920.2010.02357.x

Pu, Y., Zhao, Z., Li, Y., Zou, J., Ma, Q., Zhao, Y., Ke, Y., Zhu, Y., Chen, H., Baker, M. A. B., Ge, H., Sun, Y., Xie, X. S., & Bai, F. (2016). Enhanced Efflux Activity Facilitates Drug Tolerance in Dormant Bacterial Cells. *Molecular Cell*, *62*(2), 284–294. https://doi.org/10.1016/j.molcel.2016.03.035

Py, B., Gerez, C., Huguenot, A., Vidaud, C., Fontecave, M., Ollagnier de Choudens, S., & Barras, F. (2018). The ErpA/NfuA Complex Builds an Oxidation-Resistant Fe-S Cluster Delivery Pathway. *Journal of Biological Chemistry*, *293*(20), 7689–7702. https://doi.org/10.1074/jbc.RA118.002160

Reimmann, C., Patel, H. M., Serino, L., Barone, M., Walsh, C. T., & Haas, D. (2001). Essential PchG-Dependent Reduction in Pyochelin Biosynthesis of *Pseudomonas aeruginosa*. *Journal of Bacteriology*, *183*(3), 813–820. https://doi.org/10.1128/JB.183.3.813-820.2001

Ritchie, M. E., Phipson, B., Wu, D., Hu, Y., Law, C. W., Shi, W., & Smyth, G. K. (2015). *limma* Powers Differential Expression Analyses for RNA-Sequencing and Microarray Studies. *Nucleic Acids Research*, *43*(7), e47–e47. https://doi.org/10.1093/nar/gkv007

Roche, B., Garcia-Rivera, M. A., Normant, V., Kuhn, L., Hammann, P., Brönstrup, M., Mislin, G. L. A., & Schalk, I. J. (2022). A Role for <scp>PchHI</scp> as the <scp>ABC</scp> Transporter in Iron Acquisition by the Siderophore Pyochelin in *Pseudomonas aeruginosa*. *Environmental Microbiology*, *24*(2), 866–877. https://doi.org/10.1111/1462-2920.15811

Rotem, E., Loinger, A., Ronin, I., Levin-Reisman, I., Gabay, C., Shoresh, N., Biham, O., & Balaban, N. Q. (2010). Regulation of Phenotypic Variability by a Threshold-Based Mechanism Underlies Bacterial Persistence. *Proceedings of the National Academy of Sciences*, *107*(28), 12541–12546. https://doi.org/10.1073/pnas.1004333107

Rowe, S. E., Conlon, B. P., Keren, I., & Lewis, K. (2016). *Persisters: Methods for Isolation and Identifying Contributing Factors—A Review* (pp. 17–28). https://doi.org/10.1007/978-1-4939-2854-5_2

Schalk, I. J., Rigouin, C., & Godet, J. (2020). An Overview of Siderophore Biosynthesis among Fluorescent *Pseudomonads* and New Insights into Their Complex Cellular Organization. *Environmental Microbiology*, *22*(4), 1447–1466. https://doi.org/10.1111/1462-2920.14937

Schwanhäusser, B., Busse, D., Li, N., Dittmar, G., Schuchhardt, J., Wolf, J., Chen, W., & Selbach, M. (2011). Global Quantification of Mammalian Gene Expression Control. *Nature*, *473*(7347), 337–342. https://doi.org/10.1038/nature10098

Semanjski, M., Gratani, F. L., Englert, T., Nashier, P., Beke, V., Nalpas, N., Germain, E., George, S., Wolz, C., Gerdes, K., & Macek, B. (2021). Proteome Dynamics during Antibiotic Persistence and Resuscitation. *MSystems*, *6*(4). https://doi.org/10.1128/mSystems.00549-21

Shan, Y., Brown Gandt, A., Rowe, S. E., Deisinger, J. P., Conlon, B. P., & Lewis, K. (2017). ATP-Dependent Persister Formation in *Escherichia coli*. *MBio*, *8*(1). https://doi.org/10.1128/mBio.02267-16

Silby, M. W., Winstanley, C., Godfrey, S. A. C., Levy, S. B., & Jackson, R. W. (2011). *Pseudomonas* Genomes: Diverse and Adaptable. *FEMS Microbiology Reviews*, *35*(4), 652–680. https://doi.org/10.1111/j.1574-6976.2011.00269.x

Sokol, P. A. (1987). Surface Expression of Ferripyochelin-Binding Protein is Required for Virulence of *Pseudomonas aeruginosa*. *Infection and Immunity*, *55*(9), 2021–2025. https://doi.org/10.1128/iai.55.9.2021-2025.1987

Spanka, D.-T., Konzer, A., Edelmann, D., & Berghoff, B. A. (2019). High-Throughput Proteomics Identifies Proteins with Importance to Postantibiotic Recovery in Depolarized Persister Cells. *Frontiers in Microbiology*, *10*. https://doi.org/10.3389/fmicb.2019.00378

Spoering, A. L., & Lewis, K. (2001). Biofilms and Planktonic Cells of *Pseudomonas aeruginosa* Have Similar Resistance to Killing by Antimicrobials. *Journal of*

Bacteriology, *183*(23), 6746–6751. https://doi.org/10.1128/JB.183.23.6746-6751.2001

Stojiljkovic, I., Bäumler, A. J., & Hantke, K. (1994). Fur Regulon in Gram-Negative Bacteria. *Journal of Molecular Biology*, *236*(2), 531–545. https://doi.org/10.1006/jmbi.1994.1163

Svenningsen, M. S., Veress, A., Harms, A., Mitarai, N., & Semsey, S. (2019). Birth and Resuscitation of (p)ppGpp Induced Antibiotic Tolerant Persister Cells. *Scientific Reports*, *9*(1), 6056. https://doi.org/10.1038/s41598-019-42403-7

Takahashi, Y., & Nakamura, M. (1999). Functional Assignment of the ORF2-*iscS-iscU-iscA-hscB-hscA-fdx*-ORF3 Gene Cluster Involved in the Assembly of Fe-S Clusters in *Escherichia coli*. *Journal of Biochemistry*, *126*(5), 917–926. https://doi.org/10.1093/oxfordjournals.jbchem.a022535

Takase, H., Nitanai, H., Hoshino, K., & Otani, T. (2000). Requirement of the *Pseudomonas aeruginosa tonB* Gene for High-Affinity Iron Acquisition and Infection. *Infection and Immunity*, *68*(8), 4498–4504. https://doi.org/10.1128/IAI.68.8.4498-4504.2000

Tanrikulu, I. C., Schmitt, E., Mechulam, Y., Goddard, W. A., & Tirrell, D. A. (2009). Discovery of *Escherichia coli* Methionyl-tRNA Synthetase Mutants for Efficient Labeling of Proteins with Azidonorleucine in *vivo*. *Proceedings of the National Academy of Sciences*, *106*(36), 15285–15290. https://doi.org/10.1073/pnas.0905735106

Tsakou, F., Jersie-Christensen, R., Jenssen, H., & Mojsoska, B. (2020). The Role of Proteomics in Bacterial Response to Antibiotics. *Pharmaceuticals*, *13*(9), 1–27. https://doi.org/10.3390/ph13090214

Völzing, K. G., & Brynildsen, M. P. (2015). Stationary-Phase Persisters to Ofloxacin Sustain DNA Damage and Require Repair Systems Only during Recovery. *MBio*, *6*(5). https://doi.org/10.1128/mBio.00731-15

Wang, J., Mushegian, A., Lory, S., & Jin, S. (1996). Large-Scale Isolation of Candidate Virulence Genes of *Pseudomonas aeruginosa* by in *vivo* Selection.

Proceedings of the National Academy of Sciences, *93*(19), 10434–10439. https://doi.org/10.1073/pnas.93.19.10434

Wilmaerts, D., Windels, E. M., Verstraeten, N., & Michiels, J. (2019). General Mechanisms Leading to Persister Formation and Awakening. *Trends in Genetics*, *35*(6), 401–411. https://doi.org/10.1016/j.tig.2019.03.007

Winsor, G. L., Griffiths, E. J., Lo, R., Dhillon, B. K., Shay, J. A., & Brinkman, F. S. L. (2016). Enhanced Annotations and Features for Comparing Thousands of *Pseudomonas* Genomes in the *Pseudomonas* Genome Database. *Nucleic Acids Research*, *44*(D1), D646–D653. https://doi.org/10.1093/nar/gkv1227

Winsor, G. L., Lam, D. K. W., Fleming, L., Lo, R., Whiteside, M. D., Yu, N. Y., Hancock, R. E. W., & Brinkman, F. S. L. (2011). Pseudomonas Genome Database: Improved Comparative Analysis and Population Genomics Capability for *Pseudomonas* Genomes. *Nucleic Acids Research*, *39*(Database), D596–D600. https://doi.org/10.1093/nar/gkq869

Wood, T. L., & Wood, T. K. (2016). The HigB/HigA Toxin/Antitoxin System of *Pseudomonas aeruginosa* Influences the Virulence Factors Pyochelin, Pyocyanin, and Biofilm Formation. *MicrobiologyOpen*, *5*(3), 499–511. https://doi.org/10.1002/mbo3.346

Xiao, G., Déziel, E., He, J., Lépine, F., Lesic, B., Castonguay, M.-H., Milot, S., Tampakaki, A. P., Stachel, S. E., & Rahme, L. G. (2006). MvfR, a Key *Pseudomonas aeruginosa* Pathogenicity LTTR-class Regulatory Protein, Has Dual Ligands. *Molecular Microbiology*, *62*(6), 1689–1699. https://doi.org/10.1111/j.1365-2958.2006.05462.x

Yamasaki, R., Song, S., Benedik, M. J., & Wood, T. K. (2020). Persister Cells Resuscitate Using Membrane Sensors that Activate Chemotaxis, Lower cAMP Levels, and Revive Ribosomes. *IScience*, *23*(1), 100792. https://doi.org/10.1016/j.isci.2019.100792

Zhou, J., Li, S., Li, H., Jin, Y., Bai, F., Cheng, Z., & Wu, W. (2021). Identification of a Toxin–Antitoxin System That Contributes to Persister Formation by

Reducing NAD in *Pseudomonas aeruginosa*. *Microorganisms*, *9*(4), 753. https://doi.org/10.3390/microorganisms9040753

3.9. Supplementary information

3.9.1. Gel visualization of Anl-labeled PA14 proteins in stationary phase

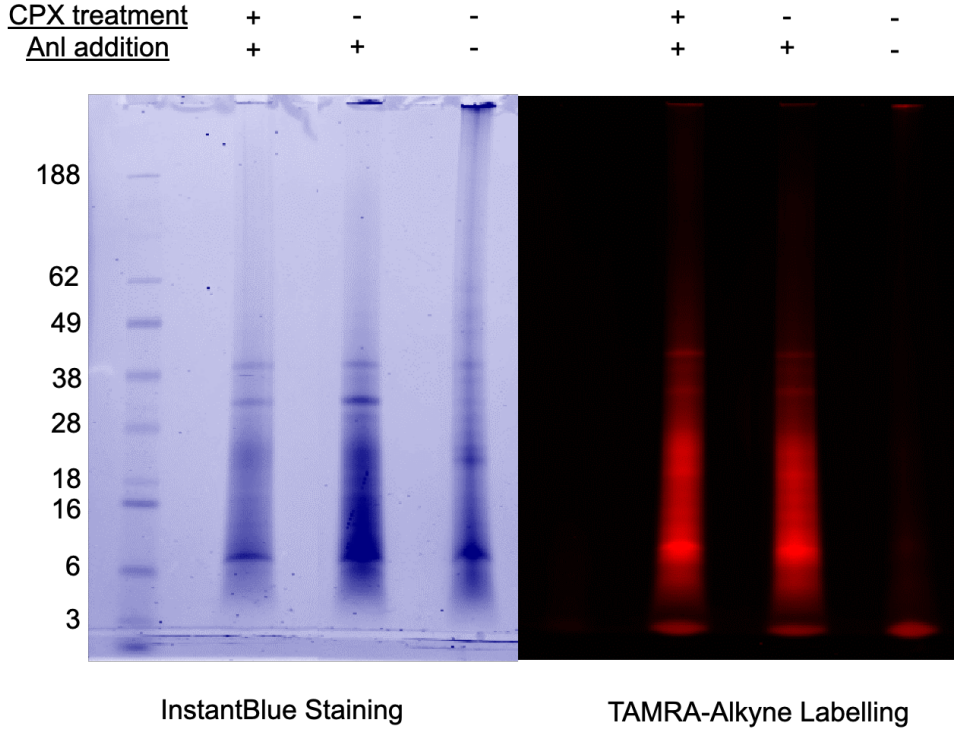

Figure 3.S1. Gel visualization of Anl-labeled proteins in each condition. Left: InstantBlue. Right: TAMRA labeling. Lane 1 refers to proteins extracted from lysates of recovered persister in stationary phase. Lane 2 refers to proteins extracted from untreated cell lysates. Lane 3 refers to negative control.

3.9.2. Comparison between proteome of recovered persisters and untreated cells in the stationary phase with BONCAT.

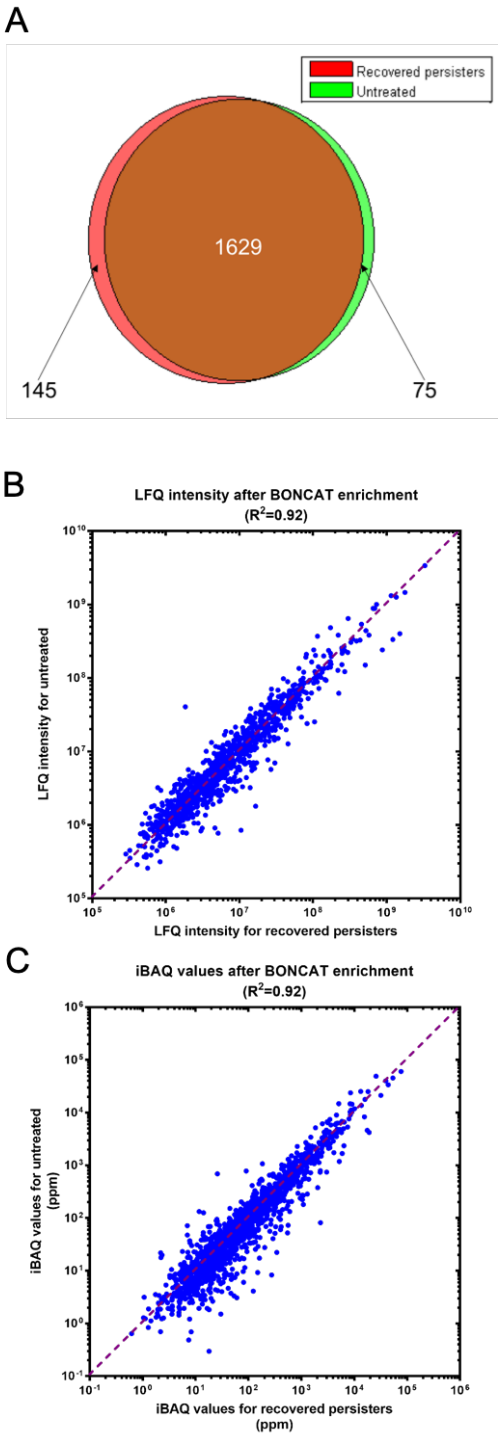

Figure 3.S2. Proteomic comparison between recovered persisters and untreated cells. (A) Venn diagram shows the total number of identified proteins in each condition and shared proteins between recovered persisters and untreated cells in section 3.3.4. (B) LFQ intensity for the two conditions after BONCAT enrichment experiment. (C) iBAQ values after BONCAT enrichment experiment.

3.9.3. Comparison between proteome of recovered persisters and untreated cells in the early exponential phase labeled with BONCAT.

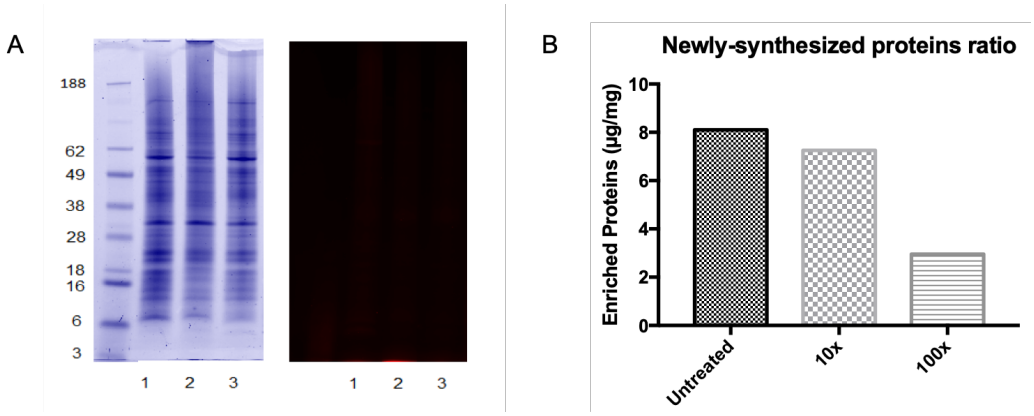

Figure 3.S3. Proteomic comparison at the early exponential phase. (A) Gel visualization of Anl-labeled proteins in early exponential phase in (1) untreated cells, (2) resuscitated persister initially diluted by 10x, and (3) resuscitated persister initially diluted by 100x, stained with InstantBlue (left) and TAMRA (right). (B) The ratios of the mass of newly-synthesized proteins over total loaded proteins for three conditions. The newly synthesized proteins were quantified by HPLC after the enrichment step. The loaded proteins were quantified by BCA assays before the enrichment step.

3.9.4. Revised labeling strategies for section 3.3.5 and 3.5.3.

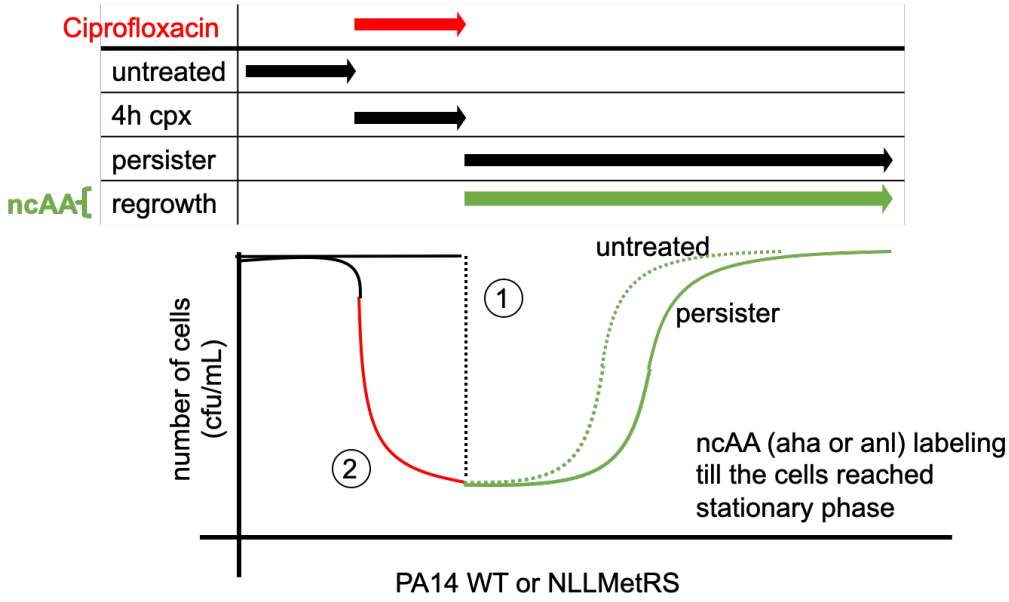

Figure 3.S4. Labeling strategies for cumulatively temporal comparison between untreated cells and persister cells. Stationary-phase cell cultures were (1) diluted or (2) treated with ciprofloxacin for 4 h. Starting from the time where the cells were suspended into fresh medium, the regrowth period was referring to the first 10 h for untreated cells, and the first 20 h for persister cells with a dilution factor of 100.

3.9.5. Gel visualization of Anl-labeled PA14 proteins during regrowth

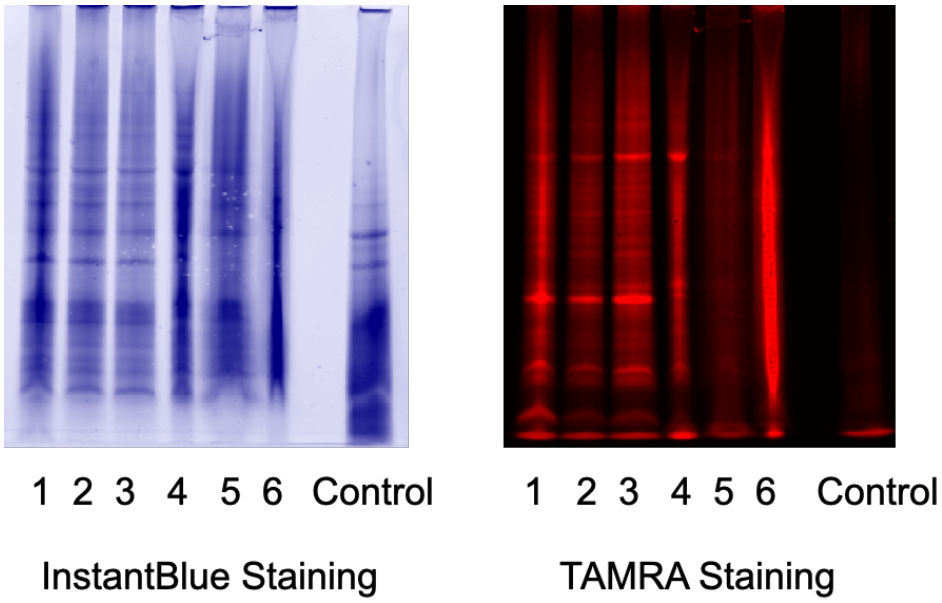

Figure 3.S5. In-gel visualization of Anl-labeled samples. Gel visualization of Anl-labeled proteins in untreated cells (1-3), recovered persister initially diluted by 100x (4-6), and a negative control without adding Anl, stained with InstantBlue (left) and TAMRA (right). For untreated cells, stationary-phase cells were diluted to 10^6 CFU/mL and resuspended into LB medium with Anl added and cultured for 10 h. For persisters, cultures at stationary phase were treated with ciprofloxacin (20 μg/ml) for 4 h. Washed cell pellets were diluted 100x and resuspended into fresh LB medium with Anl added and cultured for 20 h. Each condition was repeated three times. For control cells, stationary-phase cells were diluted to 10^6 CFU/mL and resuspended into LB medium without Anl and cultured for 10 h.

3.9.6. Survival rates of the transposon insertion mutants of pyochelin-related genes

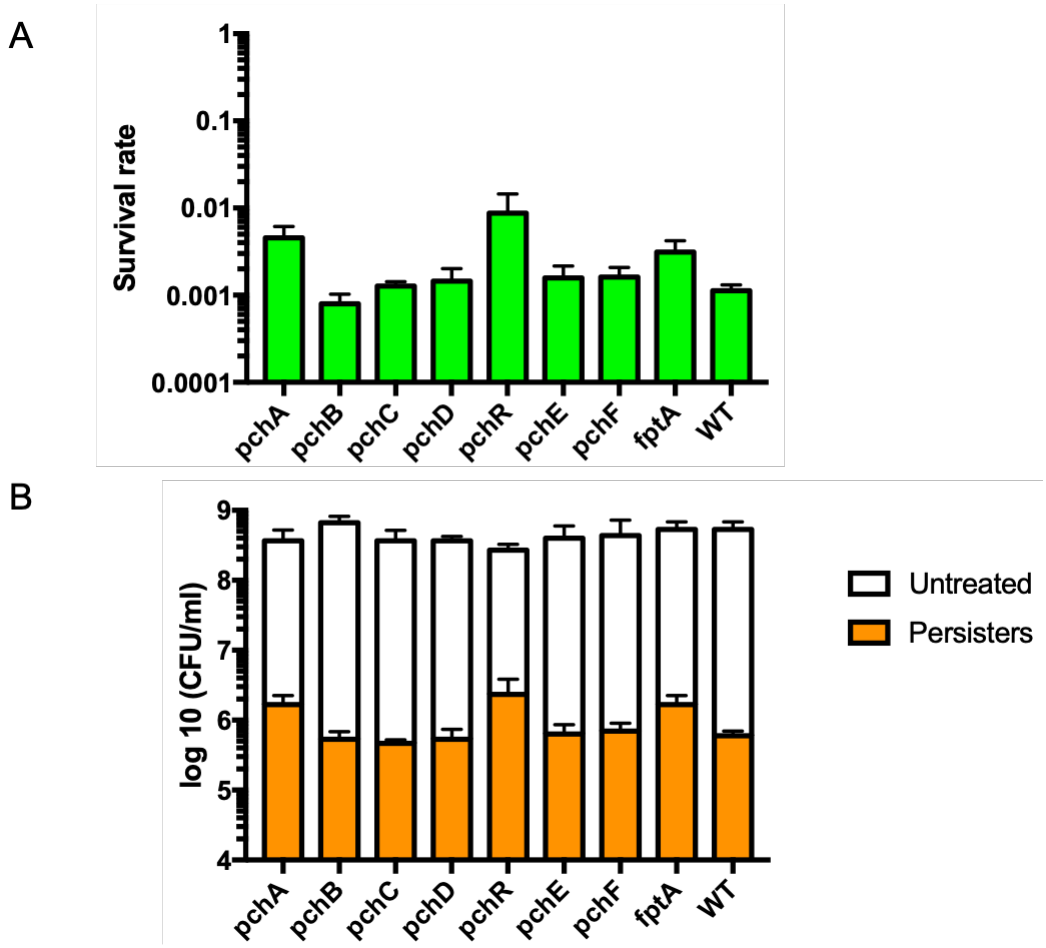

Figure. 3.S6. Effect of pyochelin-related genes on survival rates. (A) Survival rates of the transposon insertion mutants of pyochelin-related genes. (B) Survival rates of the above shown with the total population in CFU/ml. Ciprofloxacin was added to stationary-phase cell culture at 20 μg/ml for 4 h. CFU was recorded before and after ciprofloxacin treatment. CFUs were measured from three replicates at each condition.

3.9.7. Appearance times of the persisters of transposon insertion mutants of pyochelin-related genes

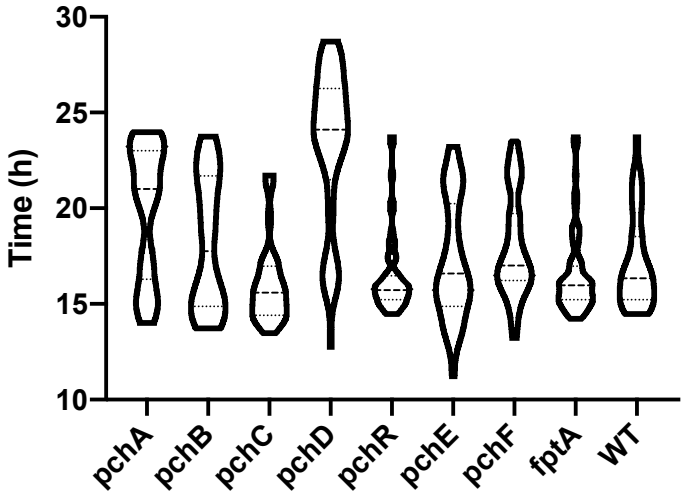

Figure 3.S7. Violin diagrams of the appearance times of the transposon insertion mutants of pyochelin-related genes with ScanLag. Persisters were obtained by treating stationary-phase cells with ciprofloxacin for 4 h. After washing the cell pellets, the appearance times were recorded with ScanLag.

3.9.8. Locating HigA in the BONCAT enrichment results

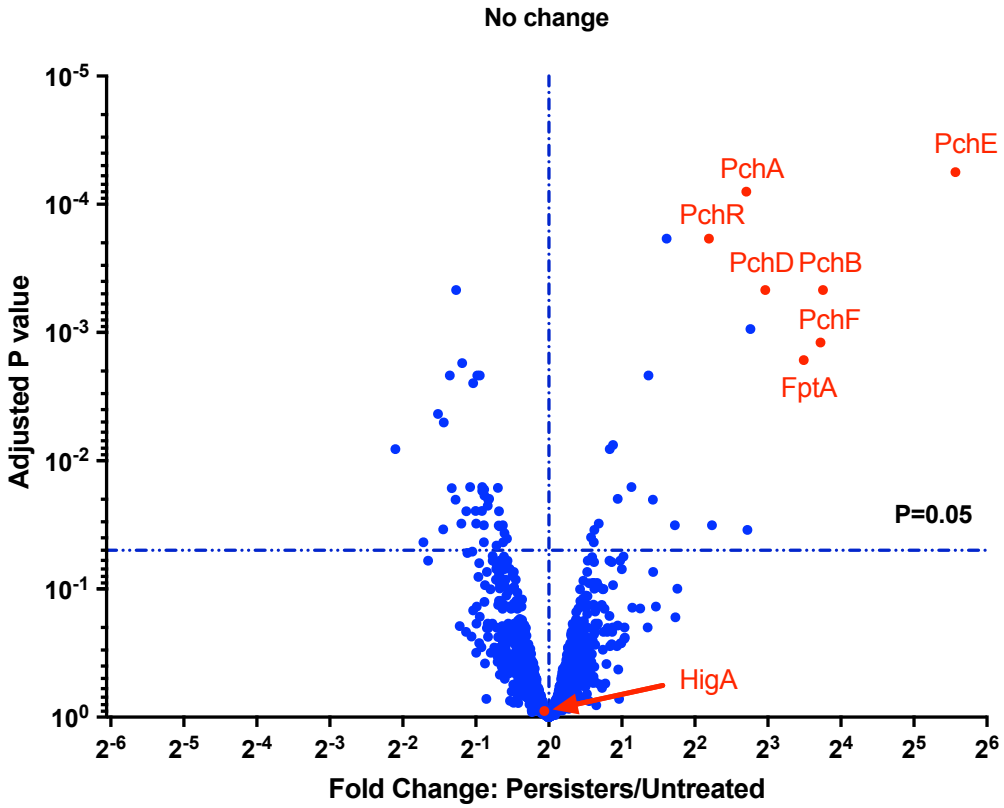

Figure 3.S8. HigA was located in the identified proteome of BONCAT enrichment results (red arrow). Position of HigA was marked in the volcano plot in Figure 3.3A.

3.9.9. Gel visualization of Aha-labeled proteins

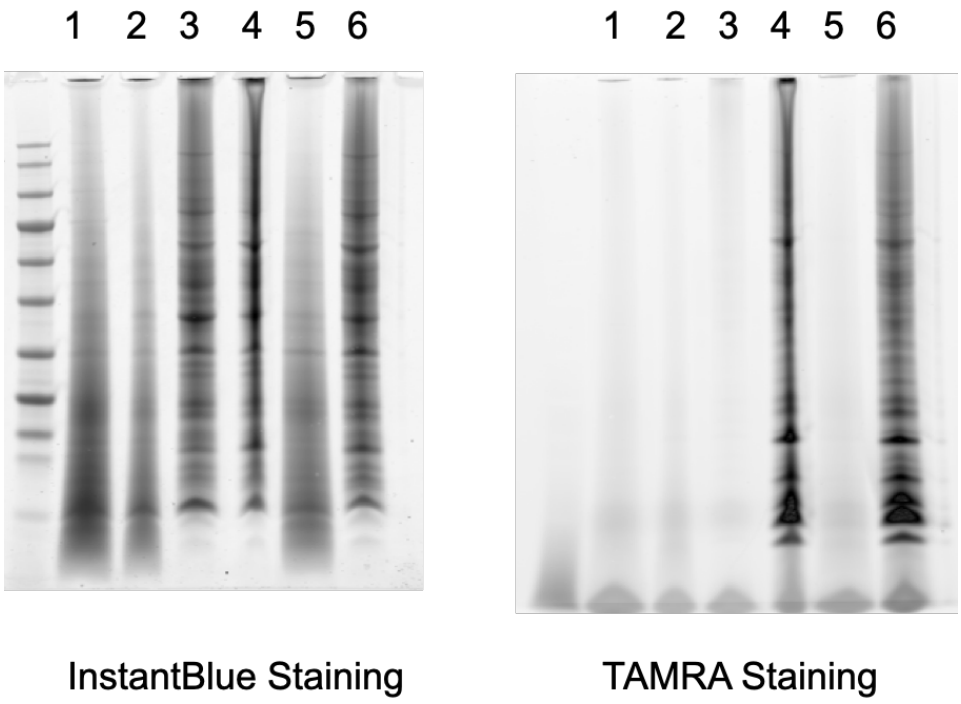

Figure 3.S9. In-gel visualation of Aha-labeled proteins. Gel visualization of Aha-labeled proteins in PA14 (1) WT proteins in LB medium, (2) WT proteins in LB medium + Aha, (3) WT proteins in minimal medium + (19 AAs + methionine (Met), (4) WT proteins in minimal medium + 19 AAs + Aha: Met = 30:1, (5) *higA*::Tn proteins in LB + Aha, (6) *higA*::Tn proteins + 19 AAs + Aha: Met = 30:1, stained with InstantBlue (left) and TAMRA (right)

3.9.10. Gel visualization of Aha-labeled proteins in the regrowth experiments

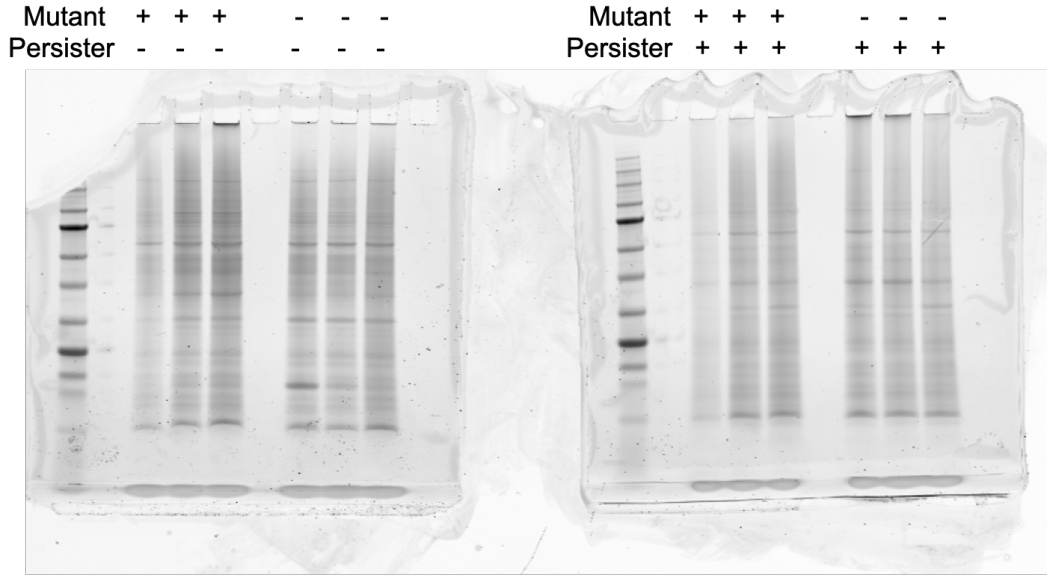

Figure 3.S10. Gel visualization of Aha-labeled proteins in three biological replicates of the samples in section 3.3.10 and 3.3.11. Persister (+) means proteins collected from the regrowth of persister cells; persister (-) means proteins collected from the regrowth of untreated cells; mutant (+) means proteins collected from the

regrowth of *higA*::Tn cells; mutant (-) means proteins collected from the regrowth of WT cells, stained with InstantBlue (top) and TAMRA (bottom).

3.9.11. Comparison between Anl-labeled method and Aha-labeled method

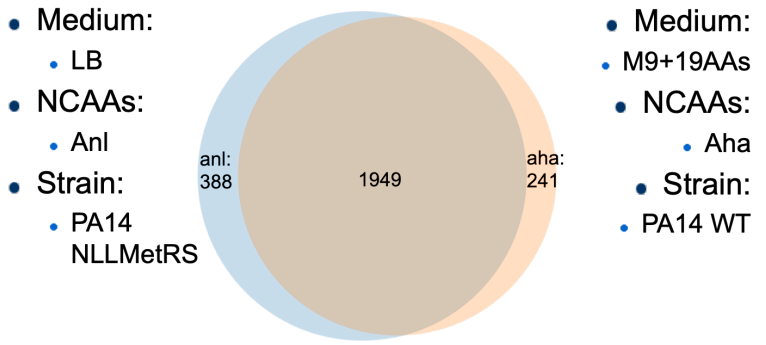

Figure 3.S11. Comparison of proteins identified in the BONCAT enrichment experiments: (left) PA14 NLL-MetRS strain labeled with Anl, as described in section 3.3.6; (right) PA14 WT strain labeled with Aha, as described in section 3.3.8.

3.9.12. Summary of the results of BONCAT enrichment experiments

PA Locus Tag	Protein Description	Gene Name	Fold Change (Persisters/Untreated)	Adjusted p value
PA14_09270	Pyochelin synthetase	*pchE*	47.48	5.62E-05
PA14_09220	Salicylate biosynthesis protein PchB	*pchB*	13.50	4.67E-04
PA14_09280	Pyochelin synthetase PchF	*pchF*	13.20	1.19E-03
PA14_09340	Fe(III)-pyochelin outer membrane receptor	*fptA*	11.23	1.64E-03
PA14_09240	Pyochelin biosynthesis protein PchD	*pchD*	7.80	4.67E-04
PA14_38220	Putative siderophore-interacting protein	-	6.79	9.40E-04
PA14_58000	Superoxide dismutase	*sodM*	6.59	3.46E-02
PA14_09210	Salicylate biosynthesis isochorismate synthase	*pchA*	6.51	7.95E-05

PA14_09380	Putative transporter	-	4.71	3.19E-02
PA14_09260	Transcriptional regulator PchR	*pchR*	4.58	1.85E-04
PA14_70740	Putative exported protein	-	3.31	3.19E-02
PA14_08070	Putative prophage major tail sheath protein	*gpFI*	3.06	1.85E-04
PA14_04150	Putative fumarylacetoacetate hydrolase family protein	*ycgM*	2.69	2.01E-02
PA14_70590	Uncharacterized protein	-	2.57	2.16E-03
PA14_28600	Uncharacterized protein	-	2.19	1.61E-02
PA14_61650	Lipid A deacylase	*pagL*	1.93	1.98E-02
PA14_56830	Insulin-cleaving metalloproteinase outer membrane	*icmP*	1.84	7.53E-03
PA14_03490	Alkyl hydroperoxide reductase AhpD	-	1.78	8.12E-03
PA14_72970	Protein TonB	*tonB*	1.61	3.09E-02

PA14_58870	NADH dehydrogenase	*ndh*	1.54	3.46E-02
PA14_51670	7-cyano-7-deazaguanine synthase	*queC*	1.53	4.32E-02
PA14_62200	Penicillin-binding protein 1B	*mrcB*	1.49	3.95E-02
PA14_22930	Glucokinase	*glk*	0.67	4.06E-02
PA14_58375	Probable metallopeptidase	-	0.66	3.67E-02
PA14_44030	Succinate dehydrogenase flavoprotein subunit	*sdhA*	0.65	4.32E-02
PA14_10550	Putative sulfite or nitrite reductas	*cysI*	0.65	3.19E-02
PA14_61010	Uncharacterized protein	-	0.64	3.25E-02
PA14_08880	50S ribosomal protein L2	*rplB*	0.63	3.25E-02
PA14_11810	Putative aldehyde dehydrogenase; NAD+ dependent	*exaC, -(front)*	0.62	2.47E-02

	acetaldehyde dehydrogenase			
PA14_09100	30S ribosomal protein S4	*rpsD*	0.62	3.20E-02
PA14_09440	Phenazine biosynthesis protein PhzE; Phenazine biosynthesis protein PhzE	*phzE1, phzE2*	0.62	1.62E-02
PA14_53510	Uncharacterized protein	*ycbL*	0.61	4.59E-02
PA14_44300	Aerotaxis receptor Aer	*aer, -*	0.57	1.98E-02
PA14_36870	Putative short-chain dehydrogenase	-	0.56	2.01E-02
PA14_01030	Uncharacterized protein	-	0.56	2.24E-02
PA14_44360	Cbb3-type cytochrome c oxidase subunit	*ccoP*	0.54	1.87E-02
PA14_36320	Hydrogen cyanide synthase HcnB	*hcnB*	0.54	1.67E-02
PA14_33300	CRISPR-associated endonuclease Cas6/Csy4	*cas6f*	0.54	4.32E-02

PA14_31430	Uncharacterized protein	-	0.54	3.19E-02
PA14_40200	Putative exported oxidoreductase	-	0.53	1.61E-02
PA14_22980	Putative binding protein component of ABC sugar transporter	*gltF*	0.53	1.72E-02
PA14_23750	3-isopropylmalate dehydratase large subunit	*leuC*	0.53	2.46E-02
PA14_36310	Hydrogen cyanide synthase HcnC	*hcnC*	0.52	2.16E-03
PA14_54490	Uncharacterized protein	-	0.51	2.16E-03
PA14_60700	Cytochrome c551 peroxidase	*ccpR*	0.50	3.09E-02
PA14_38430	Regulatory gene of gnyRDBHAL cluster, GnyR	*gnyR*	0.50	2.46E-02
PA14_49250	Periplasmic nitrate reductase	*napA*	0.49	2.48E-03
PA14_20890	ADP-L-glycero-D-manno-	*hldD*	0.47	1.61E-02

	heptose-6-epimerase			
PA14_18670	Ferroxidase	*bfrB*	0.46	2.47E-02
PA14_51530	ExoU	*exoU*	0.44	1.73E-03
PA14_07070	Putative reductase	-	0.44	3.09E-02
PA14_23010	Putative ATP-binding component of ABC transporter	*gltK*	0.41	4.67E-04
PA14_42440	Translocator outer membrane protein PopD	*popD*	0.41	2.01E-02
PA14_44340	Putative cytochrome oxidase subunit (Cbb3-type)	*ccoN*	0.40	1.64E-02
PA14_10540	Putative iron-sulfur cluster-binding protein	*fixG*	0.39	2.16E-03
PA14_22990	Putative permease of ABC sugar transporter	-	0.37	5.02E-03
PA14_00820	Uncharacterized protein	-	0.37	3.43E-02
PA14_39945	Phospho-2-dehydro-3-	*phzC2, phzC1*	0.35	4.31E-03

	deoxyheptonate aldolase; Phospho-2-dehydro-3-deoxyheptonate aldolase			
PA14_66760	Putative cell division protein	-	0.30	4.32E-02
PA14_36520	Uncharacterized protein	-	0.23	8.12E-03

Table 3.S1. Table of proteins significantly up- or down-regulated in PA14 NLL-MetRS mutant persisters versus untreated cells.

3.9.13. Summary of whole genome searching results

Gene ID	Gene name	Gene description/function	HigA or HigA-like palindrome
PA14_10650		Hypothetical protein	TTAAC GTTAT
PA14_17270	accA	acetyl-CoA carboxylase carboxyltransferase subunit alpha	TTATC GTTAA
PA14_22250		Hypothetical protein	TTAAC GTCAA
PA14_24480	*pelA*	Hypothetical protein	TTGAC GTTAA
PA14_28800		Hypothetical protein	TTGAC GTTAA
PA14_31460		Transporter	TTTAC GTTAA
PA14_38430	*gnyR*	Regulatory gene of gnyRDBHAL cluster	TTTAC GTTAA
PA14_51330	*nadA*	Quinolinate synthetase	TTAGC GTTAA
PA14_57680		Hypothetical protein	TTAAC GTAAA
PA14_58650		Chemotaxis transducer	TTAAG GTTAA
PA14_59840		Hypothetical protein	TTAAC GTTAG
PA14_61845	*higB*	Toxin of *higBA*	TTAAC GTTAA

Table 3.S2. List of all PA14 genes with HigA or HigA-like palindrome (5′-TTAAC GTTAA-3′) in the promoter region identified by whole genome searching.

Chapter 4

PYOCHELIN CONFERS A FITNESS ADVANTAGE IN BACTERIAL PERSISTER CELLS UNDER CARBON-LIMITED CONDITIONS

4.1. Abstract

Bacteria have multiple molecular mechanisms to adapt to changing environments. For example, *P. aeruginosa* has two major siderophores for iron uptake: pyoverdine and pyochelin. Pyoverdine has been viewed as the predominant siderophore given its high affinity towards iron. However, in this study, we discovered that the pyochelin-mediated pathway is predominant during persister regrowth. In this chapter, we discuss the hypothesis that pyochelin confers a growth advantage in persister cells subject to carbon-limited conditions. In addition, we discuss the potential role of Fur, a ferric uptake regulator, in bacterial persistence.

4.2. Introduction

P. aeruginosa is a common pathogen causing opportunistic infections (Costerton et al., 1999). It can cause many types of infections (Lyczak et al., 2002), including both acute and chronic infections (Goodman et al., 2004; Mikkelsen et al., 2011), due to its ability to colonize different hosts (Goldberg, 2000), utilize multiple secretion systems (Juhas et al., 2005), and produce various virulence factors (Girard & Bloemberg, 2008; Venturi, 2006). In particular, *P. aeruginosa* is the major pathogen that infects patients with cystic fibrosis (CF) and is recalcitrant to both the host immune system and to antibiotic therapies (Davies, 2002; Harrison, 2007).

With respect to bacterial infection, not only is iron an important growth factor, but also iron enables bacteria to colonize their hosts. For *P. aeruginosa*, excessive iron causes the bacteria to aggregate from a motile unicellular form to a sessile biofilm form (Banin et al., 2005; Berlutti et al., 2005; Mikkelsen et al., 2011; Patriquin et al., 2008; Singh et al., 2002). However, iron is often available in Fe(III) form and tightly bound to host Fe(III)-sequestering heme molecules or circulating proteins, and thus not easily accessible to bacteria (Ratledge & Dover, 2000). Bacteria have developed several strategies for iron acquisition (Cornelis & Dingemans, 2013). For example, *P. aeruginosa* can acquire iron via the production of siderophores (Banin et al., 2005), the uptake of ferrisiderophores (Schalk & Guillon, 2013) or xenosiderophores (Cornelis et al., 2009; Cornelis & Bodilis, 2009), the uptake of host heme molecules (Ochsner et al., 2000), and the extracellular reduction of Fe^{3+} to Fe^{2+} through the phenazine-involved Feo system (Wang et al., 2011).

Among these strategies, siderophore-mediated iron uptake pathways allow bacteria to react quickly in iron-deficient environments and to compete for iron with host heme molecules or circulating proteins. These pathways play important roles in bacterial survival and biofilm formation, and are crucial for the virulence of *P. aeruginosa* (Banin et al., 2005; Poole, 2003). *P. aeruginosa* is known to synthesize

two major siderophores, pyoverdine (Pvd; Figure 4.1B) and pyochelin (Pch; Figure 4.1A) (Cornelis et al., 2009). Pyoverdine is a high-affinity siderophore produced by bacteria when the iron concentration is low (Meyer, 2000). Pyochelin is considered to be a secondary siderophore as its affinity toward iron is much lower than that of pyoverdine (Cornelis & Dingemans, 2013). Both siderophores are regulated by Fur, a ferric uptake regulator which negatively regulates the expression of the biosynthesis of pyoverdine and pyochelin (Figure 4.1C) (Banin et al., 2005; Kim et al., 2017).

Pyochelin is a small thiazoline derivative with low solubility in water (Braud et al., 2009). Since pyoverdine has a much higher affinity toward ferric iron and acts as the predominant siderophore for iron uptake (Serino et al., 1997), pyochelin is suspected to have other roles. For example, it might transport other metals into bacteria (Braud et al., 2009). It is also known as a virulence factor (Cox, 1982). In addition, pyochelin might play a role in the chronic infection (Lyczak et al., 2002). However, the role of pyochelin and its regulation remain unclear.

Pyochelin has been reported to be associated with bacterial persistence (Li et al., 2016; Wood & Wood, 2016). In addition, as described in Chapter 3, we have demonstrated via Bioorthogonal Noncanonical Amino Acid Tagging (BONCAT) that the biosynthesis of pyochelin was down-regulated when bacteria entered the persistence state and up-regulated when bacteria exit the persistence state. Surprisingly, differences in the abundances of pyoverdine biosynthesis proteins were not observed when we compared the regrowth of persisters and untreated cells. In addition, it has been shown that the production of pyoverdine was gradually lost in clinical isolates from patients with long-term CF infections (Smith et al., 2006) and the production of pyochelin was increased in conditions mimicking the CF lung (Hare et al., 2012). As bacterial persistence is closely related to chronic infection, these observations raise questions about whether and why persisters rely on pyochelin instead of pyoverdine in these processes.

In this study, we studied *P. aeruginosa* strains that have had either one or both siderophore biosynthesis pathways knocked out. We found that persister cells that have had pyoverdine biosynthesis knocked out were almost identical to WT cells when they resumed growth upon the removal of antibiotics. We also found that bacteria relying on the pyochelin biosynthesis pathway had a growth advantage under low energy conditions, compared to bacteria relying on the pyoverdine biosynthesis pathway.

4.3. Results

4.3.1. Differences in the abundances of pyoverdine biosynthesis proteins were not observed when we compared the regrowth of persisters and untreated cells

We reported the functional group *pyochelin biosynthesis and metabolism* to be strikingly up-regulated during the regrowth of persisters in both Anl-labeled and Aha-labeled BONCAT enrichment experiments (Table 3.1). However, our BONCAT results (including van Eldijk's independent BONCAT studies of persister formation) did not detect significant changes in pyoverdine-related genes/proteins (Figure 4.S1), which constitute the predominant iron acquisition pathway in *P. aeruginosa* (Cornelis & Dingemans, 2013).

We compared our results with two papers which studied *P. aeruginosa* persister formation (Li et al., 2016; Wood & Wood, 2016). Both papers reported only one gene related to pyoverdine biosynthesis and metabolism to be up-regulated when cells enter the persistence state: *fpvA*, which encodes the outer membrane receptor of pyoverdine (Figure 4.S1). But they also did not detect any other significant changes in the pyoverdine biosynthesis pathway, suggesting that pyoverdine does not participate the regulation of bacterial persistence.

4.3.2. Point mutations in PA14 fur increase bacterial survival rates under antibiotic treatment

The regulatory mechanisms governing siderophore switching remain unclear. But it is known that Fur, a global ferric uptake regulator, can regulate the expression of the genes involved in the biosynthesis of both pyoverdine and pyochelin. We have found that strains carrying point mutations in PA14 *fur* exhibit changes in survival rates under ciprofloxacin treatment (Figure 4.2A). We tested four strains: PA14-Fur:H86R, Y42C, L22Q, and L17R. H86R and L22Q each carry a point mutation in the metal binding domain of Fur. Y42C and L17R each carry a point mutation in the DNA binding domain of Fur. All the mutants were generated by Mn^{2+} mutagenesis

procedure as described by Hantke (Hantke, 1987). The survival rates of Fur:H86R, Y42C, L22Q, and L17R were 5.99, 9.29, 12.36, and 4.27 times higher than WT strain (*p* values obtained from t test: 0.0022, 0.0072, 0.0205, and 0.0005, respectively). Point mutations on either the metal- or DNA-binding domains of Fur can increase bacterial antibiotic tolerance significantly, which suggests the importance of iron uptake in bacterial response to antibiotics. We are unaware of previous reports of this kind, possibly due to the lethality of *fur* deletion; for example, *fur*::Tn did not exist in the PA14 transposon insertion library and Δ*fur* could not be cultured (Liberati et al., 2006; Pasqua et al., 2017). We located Fur-binding sites in both the pyochelin and pyoverdine biosynthesis pathways (Figure 4.2B) (Cunrath et al., 2020; Ochsner & Vasil, 1996). We propose that there may be auxiliary proteins that bind to Fur, resulting in conformational changes and regulating the release of Fur from the binding sites of genes responsible for siderophore biosynthesis. There are no relevant studies of this idea in *Pseudomonas* so far. But from a His-Fur pull-down experiment in *E. coli*, it appears that there are several proteins that could be potential targets for this function (Zhang et al., 2020). For example, Crp is a cAMP-activated global transcriptional regulator in *E. coli*. It has been shown that cAMP, a second messenger, has been linked to both persister resuscitation and nutrient transport (Yamasaki et al., 2020). In addition, *vfr* (PA14_08370) is the analog of *crp* (P0ACJ8) in PA14 (Figure 4.S4). It will be interesting to investigate whether Vfr could affect persistence-related phenotypic switching by binding to PA14 Fur and regulating the release of Fur from its binding sites for pyochelin or pyoverdine biosynthesis.

4.3.3. Bacteria relying on the pyochelin biosynthesis pathway had a growth advantage under low energy conditions

A majority of *Pseudomonas* strains produce secondary siderophores in addition to pyoverdine (Cornelis, 2010). Under iron-limited conditions, the biosynthesis of secondary siderophores is usually undetectable or expressed only weakly (Dumas et al., 2013). It is not clear why bacteria retain “redundant” molecular pathways to perform similar roles. It has been suggested that secondary siderophores might have

additional functions, for example, in transporting metals other than iron (Braud et al., 2009). But these scenarios are not directly or indirectly relevant to bacterial persistence. In addition, deletion of siderophores has not been reported to be associated with antibiotic resistance, tolerance, or persistence. However, it is known that the number of genes involved in the synthesis of secondary siderophores is generally smaller than the number involved in pyoverdine biosynthesis (Ravel & Cornelis, 2003; Schalk et al., 2020; Serino et al., 1997). We imagined that there might be a tradeoff between iron uptake efficiencies and the production cost of siderophore synthesis machinery and building blocks. For example, it was observed that *P. aeruginosa* produces pyochelin first at moderate iron concentration and switches to pyoverdine production in iron-starving conditions (Dumas et al., 2013). However, no evidence has been provided to prove the observation was related to the level of nutrients in the environments.

The persister cell phenotype arises not only after antibiotic treatment; nutrient stress also creates persisters (Maisonneuve & Gerdes, 2014; Yamasaki et al., 2020). It was demonstrated that persister cells, either spontaneous or triggered persisters, are a subpopulation of cells facing nutrient stress with low level of ATP (Manuse et al., 2021; Ravel & Cornelis, 2003; Song & Wood, 2020). We hypothesize that bacteria relying on the pyochelin biosynthesis pathway, compared to those relying on the pyoverdine biosynthesis pathway, might have a growth advantage under low nutrient conditions. This advantage might help bacteria exit the persistence state. To test this hypothesis, we checked bacterial resuscitation under carbon-limited conditions. In previous studies, Basta et al demonstrated bacteria could remain viable in minimal medium with 1 mM pyruvate and are capable of regrowth once the limiting energy is replenished (40 mM pyruvate) (Basta et al., 2017). The growth arrest under energy-limited conditions and the resuscitation under energy-sufficient conditions overlap with the phenotypic switching of persister cells. To create the energy-varying conditions, the carbon source of the minimal growth medium was removed and replaced with pyruvate concentrations ranging from 0 to 40 mM as the only carbon

source (Basta et al., 2017). We tested the planktonic regrowth of either untreated or persister cells of WT *P. aeruginosa*, as well as strains bearing clean deletions of genes involved in the synthesis of pyochelin or pyoverdine (pyochelin-producing strain Δ*pvdA*, pyoverdine-producing strain Δ*pchE*, and double deletion mutant strain Δ*pvdA*Δ*pchE*). Surprisingly, untreated cells with siderophore(s) deleted did not exhibit growth defects (Figure 4.S2 and S3). In contrast, persister cells with *pchE* deleted showed fitness defects, while the Δ*pvdA* strain was almost identical to the WT strain. Under low-carbon conditions (5 and 7.5 mM pyruvate), the Δ*pvdA* strain grows faster than the Δ*pchE* strain (p value from CGGC permutation test: 0.03 and 0.05 for 5 and 7.5 mM pyruvate), suggesting that pyochelin may confer a fitness advantage compared to pyoverdine-mediated regrowth. The advantage disappeared at higher energy levels (10 mM pyruvate and above) (Figure 4.3).

We note that the difference between the growth curves of Δ*pvdA* and Δ*pchE* is small, which might be related to the small OD 500 values at the beginning of resuscitation. The number of biological replicates in our experiments was three. The statistical significance can be improved if the number of replicates increases. In general, measuring the statistical significance of growth curves is challenging. Statistical methods for this purpose usually require fitting of the data to a specific model, for example, using the function grofit in R (Dumas et al., 2013).

In addition, the difference we observed between Δ*pvdA* and Δ*pchE* could be strain-specific. In our experiments, we tested Δ*pvdA* for knocking out the pyoverdine biosynthesis pathway and Δ*pchE* for knocking out the pyochelin biosynthesis pathway. It is possible that other changes due to the deletion of *pvdA* or *pchE* led to the difference we observed between these two strains. The hypothesis could be further tested by knocking out other genes in the biosynthesis pathway of pyochelin and pyoverdine, or by examining the behavior of strains in which the knocked-out genes have been complemented by plasmid-borne copies.

Overall, our results indicate the importance of understanding bacterial strategies for switching between siderophores in response to changing environments. We suggest that bacteria may produce metabolically cheap siderophores when nutrients are limited. Once the environment becomes more favorable, bacteria can adapt their iron acquisition strategies to produce metabolically expensive siderophores. Much remains to be done to test this hypothesis.

4.4. Discussion

Bacteria often possess multiple molecular systems to achieve similar purposes. Why would cells maintain redundant systems? In this study, we have investigated several *P. aeruginosa* strains that lack one or two siderophores and identified pyochelin-mediated pathway as the major siderophore-mediated pathway that has been utilized during the regrowth of persisters. The results highlighted the importance of the pyochelin biosynthesis pathway in persister awakening and regrowth, which also challenged the traditional views on the predominant position of the pyoverdine-mediated pathway and demonstrated the advantage of pyochelin biosynthesis under energy-limited conditions. Previous simulation studies demonstrated that the two siderophores facilitate adaptive responses (Dumas et al., 2013). The simulated competitions by Dumas et al between bacteria having either pyoverdine or pyochelin biosynthesis pathway knocked out demonstrated that fluctuating environmental factors (pH levels, temperature, and iron chelators) favor pyoverdine-producing bacteria; as the constancy of environment increases, pyochelin-producing bacteria gradually outcompete pyoverdine-producing bacteria. Here we provided experimental evidence for association between carbon levels and bacterial switching of strategies for siderophores, which could benefit their survival in fluctuating environments.

Bacterial persistence is one of the major causes of recurrent chronic infectious disease, even though it is defined as a transient and non-heritable phenotype. Our results might explain the decreased production or loss of pyoverdine in clinical isolates from patients with long-term CF infections (Smith et al., 2006) and the increased production of pyochelin in synthetic CF sputum medium (Hare et al., 2012).

In addition, our results could be extended to the improvement of drugs to treat *P. aeruginosa* infection. We propose that pyochelin can be used in a Trojan horse strategy to design a new class of siderophore conjugates (Mislin & Schalk, 2014).

The major cause of the multi-drug resistance of *P. aeruginosa* is the extremely low permeability of its outer membrane (Livermore, 2002). Siderophore conjugates have been used to prepare Trojan horse antibiotic prodrugs as a promising treatment strategy. A few conjugates have been demonstrated to affect the growth of *P. aeruginosa* with improved antibacterial level compared to the original antibiotic molecule (Hennard et al., 2001; Kinzel et al., 1998). However, most molecules have structures based on tris-hydroxamate or bis- or tris-catecholate scaffolds, mimicking exogenous siderophores including ferrichrome, enterobactin and other catecholate siderophores (Miller et al., 2009; Mislin & Schalk, 2014; Möllmann et al., 2009). The application of endogenous siderophores has been limited in the past. For pyoverdine conjugates, the major difficulty comes from the diversity of pyoverdine structures across different *P. aeruginosa* strains, thus limiting cross-feeding use (Noël et al., 2011). Pyochelin has been considered as a good candidate for siderophore conjugates since its structure is common to all *P. aeruginosa* strains. However, the solubility of pyochelin is very low and previous efforts have not been very successful (Noël et al., 2011; Rivault et al., 2007). For example, Rivault et al reported the synthesis of a pyochelin conjugate with norfloxacin, functionalized with an amine group in the C5 position of the phenol ring of pyochelin (Rivault et al., 2007). But the conjugate was not shown to bind to FptA, the outer membrane receptor for pyochelin, and had only moderate antibacterial activity (below the levels observed for norfloxacin). Noël et al functionalized N3'' position with a propyl-amine extension and the new design was shown to bind to FptA (Noël et al., 2011). However, the spacer arm between pyochelin and antibiotic molecule was not cleavable, thus limiting the antibacterial activity. They also reported the use of several cleavable linkers but the antibiotic prodrugs were cleaved extracellularly in all cases. Therefore, a future development could be adding a cleavable linker between pyochelin and the antibiotic prodrug that can only become cleavable in bacterial cytoplasm (Wencewicz et al., 2009). The results reported here have highlighted the importance of pyochelin and the potential application of pyochelin conjugates in killing persisters. Success in this endeavor would constitute a meaningful step forward in the treatment of chronic infection.

4.5. Materials and methods

4.5.1. Strains and growth conditions

P. aeruginosa PA14 strain was used in this study. Clean deletions of Δ*pchE*, Δ*pvdA*, and Δ*pchE*Δ*pvdA* were designed by Chelsay VanDrisse from the Newman laboratory at the California Institute of Technology following the previous developed methods by Hmelo et al (Hmelo et al., 2015). *fur* mutants (PA14-Fur:H86R, Y42C, L22Q, L17R) were designed by Paul Morale from the Newman laboratory at the California Institute of Technology following the previous developed methods by Hantke (Hantke, 1987).

The growth medium used in the energy-limited conditions was based on the modified minimal medium following the previous developed recipe (Widdel & Pfennig, 1981). After autoclaving the base medium, 1 mL of 1 M $MgSO_4$, 100 µL of 1 M $CaCl_2$, and 0.5 g NH_4Cl (Fisher Scientific) were added into 1L minimal medium. Pyruvate (Thermo Scientific) ranging from 0 mM to 40 mM was added into the minimal medium.

Trace metals were also added to the minimal medium to ensure sufficient metals especially iron. 1000x trace metals (per L) contains $Fe(III)Cl_3 \cdot 6H_2O$ (2.03g), $Co(II)Cl_2 \cdot 6H_2O$ (190mg); $Mn(II)Cl_2 \cdot 4H_2O$ (99mg); $ZnCl_2$ (68mg); $NaMoO_4 \cdot 2H_2O$ (48 mg); $Ni(II)SO_4 \cdot 6H_2O$ (26 mg); $Cu(II)SO_4 \cdot 5H_2O$ (2.5 mg); H_3BO_3 (6 mg) (Sigma-Aldrich).

4.5.2. Antibiotic treatment

Bacterial cells were cultured overnight with shaking at 37˚C to reach stationary phase. Ciprofloxacin (Life Technologies) was dissolved in 0.1 M NaOH solution and the pH was adjusted to 7. The ciprofloxacin was then filtered and added to cultures at stationary phase at a final concentration of 20 µg/mL, 100x the reported minimum inhibitory concentration (MIC). The duration of antibiotic treatment was 4 h. Culture

tubes containing the persister cells and cell debris were centrifuged at 5,000 g for 5 mins and the cell pellets were washed with sterile 0.9% NaCl solution twice.

4.5.3. Survival rates characterization

Survival rates were characterized by counting colony forming unit (CFU). At the desired timepoint, 100 mL of cell suspension was collected from the culture tubes, followed by washing with 0.9% NaCl solution (an extra wash was performed if the cell suspension contained antibiotics). The cells were then diluted in series, up to 10^9 for untreated cells and up to 10^7 for persisters. Three drops from each diluted sample were collected and plated on LB agar plates. The plates were then cultured overnight at 37˚C.

4.5.4. Absorbance

Cultures were grown overnight in LB medium and diluted 1:100 into corresponding minimal medium with desired pyruvate concentration. 200 µL of each diluted culture was transferred to 96-well flat-bottom polystyrene plates (Falcon). Plates were capped and shaking at 37 ˚C. Absorbances at 500 nm were measured with Varioskan LUX Microplate Reader (Thermo Scientific).

4.5.5. Statistical analysis

We tested with student's t-test for PA14 *fur* mutants and WT strain. In the case of growth curves analyses, we used the CGGC permutation test, which computes a permutation p-value for each pair of groups, using the average t-statistic between the groups as the test statistic. The method was used and described in these studies (Baldwin et al., 2007; Elso et al., 2004).

4.6. Acknowledgements

We thank Dr. Brett M. Babin for his help in BONCAT experiments and Dr. Mark van Eldijk for his assistance in proteomic analysis. We thank Roxana Eggleston-Rangel, Michael J. Sweredoski, Annie Moradian, Dr. Jeff Jones, and Brett Lomenick from Caltech Proteome Exploration Laboratory for LC-MS/MS experiments and analysis. We thank Dr. Chelsey VanDrisse for her help in making PA14 clean deletions. We also thank Dr. Megan Bergkessel, Dr. Paul Morale, and Prof. Dianne K. Newman for their help in PA14 strains and their insights in this project.

4.7. List of figures

Figure 4.1. Pyochelin and pyoverdine. (A) Chemical structure of pyochelin. (B) Chemical structure of pyoverdine in *P. aeruginosa*. (C) Schematic model of the role of siderophores in iron uptake. Siderophores (pyochelin or pyoverdine) are secreted and bound with ferric iron extracellularly. Iron-bound siderophores are transported across the outer membrane through TonB-dependent receptors (FptA for pyochelin and FpvA for pyoverdine) and the inner membrane through ATP binding cassette (ABC) transporters. Once in the cytoplasm, ferrous ion is detached from the siderophores and participates in cellular activity. Excessive ferrous ion is bound to Fur protein to regulate the biosynthesis of siderophores (pyochelin system or pyoverdine system). The pyoverdine biosynthesis is additionally regulated by sigma factors PvdS and FpvI that are bound to anti-sigma factor FpvR. Purple refers to pyochelin (Pch). Green refers to pyoverdine (Pvd).

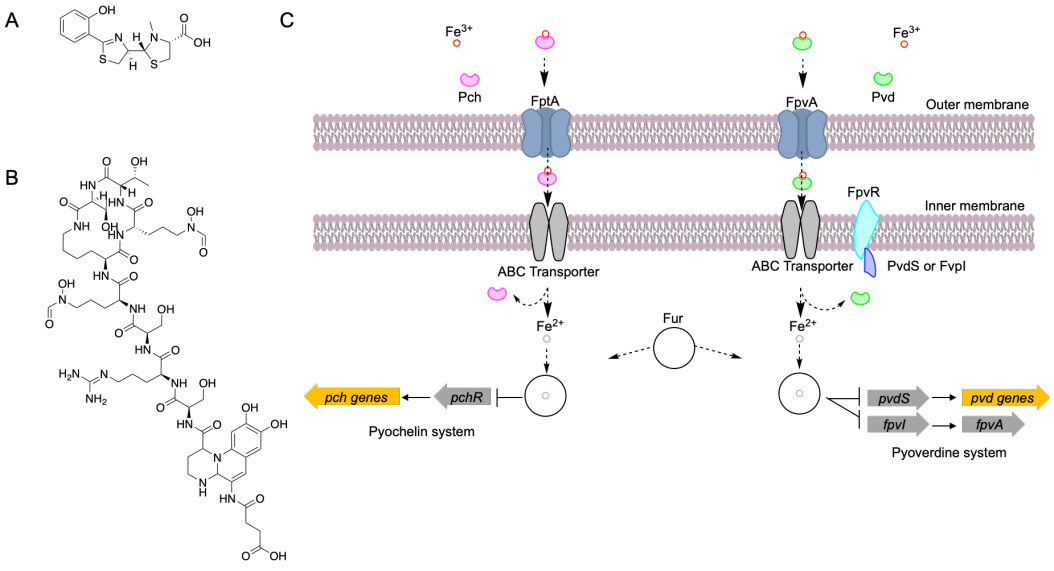

Figure 4.2. *fur* mutants and Fur binding sites. (A) Survival rates of PA14 *fur* mutants (PA14-Fur:H86R, Y42C, L22Q, L17R). The antibiotics used in this study was ciprofloxacin. Error bars refers to SDE. N = 3. Statistical test: student's t-test. (B) Fur binding sites were located on the promoter regions of *pchD*, *pchE*, and *pvdS* with comparison to the Fur consensus binding box.

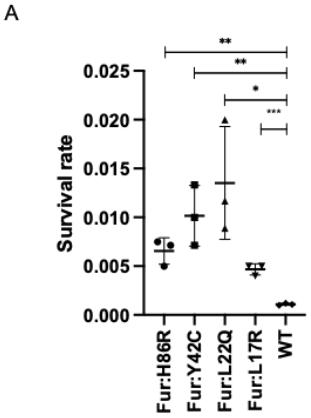

B

Fur box		**GATAATGATAATCATTATC**
pchD	-57	…AAT**GATAATAA**ATC**TCATT**…**TC**CCA…
pchE	-72	…TTT**GATAAT**CG**T**TGC**CA**GG**AAC**TGG…
pvdS	-102	…TTC**G**…**TAAT**T**GAC****AATCATTATC**AT…

Figure 4.3. Regrowth of persisters of each strain under energy-limited conditions. Persisters of each strain (WT, clean deletions of Δ*pchE*, Δ*pvdA*, and Δ*pvdA*Δ*pchE*), were obtained by treating stationary-phase cells with ciprofloxacin for 4 hours. Absorbance at OD 500 of each strain was measured in carbon-limited media with pyruvate concentrations ranging from 0 mM to 10 mM. The number in the subtitle MMX means that the pyruvate concentration is X mM. Error bars refer to SDE. Measurements were repeated 3 times.

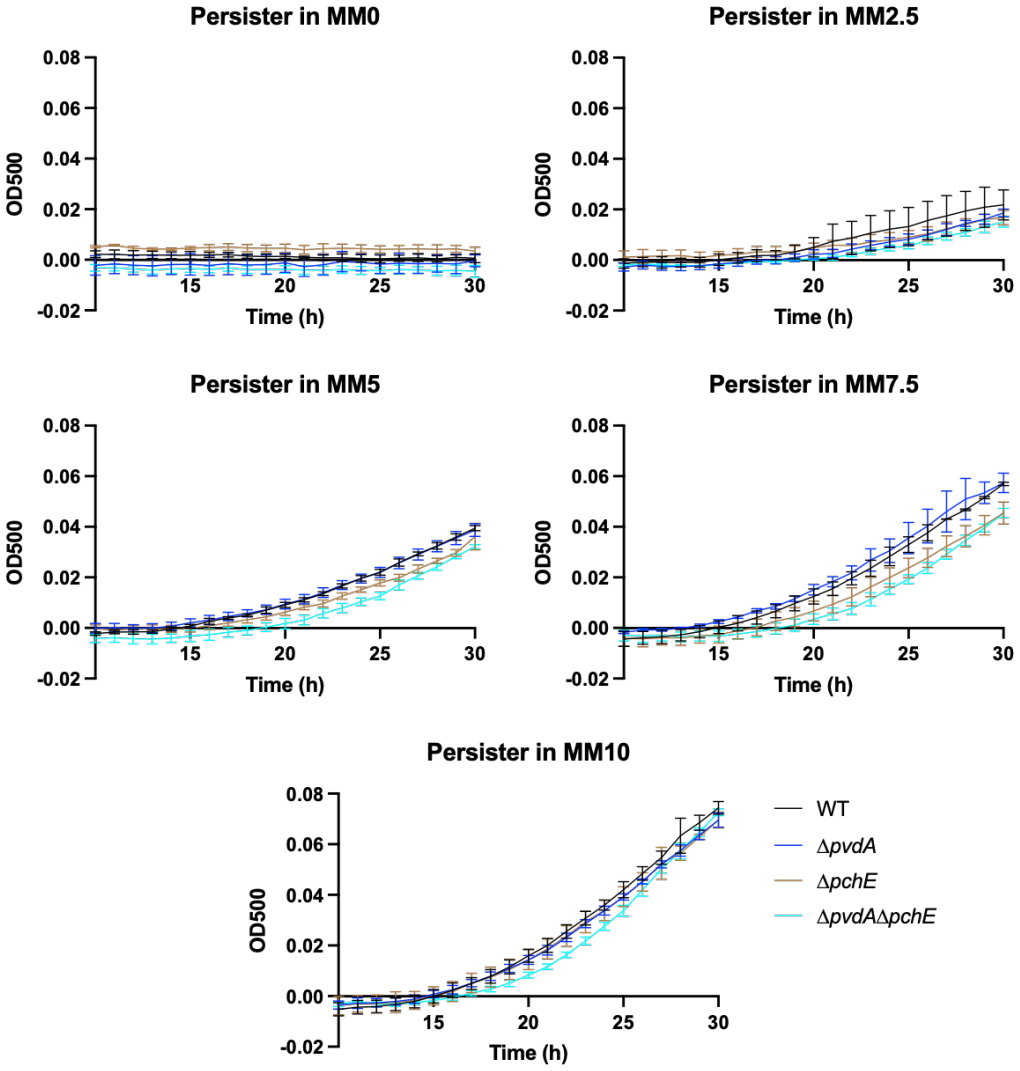

4.8. References

Baldwin, T., Sakthianandeswaren, A., Curtis, J. M., Kumar, B., Smyth, G. K., Foote, S. J., & Handman, E. (2007). Wound Healing Response is a Major Contributor to the Severity of Cutaneous Leishmaniasis in the Ear Model of Infection. *Parasite Immunology*, *29*(10), 501–513. https://doi.org/10.1111/j.1365-3024.2007.00969.x

Banin, E., Vasil, M. L., & Greenberg, E. P. (2005). Iron and *Pseudomonas aeruginosa* Biofilm Formation. *Proceedings of the National Academy of Sciences*, *102*(31), 11076–11081. https://doi.org/10.1073/pnas.0504266102

Basta, D. W., Bergkessel, M., & Newman, D. K. (2017). Identification of Fitness Determinants during Energy-Limited Growth Arrest in *Pseudomonas aeruginosa*. *MBio*, *8*(6). https://doi.org/10.1128/mBio.01170-17

Berlutti, F., Morea, C., Battistoni, A., Sarli, S., Cipriani, P., Superti, F., Ammendolia, M. G., & Valenti, P. (2005). Iron Availability Influences Aggregation, Biofilm, Adhesion and Invasion of *Pseudomonas Aeruginosa* and *Burkholderia Cenocepacia*. *International Journal of Immunopathology and Pharmacology*, *18*(4), 661–670. https://doi.org/10.1177/039463200501800407

Braud, A., Hannauer, M., Mislin, G. L. A., & Schalk, I. J. (2009). The *Pseudomonas aeruginosa* Pyochelin-Iron Uptake Pathway and Its Metal Specificity. *Journal of Bacteriology*, *191*(11), 3517–3525. https://doi.org/10.1128/JB.00010-09

Cornelis, P. (2010). Iron Uptake and Metabolism in *Pseudomonads*. *Applied Microbiology and Biotechnology*, *86*(6), 1637–1645. https://doi.org/10.1007/s00253-010-2550-2

Cornelis, P., & Bodilis, J. (2009). A Survey of TonB-Dependent Receptors in Fluorescent *Pseudomonads*. *Environmental Microbiology Reports*, *1*(4), 256–262. https://doi.org/10.1111/j.1758-2229.2009.00041.x

Cornelis, P., & Dingemans, J. (2013). *Pseudomonas aeruginosa* Adapts Its Iron Uptake Strategies in Function of the Type of Infections. *Frontiers in Cellular and Infection Microbiology*, *3*. https://doi.org/10.3389/fcimb.2013.00075

Cornelis, P., Matthijs, S., & van Oeffelen, L. (2009). Iron Uptake Regulation in *Pseudomonas aeruginosa*. *BioMetals*, *22*(1), 15–22. https://doi.org/10.1007/s10534-008-9193-0

Costerton, J. W., Stewart, P. S., & Greenberg, E. P. (1999). Bacterial Biofilms: A Common Cause of Persistent Infections. *Science*, *284*(5418), 1318–1322. https://doi.org/10.1126/science.284.5418.1318

Cox, C. D. (1982). Effect of Pyochelin on the Virulence of *Pseudomonas aeruginosa*. *Infection and Immunity*, *36*(1), 17–23. https://doi.org/10.1128/iai.36.1.17-23.1982

Cunrath, O., Graulier, G., Carballido-Lopez, A., Pérard, J., Forster, A., Geoffroy, V. A., saint Auguste, P., Bumann, D., Mislin, G. L. A., Michaud-Soret, I., Schalk, I. J., & Fechter, P. (2020). The Pathogen *Pseudomonas aeruginosa* Optimizes the Production of the Siderophore Pyochelin upon Environmental Challenges. *Metallomics*, *12*(12), 2108–2120. https://doi.org/10.1039/d0mt00029a

Davies, J. C. (2002). *Pseudomonas aeruginosa* in Cystic Fibrosis: Pathogenesis and Persistence. *Paediatric Respiratory Reviews*, *3*(2), 128–134. https://doi.org/10.1016/S1526-0550(02)00003-3

Dumas, Z., Ross-Gillespie, A., & Kümmerli, R. (2013). Switching Between Apparently Redundant Iron-Uptake Mechanisms Benefits Bacteria in Changeable Environments. *Proceedings of the Royal Society B: Biological Sciences*, *280*(1764), 20131055. https://doi.org/10.1098/rspb.2013.1055

Elso, C. M., Roberts, L. J., Smyth, G. K., Thomson, R. J., Baldwin, T. M., Foote, S. J., & Handman, E. (2004). Leishmaniasis Host Response Loci (*lmr1–3*) Modify Disease Severity through a Th1/Th2-Independent Pathway. *Genes & Immunity*, *5*(2), 93–100. https://doi.org/10.1038/sj.gene.6364042

Girard, G., & Bloemberg, G. v. (2008). Central Role of Quorum Sensing in Regulating the Production of Pathogenicity Factors in *Pseudomonas aeruginosa*. *Future Microbiology*, *3*(1), 97–106. https://doi.org/10.2217/17460913.3.1.97

Goldberg, J. B. (2000). *Pseudomonas*: Global Bacteria. *Trends in Microbiology*, *8*(2), 55–57. https://doi.org/10.1016/S0966-842X(99)01671-6

Goodman, A. L., Kulasekara, B., Rietsch, A., Boyd, D., Smith, R. S., & Lory, S. (2004). A Signaling Network Reciprocally Regulates Genes Associated with Acute Infection and Chronic Persistence in *Pseudomonas aeruginosa*. *Developmental Cell*, *7*(5), 745–754. https://doi.org/10.1016/j.devcel.2004.08.020

Hantke, K. (1987). Selection Procedure for Deregulated Iron Transport Mutants (*fur*) in *Escherichia coli* K 12: Fur Not Only Affects Iron Metabolism. *Molecular and General Genetics MGG*, *210*(1), 135–139. https://doi.org/10.1007/BF00337769

Hare, N. J., Soe, C. Z., Rose, B., Harbour, C., Codd, R., Manos, J., & Cordwell, S. J. (2012). Proteomics of *Pseudomonas aeruginosa* Australian Epidemic Strain 1 (AES-1) Cultured under Conditions Mimicking the Cystic Fibrosis Lung Reveals Increased Iron Acquisition via the Siderophore Pyochelin. *Journal of Proteome Research*, *11*(2), 776–795. https://doi.org/10.1021/pr200659h

Harrison, Freya. (2007). Microbial Ecology of the Cystic Fibrosis Lung. *Microbiology*, *153*(4), 917–923. https://doi.org/10.1099/mic.0.2006/004077-0

Hennard, C., Truong, Q. C., Desnottes, J.-F., Paris, J.-M., Moreau, N. J., & Abdallah, M. A. (2001). Synthesis and Activities of Pyoverdin−Quinolone Adducts: A Prospective Approach to a Specific Therapy Against *Pseudomonas aeruginosa*. *Journal of Medicinal Chemistry*, *44*(13), 2139–2151. https://doi.org/10.1021/jm990508g

Hmelo, L. R., Borlee, B. R., Almblad, H., Love, M. E., Randall, T. E., Tseng, B. S., Lin, C., Irie, Y., Storek, K. M., Yang, J. J., Siehnel, R. J., Howell, P. L., Singh, P. K., Tolker-Nielsen, T., Parsek, M. R., Schweizer, H. P., & Harrison, J. J. (2015). Precision-Engineering the *Pseudomonas aeruginosa* Genome with Two-Step Allelic Exchange. *Nature Protocols*, *10*(11), 1820–1841. https://doi.org/10.1038/nprot.2015.115

Juhas, M., Eberl, L., & Tummler, B. (2005). Quorum Sensing: The Power of Cooperation in the World of *Pseudomonas*. *Environmental Microbiology*, *7*(4), 459–471. https://doi.org/10.1111/j.1462-2920.2005.00769.x

Kim, T.-S., Ham, S.-Y., Park, B. B., Byun, Y., & Park, H.-D. (2017). Lauroyl Arginate Ethyl Blocks the Iron Signals Necessary for *Pseudomonas aeruginosa* Biofilm Development. *Frontiers in Microbiology*, *8*. https://doi.org/10.3389/fmicb.2017.00970

Kinzel, O., Tappe, R., Gerus, I., & Budzikiewicz, H. (1998). The Synthesis and Antibacterial Activity of Two Pyoverdin-Ampicillin Conjugates, Entering *Pseudomonas aeruginosa* via the Pyoverdin-Mediated Iron Uptake Pathway. *The Journal of Antibiotics*, *51*(5), 499–507. https://doi.org/10.7164/antibiotics.51.499

Li, M., Long, Y., Liu, Y., Liu, Y., Chen, R., Shi, J., Zhang, L., Jin, Y., Yang, L., Bai, F., Jin, S., Cheng, Z., & Wu, W. (2016). HigB of *Pseudomonas aeruginosa* Enhances Killing of Phagocytes by Up-Regulating the Type III Secretion System in Ciprofloxacin Induced Persister Cells. *Frontiers in Cellular and Infection Microbiology*, *6*. https://doi.org/10.3389/fcimb.2016.00125

Liberati, N. T., Urbach, J. M., Miyata, S., Lee, D. G., Drenkard, E., Wu, G., Villanueva, J., Wei, T., & Ausubel, F. M. (2006). An Ordered, Nonredundant Library of *Pseudomonas aeruginosa* Strain PA14 Transposon Insertion Mutants. *Proceedings of the National Academy of Sciences*, *103*(8), 2833–2838. https://doi.org/10.1073/pnas.0511100103

Livermore, D. M. (2002). Multiple Mechanisms of Antimicrobial Resistance in *Pseudomonas aeruginosa*: Our Worst Nightmare? *Clinical Infectious Diseases*, *34*(5), 634–640. https://doi.org/10.1086/338782

Lyczak, J. B., Cannon, C. L., & Pier, G. B. (2002). Lung Infections Associated with Cystic Fibrosis. *Clinical Microbiology Reviews*, *15*(2), 194–222. https://doi.org/10.1128/CMR.15.2.194-222.2002

Maisonneuve, E., & Gerdes, K. (2014). Molecular Mechanisms Underlying Bacterial Persisters. *Cell*, *157*(3), 539–548. https://doi.org/10.1016/j.cell.2014.02.050

Manuse, S., Shan, Y., Canas-Duarte, S. J., Bakshi, S., Sun, W.-S., Mori, H., Paulsson, J., & Lewis, K. (2021). Bacterial Persisters are a Stochastically Formed Subpopulation of Low-Energy Cells. *PLOS Biology*, *19*(4), e3001194. https://doi.org/10.1371/journal.pbio.3001194

Meyer, J.-M. (2000). Pyoverdines: Pigments, Siderophores and Potential Taxonomic Markers of Fluorescent *Pseudomonas* Species. *Archives of Microbiology*, *174*(3), 135–142. https://doi.org/10.1007/s002030000188

Mikkelsen, H., McMullan, R., & Filloux, A. (2011). The *Pseudomonas aeruginosa* Reference Strain PA14 Displays Increased Virulence Due to a Mutation in *ladS*. *PLoS ONE*, *6*(12), e29113. https://doi.org/10.1371/journal.pone.0029113

Miller, M. J., Zhu, H., Xu, Y., Wu, C., Walz, A. J., Vergne, A., Roosenberg, J. M., Moraski, G., Minnick, A. A., McKee-Dolence, J., Hu, J., Fennell, K., Kurt Dolence, E., Dong, L., Franzblau, S., Malouin, F., & Möllmann, U. (2009). Utilization of Microbial Iron Assimilation Processes for the Development of New Antibiotics and Inspiration for the Design of New Anticancer Agents. *BioMetals*, *22*(1), 61–75. https://doi.org/10.1007/s10534-008-9185-0

Mislin, G. L. A., & Schalk, I. J. (2014). Siderophore-Dependent Iron Uptake Systems as Gates for Antibiotic Trojan Horse Strategies against *Pseudomonas aeruginosa*. *Metallomics*, *6*(3), 408–420. https://doi.org/10.1039/C3MT00359K

Möllmann, U., Heinisch, L., Bauernfeind, A., Köhler, T., & Ankel-Fuchs, D. (2009). Siderophores as Drug Delivery Agents: Application of the "Trojan Horse" Strategy. *BioMetals*, *22*(4), 615–624. https://doi.org/10.1007/s10534-009-9219-2

Noël, S., Gasser, V., Pesset, B., Hoegy, F., Rognan, D., Schalk, I. J., & Mislin, G. L. A. (2011). Synthesis and Biological Properties of Conjugates Between Fluoroquinolones and a N3″-Functionalized Pyochelin. *Organic & Biomolecular Chemistry*, *9*(24), 8288. https://doi.org/10.1039/c1ob06250f

Ochsner, U. A., Johnson, Z., & Vasil, M. L. (2000). Genetics and Regulation of Two Distinct Haem-Uptake systems, *phu* and *has*, in *Pseudomonas aeruginosa*. *Microbiology*, *146*(1), 185–198. https://doi.org/10.1099/00221287-146-1-185

Ochsner, U. A., & Vasil, M. L. (1996). Gene Repression By the Ferric Uptake Regulator in *Pseudomonas aeruginosa*: Cycle Selection of Iron-Regulated Genes. *Proceedings of the National Academy of Sciences*, *93*(9), 4409–4414. https://doi.org/10.1073/pnas.93.9.4409

Pasqua, M., Visaggio, D., lo Sciuto, A., Genah, S., Banin, E., Visca, P., & Imperi, F. (2017). Ferric Uptake Regulator Fur Is Conditionally Essential in *Pseudomonas aeruginosa*. *Journal of Bacteriology*, *199*(22). https://doi.org/10.1128/JB.00472-17

Patriquin, G. M., Banin, E., Gilmour, C., Tuchman, R., Greenberg, E. P., & Poole, K. (2008). Influence of Quorum Sensing and Iron on Twitching Motility and Biofilm Formation in *Pseudomonas aeruginosa*. *Journal of Bacteriology*, *190*(2), 662–671. https://doi.org/10.1128/JB.01473-07

Poole, K. (2003). Iron Acquisition and Its Control in *Pseudomonas aeruginosa* Many Roads Lead to Rome. *Frontiers in Bioscience*, *8*(4), 1051. https://doi.org/10.2741/1051

Ratledge, C., & Dover, L. G. (2000). Iron Metabolism in Pathogenic Bacteria. *Annual Review of Microbiology*, *54*(1), 881–941. https://doi.org/10.1146/annurev.micro.54.1.881

Ravel, J., & Cornelis, P. (2003). Genomics of Pyoverdine-Mediated Iron Uptake in *Pseudomonads*. *Trends in Microbiology*, *11*(5), 195–200. https://doi.org/10.1016/S0966-842X(03)00076-3

Rivault, F., Liébert, C., Burger, A., Hoegy, F., Abdallah, M. A., Schalk, I. J., & Mislin, G. L. A. (2007). Synthesis of Pyochelin–Norfloxacin Conjugates. *Bioorganic & Medicinal Chemistry Letters*, *17*(3), 640–644. https://doi.org/10.1016/j.bmcl.2006.11.005

Schalk, I. J., & Guillon, L. (2013). Fate of Ferrisiderophores after Import across Bacterial Outer Membranes: Different Iron Release Strategies Are Observed in

the Cytoplasm or Periplasm Depending on the Siderophore Pathways. *Amino Acids*, *44*(5), 1267–1277. https://doi.org/10.1007/s00726-013-1468-2

Schalk, I. J., Rigouin, C., & Godet, J. (2020). An Overview of Siderophore Biosynthesis among Fluorescent *Pseudomonads* and New Insights into their Complex Cellular Organization. *Environmental Microbiology*, *22*(4), 1447–1466. https://doi.org/10.1111/1462-2920.14937

Serino, L., Reimmann, C., Visca, P., Beyeler, M., Chiesa, V. D., & Haas, D. (1997). Biosynthesis of Pyochelin and Dihydroaeruginoic Acid Requires the Iron-Regulated *pchDCBA* Operon in *Pseudomonas aeruginosa*. *Journal of Bacteriology*, *179*(1), 248–257. https://doi.org/10.1128/jb.179.1.248-257.1997

Singh, P. K., Parsek, M. R., Greenberg, E. P., & Welsh, M. J. (2002). A Component of Innate Immunity Prevents Bacterial Biofilm Development. *Nature*, *417*(6888), 552–555. https://doi.org/10.1038/417552a

Smith, E. E., Buckley, D. G., Wu, Z., Saenphimmachak, C., Hoffman, L. R., D'Argenio, D. A., Miller, S. I., Ramsey, B. W., Speert, D. P., Moskowitz, S. M., Burns, J. L., Kaul, R., & Olson, M. v. (2006). Genetic Adaptation by *Pseudomonas aeruginosa* to the Airways of Cystic Fibrosis Patients. *Proceedings of the National Academy of Sciences*, *103*(22), 8487–8492. https://doi.org/10.1073/pnas.0602138103

Song, S., & Wood, T. K. (2020). ppGpp Ribosome Dimerization Model for Bacterial Persister Formation and Resuscitation. *Biochemical and Biophysical Research Communications*, *523*(2), 281–286. https://doi.org/10.1016/j.bbrc.2020.01.102

Venturi, V. (2006). Regulation of Quorum Sensing in *Pseudomonas*. *FEMS Microbiology Reviews*, *30*(2), 274–291. https://doi.org/10.1111/j.1574-6976.2005.00012.x

Wang, Y., Wilks, J. C., Danhorn, T., Ramos, I., Croal, L., & Newman, D. K. (2011). Phenazine-1-Carboxylic Acid Promotes Bacterial Biofilm Development via Ferrous Iron Acquisition. *Journal of Bacteriology*, *193*(14), 3606–3617. https://doi.org/10.1128/JB.00396-11

Wencewicz, T. A., Möllmann, U., Long, T. E., & Miller, M. J. (2009). Is Drug Release Necessary for Antimicrobial Activity of Siderophore-Drug Conjugates? Syntheses and Biological Studies of the Naturally Occurring Salmycin "Trojan Horse" Antibiotics and Synthetic Desferridanoxamine-Antibiotic Conjugates. *BioMetals*, *22*(4), 633–648. https://doi.org/10.1007/s10534-009-9218-3

Widdel, F., & Pfennig, N. (1981). Studies on Dissimilatory Sulfate-Reducing Bacteria that Decompose Fatty Acids. *Archives of Microbiology*, *129*(5), 395–400. https://doi.org/10.1007/BF00406470

Wood, T. L., & Wood, T. K. (2016). The HigB/HigA Toxin/Antitoxin System of *Pseudomonas aeruginosa* Influences the Virulence Factors Pyochelin, Pyocyanin, and Biofilm Formation. *MicrobiologyOpen*, *5*(3), 499–511. https://doi.org/10.1002/mbo3.346

Yamasaki, R., Song, S., Benedik, M. J., & Wood, T. K. (2020). Persister Cells Resuscitate Using Membrane Sensors that Activate Chemotaxis, Lower cAMP Levels, and Revive Ribosomes. *IScience*, *23*(1), 100792. https://doi.org/10.1016/j.isci.2019.100792

Zhang, F., Li, B., Dong, H., Chen, M., Yao, S., Li, J., Zhang, H., Liu, X., Wang, H., Song, N., Zhang, K., Du, N., Xu, S., & Gu, L. (2020). YdiV Regulates *Escherichia coli* Ferric Uptake by Manipulating the DNA-Binding Ability of Fur in a SlyD-Dependent Manner. *Nucleic Acids Research*, *48*(17), 9571–9588. https://doi.org/10.1093/nar/gkaa696

4.9. Supplementary information

4.9.1. Comparison of pyoverdine fold changes in various studies in persister formation and regrowth

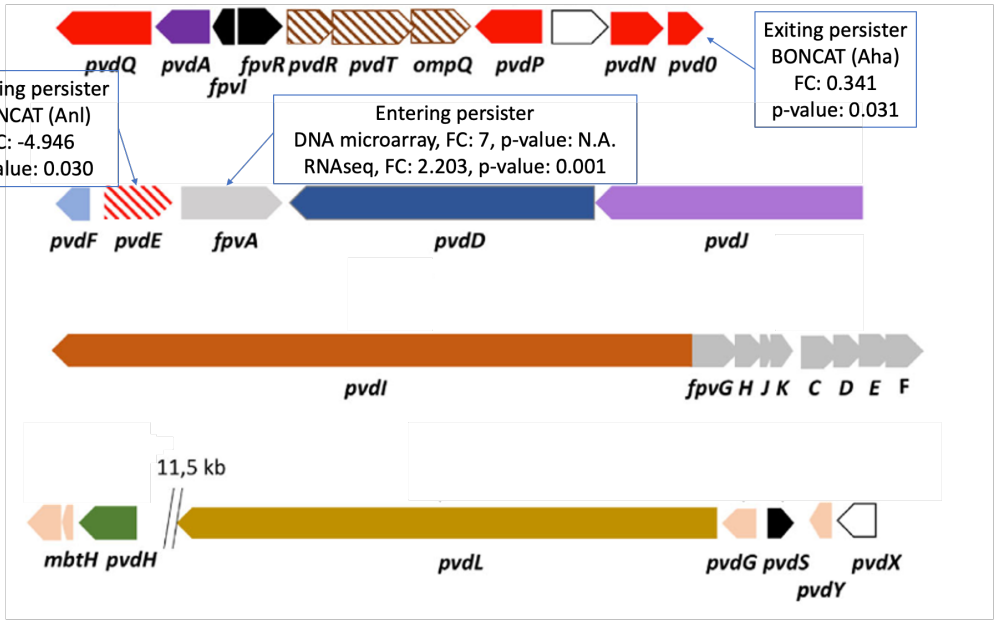

Figure 4.S1. Fold changes involved in the pyoverdine biosynthesis pathway. BONCAT results showed the fold change of PvdO was 0.341 when cells exit the persistence state and the fold change of PvdE was -4.946 when cell enter the persistence state. DNA microarrays data showed the fold change of *fpvA* was 7 (Wood & Wood, 2016). RNAseq data showed the fold change of *fpvA* was 2.203 (Li et al., 2016). Fold changes of other proteins/genes in the pyoverdine biosynthesis pathway were not found. The pyoverdine biosynthesis pathway is adapted from (Schalk et al., 2020).

4.9.2. Regrowth of untreated strains in energy-limited conditions

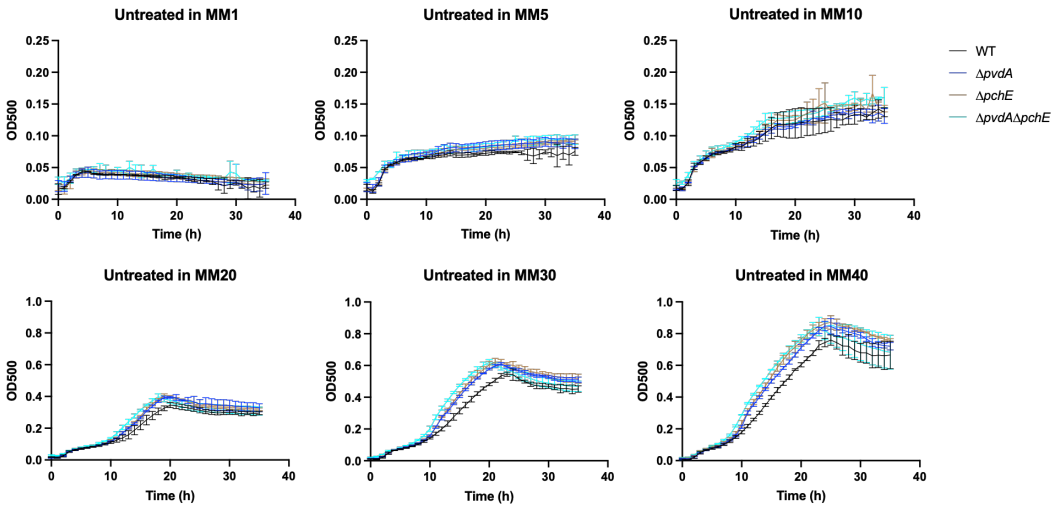

Figure 4.S2. Absorbance at OD 500 of each strain in carbon-limited medium with pyruvate concentrations ranging from 1 mM to 40 mM. Untreated cells of each strain (WT, clean deletions of Δ*pchE*, Δ*pvdA*, and Δ*pvdA*Δ*pchE*), were grown overnight in LB medium into stationary phase and diluted 1:100. Absorbance at OD 500 of each strain was measured in carbon-limited media with pyruvate concentrations ranging from 1 mM to 40 mM. The number in the subtitle MMX means that the pyruvate concentration is X mM. Error bars refer to SDE. Measurements were repeated 3 times.

4.9.3. Expanded views of the early-stage of growth for untreated cells in energy-limited conditions

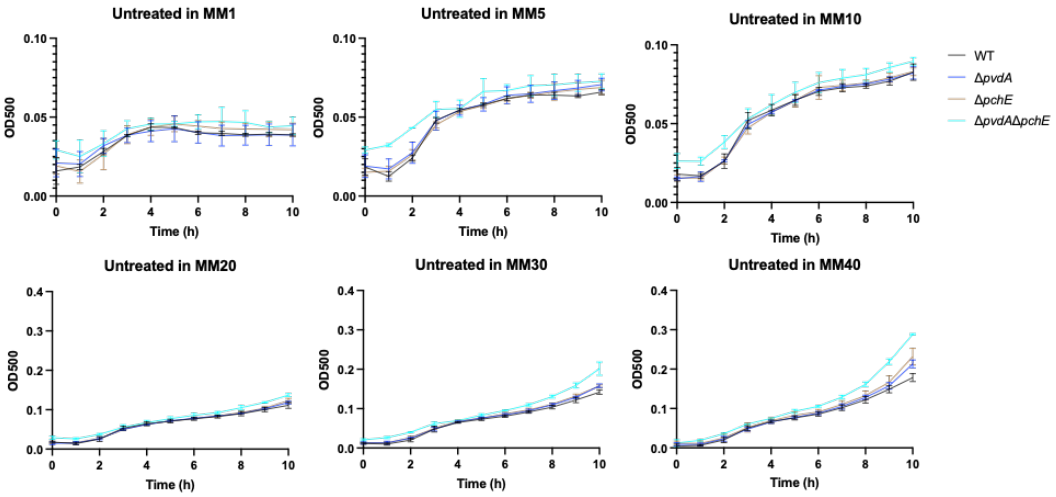

Figure 4.S3. Absorbance at OD 500 of the early-stage of growth for untreated cells in carbon-limited medium with pyruvate concentrations ranging from 1 mM to 40 mM. The figures show expanded view of the absorbance measurements during the first 10 h in Figure 4.S2.

4.9.4. BlastP results for PA14 vfr and E. coli BL21 crp

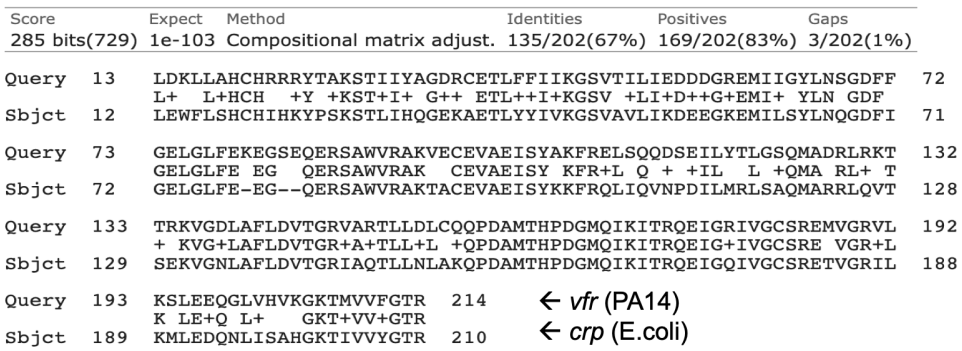

Figure 4.S4. Alignment of the protein sequences of PA14 *vfr* and *E. coli* BL21 *crp*. BLASTP (Protein BLAST; NIH website) analysis showed PA14 *vfr* and BL21 *crp* are analogous genes. The comparison of the protein sequences of two genes shows a positive rate of 83%, calculated based on the number of amino acids that are either identical or have similar chemical properties.